

ABSTRACT

Title of Document: Ecosystem Impact of Winter Dinoflagellate Blooms in the Choptank River, MD
Nicole Millette, Doctor of Philosophy, 2016

Directed By: Assistant Professor, Dr. Jamie Pierson,
Horn Point Laboratory,
University of Maryland Center of
Environmental Science

Heterocapsa rotundata is a dinoflagellate species that is known to form winter blooms in coastal and estuarine systems. Despite evidence that winter *H. rotundata* blooms are a common occurrence, there is a lack of laboratory and field-based research on the ecology of this species. My goal was to understand the impact these blooms had on the plankton food web and whether the winter blooms influenced the spring ecosystem. A majority of my research was done with water collected from the Choptank River, MD over the course of five winters. I conducted dilution and prey removal experiments to address the importance of top-down control to the formation of winter blooms. These experiments showed that appropriate environmental conditions are necessary for high *H. rotundata* growth, and that a bloom will not form unless zooplankton grazing pressure is reduced. I also used a combination of laboratory and field experiments to address whether mixotrophy helps *H. rotundata* bloom in winter, and my work showed that *H. rotundata* typically dominates winter blooms because they are a mixotrophic species that uses phagotrophy to overcome the light limitation of winter. I

used cultures of *Eurytemora carolleeae* and *H. rotundata* to test if high *H. rotundata* abundances benefit *E. carolleeae* populations. I found that *H. rotundata* has no effect on *E. carolleeae* egg production rate or hatching success rate, but that they can increase the survival *E. carolleeae* nauplii. Ultimately, through the use of historical data and a temperature based *E. carolleeae* developmental model, I discovered that lower winter temperatures improve the potential for high annual recruitment of anadromous fish larvae hatched in spring in Chesapeake Bay. Winters with below average temperatures reduce the development rate of *E. carolleeae* nauplii hatched in winter, and *H. rotundata* blooms are likely to form and that increase the survival of *E. carolleeae* nauplii. The delayed development and increased survival causes distinct peaks in *E. carolleeae* populations later in spring, increasing the chance of high *E. carolleeae* abundance when fish larvae start feeding. Overall, my research has shown the winter temperature and plankton community can influence the spring ecosystem, specifically the survival and recruitment of anadromous fish larvae.

ECOSYSTEM IMPACT OF WINTER DINOFLAGELLATE BLOOMS IN THE
CHOPTANK RIVER, MD

By

Nicole Catherine Millette

Dissertation submitted to the Faculty of the Graduate School of the
University of Maryland, College Park in partial fulfillment
of the requirements for the degree of
Doctor of Philosophy
2016

Advisory Committee:
Dr. Jamie Pierson, Chair
Dr. Diane Stoecker
Dr. Tom Fisher
Dr. Lora Harris
Dr. Kevin Sellner

© Copyright by
Nicole Catherine Millette
2016

Acknowledgements

I would like to acknowledge the various undergraduate students that helped me with my research. Leah Rechen, Alicia Klages, and Greg Remesch all volunteered their time to help me during different winters set up my numerous field experiments. Alison Aceves (REU) performed first laboratory experiments in chapter 2 looking at the effect of ammonium and light on *Heterocapsa rotundata* community grazing coefficients. Gabby King (REU) performed the *Eurytemora carolleeae* survival and grazing experiments in chapter 3. Catherine Fitzgerald, Alison Weigel, Lindy Fine, and Jacqueline Tay helped me with my experimental set up and breakdown on occasion during the past five years. I would like to give a special acknowledgement to Dr. Diane Stoecker, who served as my adviser for the first 2.5 years of my PhD studies. After Dr. Pierson became my adviser, Dr. Stoecker allowed me to still use her laboratory space and materials and maintained an unofficial co-advisor position. I would like to thank the Maryland Department of Natural Resources for use the Bill Burton Fishing Pier for sampling, without their permission my research would not have been possible. My numerous funding sources include support from Maryland Sea Grant under award 07523941 from the National Oceanic and Atmospheric Administration, U.S. Department of Commerce, the Maryland Sea Grant NSF REU program grant OCE-1262374, two years of a Horn Point Laboratory Fellowship, and two Izaak Walton League Scholarships. Equipment for and maintenance of BD Accuri C6 flow cytometer and Zeiss epifluorescence microscope used in chapter 3 was paid for by NSF grant DBI-1318455.

Table of Contents

List of Tables	v
List of Figures.....	viii
Chapter 1: Introduction	1
References.....	5
Tables and Figures.....	7
Chapter 2: Top-down control of micro- and mesozooplankton on winter dinoflagellate blooms of <i>Heterocapsa rotundata</i>	12
Introduction.....	12
Methods.....	14
Results	20
Discussion	23
References.....	29
Tables and Figures.....	33
Chapter 3: Mixotrophy in <i>Heterocapsa rotundata</i>: a mechanism for dominating the winter phytoplankton	39
Introduction.....	39
Methods.....	41
Results	47
Discussion	50
Reference	55
Tables and Figures.....	59
Chapter 4: Impact of winter temperature and <i>Heterocapsa rotundata</i> abundance on the production and survival of winter <i>Eurytemora carolleeae</i> eggs and nauplii.....	70
Introduction.....	70
Methods.....	73
Results	76
Discussion	78
Reference	83
Tables and Figures.....	85

Chapter 5: Impact of winter water temperature on timing of peak spring <i>Eurytemora carolleeae</i> abundances and implications for anadromous fish larvae survival	92
Future Research	128
Appendix.....	132
Chapter 2	132
Chapter 3	142
Chapter 5	153
Figure D.1	158

List of Tables

Table 1.1: Average temperature (°C), salinity, ammonium (μM), nitrate + nitrite (μM), phosphate (μM), μg chlorophyll *a* L^{-1} , *H. rotundata* mL^{-1} , and copepod (*E. carolleae* + *Acartia tonsa*) L^{-1} for 5 different winters. Eight samples were collected from 1/23/2012-3/13/2012, twelve samples were collected from 12/23/2012-3/10/2013, eleven samples were collected from 12/20/2013-3/10/2014 and 12/29/2014-3/9/2015, and thirty-two samples were collected from 12/30/2015-3/18/2016. Nutrient samples were not collected in winter 2012 and samples for chlorophyll *a* concentration and copepod abundance was not collected in winter 2016. Error = SE.

Table 2.1: Average percentage (\pm SD) of the total $>10\mu\text{m}$ phytoflagellate community that *H. rotundata*, cryptophytes, *P. minimum*, and *H. triquetra* accounted for in winter of 2013 and 2014.

Table 3.1. Laboratory Experiment 1-Results of two-way ANOVA with replication for community grazing coefficient experiments. Dependent variable is *H. rotundata* community grazing coefficient (d-1) on bacteria. Data are shown in Figure 3.1.

Table 3.2. Laboratory Experiment 2-*Heterocapsa rotundata* ingestion rates (I, bacteria *H. rotundata*⁻¹ hr⁻¹), cellular chlorophyll *a* concentration (Chl *a*, pg chlorophyll *a* *H. rotundata*⁻¹), population growth rate (μ , d⁻¹), cellular carbon concentration (pg carbon *H. rotundata*⁻¹), and cellular carbon:chlorophyll *a* at the different irradiance levels (PAR, $\mu\text{mol photons m}^{-2} \text{s}^{-1}$) for each treatment. The average (\pm SE) of each factor in each treatment is given.

Table 3.3. Temperature (°C), salinity, NH_4^+ ($\mu\text{M-N}$), $\text{NO}_3^- + \text{NO}_2^-$ (NO_x) ($\mu\text{M-N}$), PO_4^{3-} ($\mu\text{M-P}$), $\text{NH}_4^+ + \text{NO}_x : \text{PO}_4^{3-}$ (N:P), Irradiance at 0900 h (PAR) ($\mu\text{mol photons sec}^{-1} \text{m}^{-2}$), and day-length (hour:minute) in the Choptank River each day an experiment was set-up between 1/27/2016 and 3/18/2016.

Table 3.4. Linear regression analysis of *H. rotundata* bacterial ingestion rates collected in the Choptank River during the 2016 winter compared to ammonium ($\mu\text{M-N}$), nitrate + nitrite ($\mu\text{M-N}$), and phosphate ($\mu\text{M-P}$) concentrations and N:P. All r^2 were non-significant.

Table 4.1: Comparison of calculated and experimentally tested *E. carolleae* egg production rate (eggs female⁻¹ day⁻¹ \pm SE) at different *H. rotundata* abundances (cells ml⁻¹) in the control treatment and experimental treatment for five different weeks. *H. rotundata* abundance refers to their abundance at the start of the experiment and temperature (°C) is the temperature of the water the day the copepods and seawater were collected and experiments were set up. Calculated egg production rates were based on Lloyd et al. 2013 and Devreker et al. 2012 equations using water temperature. P-value compares the egg production rate in the control treatment to the experimental treatment each week.

Table 4.2. Average species-specific ingestion rates ($\mu\text{g C ind}^{-1} \text{d}^{-1} \pm \text{SE}$) of copepod nauplii measured in different studies. All of the studies used the Frost (1972) equations to calculate ingestion rates except for Paffenhöfer (1971), and all reported data on a range of prey items or reported multiple measurements on the same prey. Ingestion rates from other studies were calculated or converted to standardize units.

Table 5.1. The name of the stations where temperature ($^{\circ}\text{C}$) and discharge ($\text{m}^3 \text{sec}^{-1}$) data was collected in each system, number of years we had data for in each system, and a list of the years we data.

Table 5.2. The different simulations run in the temperature-dependent developmental model. Location refers to which system's (Choptank River, Head of Chesapeake Bay, or Patuxent River) the climatological daily averages of winter water temperature ($^{\circ}\text{C}$) were used (See Figure 5.2). Month altered refers to the specific month in which temperature from the climatological daily average every day was increased or decreased by 3°C .

Table 5.3. Results of Lilliefors normality test for untransformed and \log_{10} transformed YOY recruitment indices for Striped Bass and White Perch in the Choptank River, Head of Chesapeake Bay, and Patuxent River. Bold values indicate data were not normally distributed ($P < 0.05$).

Table 5.4. Results of multiple linear regression analysis, showing tests with the highest significant r^2 value. Specific factors refer to monthly averages (Jan., Feb., Mar.) of temperature and discharge.

Table 5.5. The average ($\pm \text{SE}$) generation time (d^{-1}) of *E. carolleae* that were hatched each day in winter for all the model simulations (Table 5.2). The p-value shows the result of a paired t-test comparing the *E. carolleae* generation time when temperature was increased by 3°C to when it was decreased by 3°C in each simulation.

Table A.1. The growth (μ, d^{-1}) of and grazing (g, d^{-1}) on chlorophyll *a*, *H. rotundata*, and cryptophytes in winter 2013 and 2014 based off of linear regression analysis from dilution experiments. ($\pm \text{SE}$)

Table A.2. The growth (μ, d^{-1}) of and grazing (g, d^{-1}) on chlorophyll *a*, *H. rotundata*, and cryptophytes in winter 2013 and 2014 based off of 2-point method analysis from dilution experiments. ($\pm \text{SE}$)

Table A.3. The growth (μ, d^{-1}) of *H. rotundata* based off of 2-point method analysis from dilution experiments (Exp Growth) and weekly field abundance data collected from the Choptank River (Field Growth). ($\pm \text{SE}$)

Table B.1. Weekly grazing rates on bacteria by $\leq 10 \mu\text{m}$ nanoplankton and $\leq 200 \mu\text{m}$ microplankton in the 2015 winter. $\leq 200 \mu\text{m}$ microplankton grazing rates were the difference between bacterial growth rate in the 100% whole water treatments of $10 \mu\text{m}$

and 200 μm dilution experiments. Bold numbers are significant grazing rates, for ≤ 200 μm microplankton they also note when ≤ 200 μm microplankton grazing significantly reduced < 10 μm nanoplankton grazing.

Table D.1. The average abundance of *H. rotundata* ($\text{mL}^{-1} \pm \text{SE}$) over winter when weekly abundance data was collected compared to semi-weekly data. A two-sampled unpaired t-test was used to test whether the average winter abundance from weekly and semi-weekly sampling was statistically different ($P < 0.05$).

List of Figures

Figure 1.1: Average seasonal abundances on *H. rotundata* at twelve different CBP monitoring stations from data collected from 1985 – 2011.

Figure 1.2: Location of sampling site in Choptank River, MD on the Bill Burton Fishing Pier.

Figure 1.3: Log transformation of (a) total phytoplankton cells mL⁻¹ and (b) *H. rotundata* cells mL⁻¹ abundance data collected by the Chesapeake Bay Program during winter at station ET5.2 between 1985 and 2011.

Figure 1.4: Total winter phytoplankton abundance mL⁻¹ (total bar) and *H. rotundata* winter abundance mL⁻¹ (grey) collected by the Chesapeake Bay Program at station ET5.2 between 1985 and 2011. **H. rotundata* was the most abundant phytoplankton species.

Figure 2.1: The water temperature (°C) and salinity in the Choptank River, MD, winter of (a) 2013 and (b) 2014. The ammonium, nitrate + nitrite, and phosphate concentration in Choptank River, MD, winter of (c) 2013 and (d) 2014.

Figure 2.2: Estimated carbon content of total phytoplankton based on chlorophyll *a*, *Heterocapsa rotundata*, and cryptophytes in surface waters, Choptank River, MD, winters of (a) 2013 and (b) 2014. Estimate abundance of the copepod *E. carolleae* + *Acartia tonsa* and microzooplankton in surface waters, Choptank River, MD, winters of (c) 2013 and (d) 2014.

Figure 2.3: Comparison of the abundance of phytoplankton species (cells mL⁻¹) to the percent of standing stock of that species removed by copepods and microzooplankton ingestion. (a) *Heterocapsa rotundata* 2013; (b) *Heterocapsa rotundata* 2014; (c) cryptophytes 2013; and (d) cryptophytes 2014. Note difference in right y-axis in graph b. Dates given as mm/dd/yy.

Figure 2.4: Comparison of the estimated amount of gross carbon produced per day to the estimated amount of carbon removed by copepod consumption and microzooplankton consumption of *Heterocapsa rotundata* and cryptophytes in the surface Choptank River, MD, winters of (a) 2013 and (b) 2014.

Figure 3.1. Location of sampling site in Choptank River, MD on the Bill Burton Fishing Pier.

Figure 3.2. Laboratory Experiment 1 - *Heterocapsa rotundata* community grazing coefficient g (d⁻¹) at different irradiance levels ($\mu\text{mol photons m}^{-2} \text{s}^{-1}$) for three different ammonium concentrations (μM). Bars indicate SE.

Figure 3.3. Laboratory Experiment 2 - *Heterocapsa rotundata* ingestion rates (bacteria cell⁻¹ hr⁻¹) at different irradiance levels ($\mu\text{mol photons m}^{-2} \text{s}^{-1}$).

Figure 3.4. Variation of *H. rotundata*'s cellular chlorophyll *a* concentration (pg Chl. *a* cell⁻¹) (a), carbon concentration (pg carbon cell⁻¹) (b), and C:Chl ratio (c) at different irradiance levels. Filled squares are the initial values of the *H. rotundata* culture and the open squares are experimental values after 48 hr at treatment irradiance levels. Bars = SE for initial values.

Figure 3.5. Ingestion rates of *H. rotundata* (bacteria hr⁻¹) collected from the Choptank River in winter 2016 (□) and in culture (●) at different irradiance levels (μmol photons m⁻² s⁻¹) with a log functional response curve. Grey area denotes 95% confidence intervals.

Figure 3.6. The clearance rates (nL *H. rotundata*⁻¹ hr⁻¹) (a) and ingestion rates (bacteria cell⁻¹ h⁻¹) (b) of *H. rotundata* measured at various bacterial concentrations (mL⁻¹)

Figure 3.7. Estimated bacterial standing stock (open bars) and the bacteria ingested by the *H. rotundata* population (black bars) in the Choptank River during winter 2016.

Figure 4.1: Individual *E. carolleae* (a) egg production rates (eggs female⁻¹ day⁻¹) and (b) hatching success rate (%) from control (white circle) and treatment (black circle) experiments compared to *H. rotundata* abundance (cells ml⁻¹). Error bars = SE.

Figure 4.2: Individual *E. carolleae* (a) egg production rates (eggs female⁻¹ day⁻¹) and (b) hatching success rate (%) from control (white circle) and treatment (black circle) experiments compared to the *in situ* temperature (°C) when *E. carolleae* were collected. Error bars = SE.

Figure 4.3. The ingestion rates (a, μg C copepod⁻¹ day⁻¹) and clearance rates (b, ml copepod⁻¹ day⁻¹) of *E. carolleae* nauplii measured at various carbon concentrations (μg C L⁻¹) of *H. rotundata* with a type II functional response curve. Grey area denotes 95% confidence intervals.

Figure 4.4. Percent mortality of nauplii at different *H. rotundata* concentrations. Error bars refer to standard error.

Figure 4.5. Lipid storages in *Eurytemora carolleae* collected from the Choptank River in the 2014 winter. Black arrows point to lipids.

Figure 5.1. The location of the monitoring stations from which we obtained data. Temperature data was collect by NOAA at Cambridge, Solomons, and Tolchester Beach. Discharge data was collect by USGS at Greensboro, Bowie, and Conowingo. YOY indices were collected by Maryland DNR based off of seine surveys done throughout the Choptank River, Patuxent River, and head of Chesapeake Bay.

Figure 5.2. The daily water temperature (°C) for the first four months of the year in the (a) Choptank River for 14 different years, (b) head of Chesapeake Bay for 17 different

years, and (c) Patuxent River for 16 different years. The black line is the average daily water temperature for all years.

Figure 5.3. An example of the matrix for each simulation run used to calculate the daily fractional development rate and estimate the date each cohort of *E. carolleae* would reach the adult stage. The model calculated the daily fractional developmental rate using the daily temperature input into the model, and the cumulative fractional development was tracked for each cohort in its row. These daily cohorts had no abundance and only the fractional development was tracked for a given cohort. Once the cumulative development reached 1, the cohort was assumed to have reached the adult stage.

Figure 5.4. Fractional developmental rates at the climatologically averaged daily temperature (●) and when daily temperature was increased by 3 °C (●) and decreased by 3 °C (●) during (a) January for Choptank River temperature data, (b) February for Patuxent River temperature data, (c) February for Head of the Bay temperature data, and (d) March for Head of the Bay temperature data.

Figure 5.5. The day each daily *E. carolleae* cohort hatched in winter reached the C6 stage according to my developmental model. For each model simulation I adjusted the average daily temperature ± 3 °C in (a) the Choptank River during January, (b) the Patuxent River during February, (c) the head of Chesapeake Bay during February, and (d) the head of Chesapeake Bay during March.

Figure 5.5. Conceptual diagram of how variability in the winter season impacts anadromous fish recruitment later in the year. (a) In winters with above average water temperature and below average discharge, *E. carolleae* copepodite and *H. rotundata* abundance is low. Few nauplii are produced and accumulate throughout winter. In early spring there is a small increase in *E. carolleae* adult abundances, but prey concentrations are low for first feeding larvae of anadromous fish. Young of the year (YOY) recruitment in the fall will be low. (b) In winters with above average water temperature and above average discharge, *E. carolleae* copepodite and *H. rotundata* abundance is average. A higher concentration of *E. carolleae* nauplii are produced and survive throughout winter. At the same time in spring, *E. carolleae* nauplii hatched in winter reach the adult stage. This increases the concentration of prey available to fish feeding fish larvae. As a result, YOY recruitment is higher in the fall compared to warm, dry years. (c) Discharges to no appear to have any effect on anadromous fish recruitment in winters with below average water temperature. At the beginning of winter, *H. rotundata* and *E. carolleae* copepodite abundance is similar to warm, wet winters. Later in winter, a large *H. rotundata* bloom is likely to form. The combination of high *H. rotundata* abundance and decreased developmental rates caused by low temperatures, allows *E. carolleae* nauplii abundances to accumulate over winter. Later in spring, all *E. carolleae* nauplii hatched in winter reach the adult stage over a short period of time. This causes a large, distinct peak in *E. carolleae* abundances at the same time first fish larvae of anadromous fish start feeding. As a result, YOY recruitment in the fall is likely to be very high.

Figure A.1. The ingestion rates (a, $\mu\text{g C copepod}^{-1} \text{ day}^{-1}$) and clearance rates (b, $\text{ml copepod}^{-1} \text{ day}^{-1}$) of *E. carolleeae* copepods measured at various *in situ* carbon concentrations ($\mu\text{g C L}^{-1}$) of *H. rotundata* with a type II functional response curve. Grey area denotes 95% confidence intervals.

Figure B.1. Weekly growth rates of bacteria (d^{-1}) in experimental bottles with 100% 10 μm and 200 μm filtered water during the 2015 winter. Error bars = standard error.

Figure B.2. The uptake rate of microspheres per *H. rotundata* over 120 minutes.

Figure B.3. *Heterocapsa rotundata* community grazing coefficient g (d^{-1}) at different irradiance levels ($\mu\text{mol photons m}^{-2} \text{ s}^{-1}$) for three different ammonium concentrations (μM) during (a) 0-24 hr and (b) 48-72 hr. Bars indicate SE.

Figure B.4. A comparison of a log function (black), power function (blue), and linear regression (red) fitted to ingestion rates of *H. rotundata* (bacteria hr^{-1}) at different irradiance levels. Color shaded areas denotes 95% confidence intervals.

Figure C.1. Copepodite abundances of *E. carolleeae* and *A. tonsa* in the Choptank River for winter and spring 2014 (12/30/2013-4/14/2014) and 2015 (12/29/2014-4/6/2015).

Figure D.1. A comparison of variability in winter *Heterocapsa rotundata* abundance (mL^{-1}) from weekly sampling compared to semi-weekly sampling in the Choptank River for (a) 2012, (b) 2012-2013, (c) 2013-2014, (d) 2014-2015, and (e) 2015-2016.

Chapter 1: Introduction

Heterocapsa is a genus that contains numerous bloom forming and toxic species of dinoflagellates (Salas et al. 2014). One particular species, *Heterocapsa rotundata* (Lohmann) Loeblich (Hansen, 1995), is ubiquitous and occasionally forms large blooms. *H. rotundata* has been reported in a range of environments all over the world including, Chesapeake Bay, USA (Millette et al. 2015), Masan Bay, South Korea (Seong et al. 2006), Manori Creek and Manim Bay, India (Shahi et al. 2015), Baltic Sea, Germany (Jaschinaski et al. 2015), and Kangaroo Island, Australia (Balzano et al. 2015). Where ever it is found, *H. rotundata* tends to either dominate or be a prominent part of the phytoplankton community for at least part of the year (Seong et al. 2006; Balzano et al. 2015; Millette et al. 2015a). For such a commonly occurring, global species, there is a lack of research specifically focused on the ecology of *H. rotundata*.

H. rotundata commonly appears in scientific literature as a prey item used to feed cultures of heterotrophic organisms for experimental studies. Some examples include *H. rotundata* used as prey to feed heterotrophic protists that were in turn fed to copepods to test the effect of fatty acid composition of prey on copepods feeding and reproduction (Broglio et al. 2003), to test how food uptake was effected by a mixotroph that released toxins (Skovgaard and Hansen 2003), to study a microzooplankton's feeding response to different prey types (Jakobsen et al. 2006), and to test circadian cycles of growth and feeding of heterotrophic protists (Jakobsen and Strom 2004). For all of these experiments the research was focused on the predators and not *H. rotundata*, as a result, very few studies have published data on *H. rotundata*.

A majority of the data available on *H. rotundata* comes from research done in the Potomac River (Cohen 1985) and the Patuxent River (Sellner et al. 1991) during winter blooms. The formation of winter *H. rotundata* blooms have been associated with a stratified water column caused by high freshwater flow and low temperatures (Cohen 1985; Sellner et al. 1991). A bloom tends to form around the transition zone between the shallow, up river area and deep, down river area (Cohen 1985; Sellner et al. 1991).

H. rotundata have fast swimming speeds, up to 15 m in 12 h (Thronsdon 1973), and have been observed to use vertical migration to maintain their location (Cohen 1985). During the day, *H. rotundata* is concentrated in the surface waters headed downstream, while in the evening, *H. rotundata* migrates down to bottom waters headed upstream (Cohen 1985). It has been suggested that *H. rotundata* may have a resting stage that could seed a winter bloom (Cohen 1985), but no further research has been done to confirm a resting stage of *H. rotundata*. The decline of winter blooms in the Patuxent River has been associated with an increase in grazing by copepods (Sellner et al. 1991).

Monitoring data from the Chesapeake Bay Program collected between 1985 to 2011 shows that *H. rotundata* abundances are highest in the winter in the northern Chesapeake Bay and tributaries (Figure 1.1). I downloaded phytoplankton abundance data for twelve monitoring stations in the Chesapeake Bay and averaged all the data collected over twenty-six years by season. *Heterocapsa rotundata* abundances were highest in the winter in the oligohaline region of Chesapeake Bay and the Chester, Choptank, and Patuxent River, but never existed above background abundances in the polyhaline region (Figure 1.1). This aligns with that is known about *H. rotundata* blooms,

they are rarely found above a salinity of 14, despite the individuals having a salinity tolerance higher than 14 (Cohen 1985; Sellner et al. 1991).

All of my field work was done at the Bill Burton fishing pier on the Choptank River in Cambridge, MD USA (38°34'24" N 76°4'6" W), a tributary that feeds into the mesohaline section of the Chesapeake Bay (Figure 1.2). This location was chosen because of its proximity to Horn Point Laboratory, the ability to sample in the middle of the Choptank River without a boat, and the high likelihood of a *H. rotundata* bloom forming. The Chesapeake Bay Program monitoring station ET5.2 is located near the fishing pier and has recorded high winter *H. rotundata* abundances in this section of the Choptank River.

Monitoring data available for station ET5.2 includes historical winter phytoplankton abundances from 1985 – 2011. From 1985 – 1987 water samples to estimate phytoplankton abundances were collected in the winter between January and March but since 1988 winter phytoplankton samples were only collected in March. Typically, one phytoplankton sample is collected in early to middle March each year to represent the entire winter. Despite the lack of high frequency sampling, the historical winter phytoplankton data from ET5.2 provides support for this location as a sample site to study *H. rotundata*. Since 1985 there has been a significant increase in the abundance of total winter phytoplankton in general ($r^2 = 0.38$, $p = 0.001$, linear regression, Figure 1.3a) and winter *H. rotundata* abundance in particular ($r^2 = 0.32$, $p = 0.001$, linear regression, Figure 1.3b). Since most of these data points come from one sample collected in March, the increase in winter phytoplankton abundance could be from a shift in peak abundance to later in the winter or an increase in the abundance of the winter

phytoplankton, but I cannot discern this from available data. *H. rotundata* was the most abundant winter phytoplankton species for 14 years of the 26 years sampled in the Choptank River at this station (Figure 1.4).

At least once a week during the winter from 2012 and 2016 I collected water quality data (Table 1.1). During the five years I sampled there was a large variability in average temperature and *H. rotundata* abundance between years while nutrient concentrations were relatively stable (Table 1.1). Average salinity, chlorophyll *a* concentration, and copepod abundances were typically similar between years, with the exception of winter 2012 when all factors were lower (Table 1.1) *H. rotundata* abundance was highest in winter 2014 and lowest in winter 2012 (Table 1.1). Winter 2012 was an anomalously warm and dry winter with low chlorophyll *a* and copepod concentrations (Table 1.1).

This dissertation, titled “Ecosystem Impact of Winter Dinoflagellate Blooms in the Choptank River, MD” reports on my research designed to improve our understanding of how these blooms form and what impact they have on the winter and spring ecosystem. I used a combination of weekly field sampling and *in situ* and lab experiments to achieve this goal. My project was divided into four sections, each addressing a specific question, related to the overall goal of this project. Chapter 2 looked at the top-down controls effecting the formation of winter *H. rotundata* blooms. Chapter 3 identified environmental factors that affect *H. rotundata* ingestion rates of bacteria. Chapter 4 investigated how large winter *H. rotundata* abundances affect *Eurytemora carolleeae* (a copepod) populations. Chapter 5 described how variations in the winter environment and *H. rotundata* abundances can affect anadromous fish spring recruitment.

References

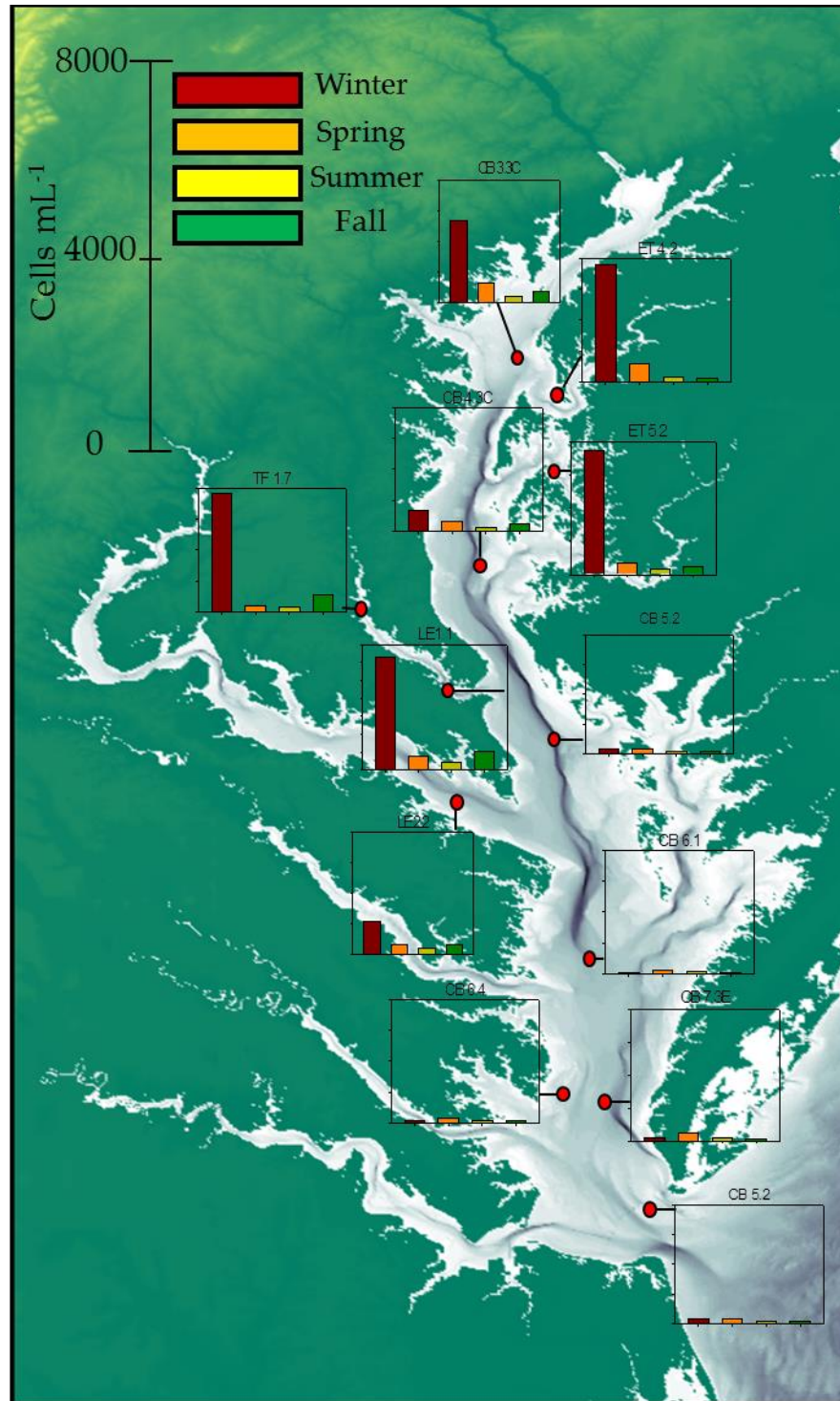
- Balzano, S., A.V. Ellis, C. Le Lan, and S.C. Leterme (2015) Seasonal changes in phytoplankton on the north-eastern shelf of Kangaroo Island (South Australia) in 2012 and 2013. *Oceanologia* 57:251-262.
- Broglio, E., S. Jonasdottir, A. Calbet, H.H. Jakobsen, and E. Saiz (2003) Effect of heterotrophic versus autotrophic food on feeding and reproduction of the calanoid copepod *Acartia tonsa*: relationship with prey fatty acid composition. *Aquat Microb Ecol* 31:267-278.
- Cohen, R. R. H. (1985) Physical processes and the ecology of a winter dinoflagellate bloom of *Katodinium rotundatum*. *Mar Ecol Prog Ser* 26:135-144.
- Hansen, G. (1995) Analysis of the thecal plate pattern in the dinoflagellate *Heterocapsa rotundata* (Lohmann) comb. nov. (= *Katodinium rotundatum* (Lohmann) Loeblich). *Phycologia* 34:166-170.
- Jakobsen, H. H. and S.L. Strom (2004) Circadian cycles in growth and feeding rates of heterotrophic protist plankton. *Limnol Oceanogr* 49:1915-1922.
- Jakobsen, H. H., L.M. Everett, and S.L. Strom (2006) Hydromechanical signaling between the ciliate *Mesodinium pulex* and motile protist prey. *Aquat Microb Ecol* 44:197-206.
- Jaschinski, S., S. Flöder, T. Petenati, and G. Göbel (2015) Effects of nitrogen concentration on the taxonomic and functional structure of phytoplankton communities in the Western Baltic Sea and implications for the European water framework directive. *Hydrobiologia* 745:201-210.
- Millette, N.C., J.J. Pierson, and D.K. Stoecker (2015) Top-down control of micro- and mesozooplankton on winter dinoflagellate blooms of *Heterocapsa rotundata*. *Aquat Microb Ecol* 76:15-25.
- Salas, R., U. Tillmann, and S. Kavanagh (2014) Morphological and molecular characterization of the small armoured dinoflagellate *Heterocapsa minima* (Peridiniales, Dinophyceae). *Europ J Phycol* 49:413-428.
- Sellner, K. G., R.V. Lacouture, S.J. Cibik, A. Brindley, and S.G. Brownlee (1991) Importance of a winter dinoflagellate-microflagellate bloom in the Patuxent River estuary. *Estuar Coast Shelf S* 32:27-42.
- Seong, K.A., H.J. Jeong, S. Kim, G.H. Kim, and J.H. Kang (2006) Bacterivory by co-occurring red-tide algae, heterotrophic nanoflagellates, and ciliates. *Mar Ecol Prog Ser* 322:85-97.

Shahi, N., A. Godhe, S.K. Mallik, K. Härnström, and B.B. Nayak (2015) The relationship between variation of phytoplankton species composition and physico-chemical parameters in northern coastal waters of Mumbai, India. *Indian Journal of Geo-Marine Sciences* 44.

Skovgaard, A. and P.J Hansen (2003) Food uptake in the harmful alga *Prymnesium parvum* mediated by excreted toxins. *Limnol Oceanogr* 48:1161-1166.

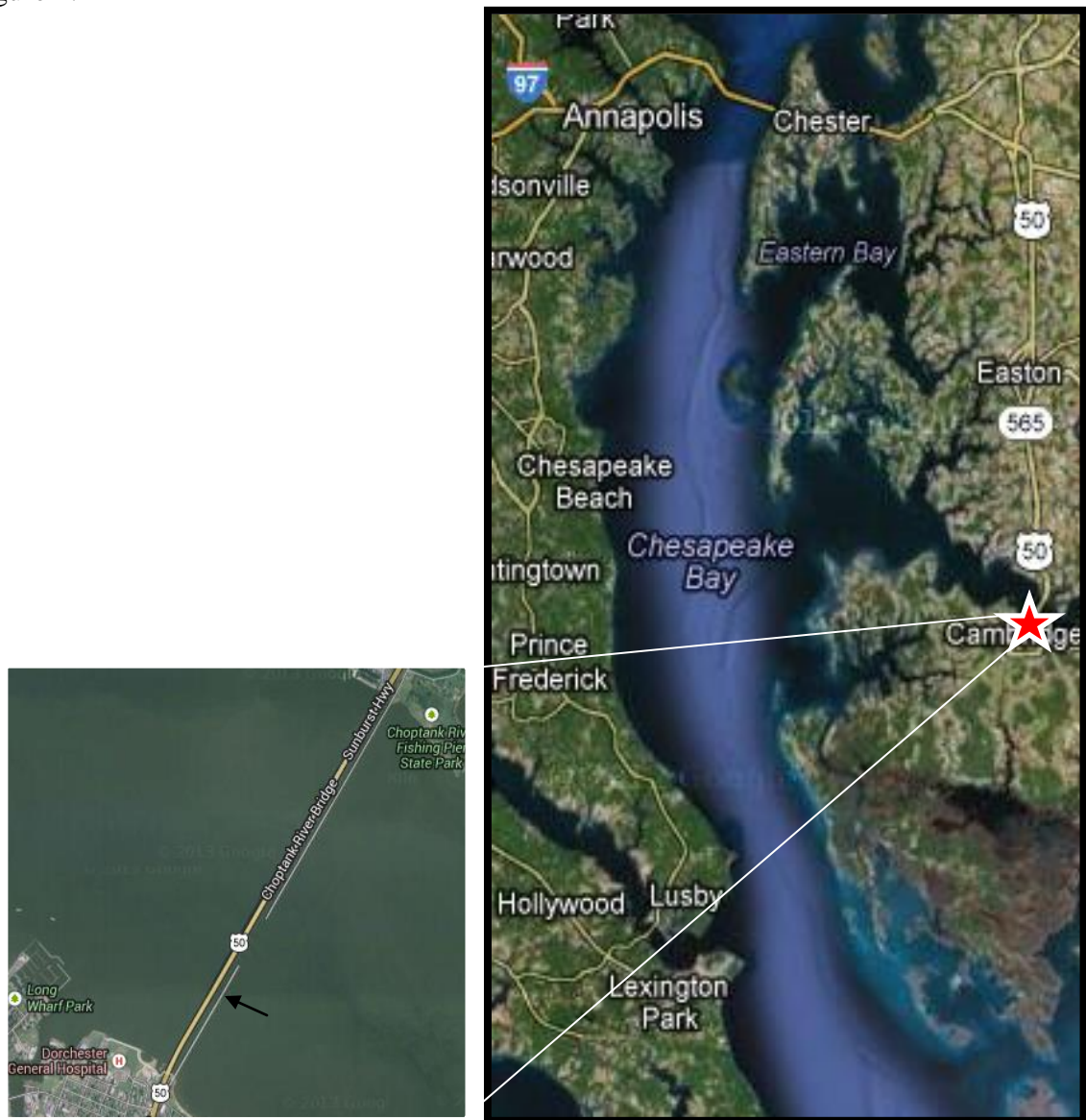
Thronsen, J (1973) Motility in some marine nanoplankton flagellates. *Norw J Zool* 21:193-200.

Tables and Figures
Figure 1.1



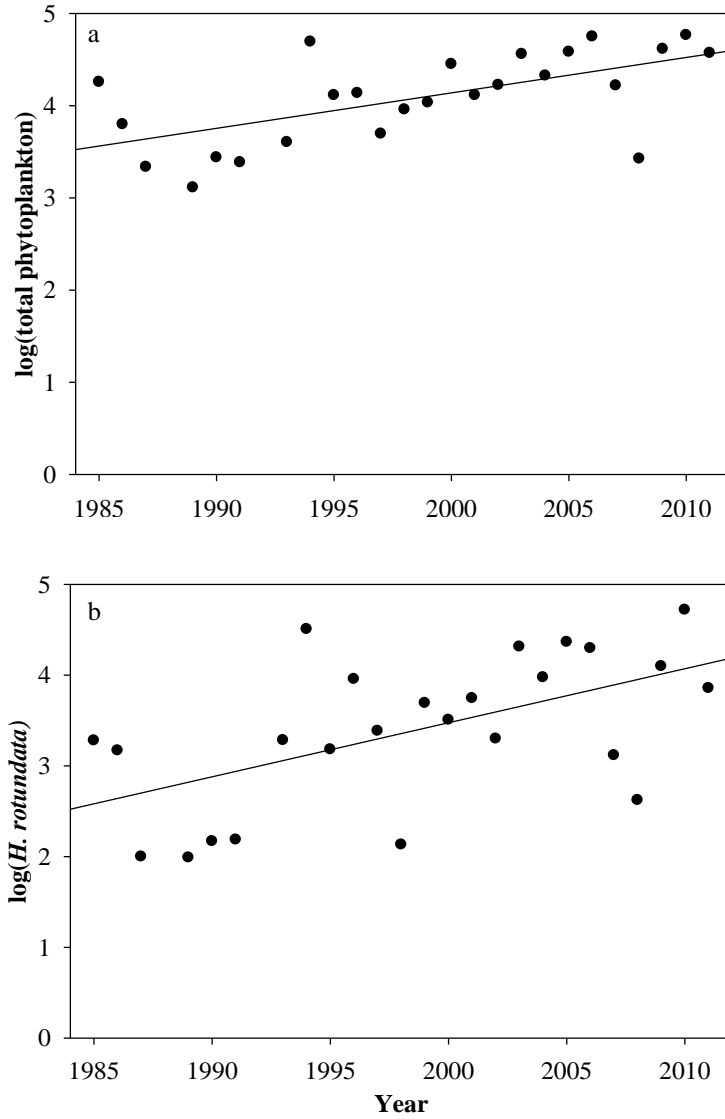
Average seasonal abundances on *H. rotundata* at twelve different CBP monitoring stations from data collected from 1985 – 2011.

Figure 1.2



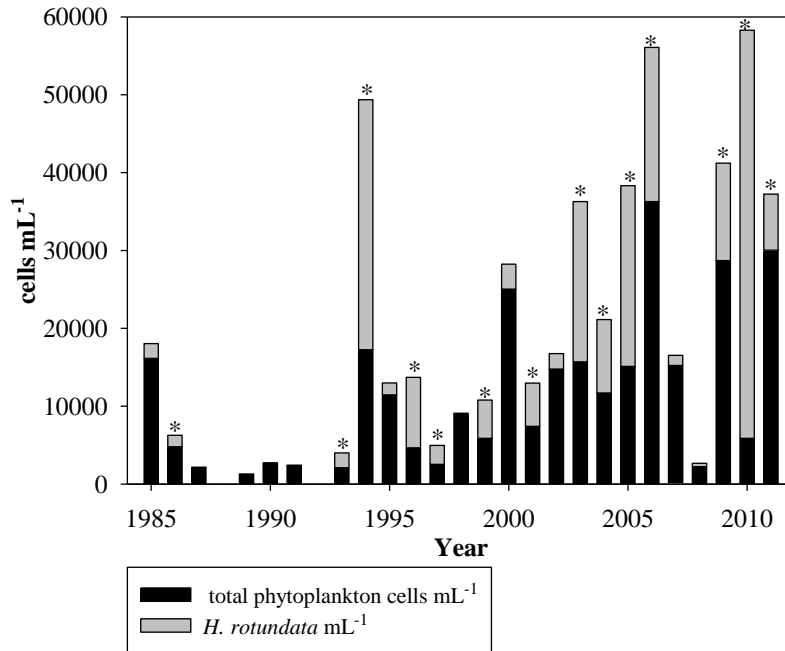
Location of sampling site in Choptank River, MD on the Bill Burton Fishing Pier.

Figure 1.3



Log transformation of (a) total phytoplankton cells mL^{-1} and (b) *H. rotundata* cells mL^{-1} abundance data collected by the Chesapeake Bay Program during winter at station ET5.2 between 1985 and 2011.

Figure 1.4



Total winter phytoplankton abundance mL⁻¹ (total bar) and *H. rotundata* winter abundance mL⁻¹ (grey) collected by the Chesapeake Bay Program at station ET5.2 between 1985 and 2011. **H. rotundata* was the most abundant phytoplankton species.

Table 1.1

Start Date	End Date	°C	Salinity	NH ₄ ⁺ μM	NO _x μM	PO ₄ ³⁻ μM	μg Chl <i>a</i> L ⁻¹	<i>H. rotundata</i> mL ⁻¹	Copepod L ⁻¹
1/23/2012	3/13/2012	5.8 ± 0.7	5.0 ± 0.4	-	-	-	4.4 ± 0.4	26 ± 6	2 ± 1
12/23/2012	3/10/2013	4.2 ± 0.4	10.1 ± 0.3	2.3 ± 0.4	39.9 ± 4.5	0.2 ± 0.1	20.5 ± 1.9	1332 ± 292	10 ± 2
12/30/2013	3/10/2014	3.0 ± 0.9	9.2 ± 2.9	4.6 ± 1.5	55.3 ± 17.5	0.2 ± 0.1	27.3 ± 6.7	7236 ± 2288	8 ± 2
12/29/2014	3/9/2015	1.6 ± 0.7	10.0 ± 0.4	5.7 ± 2.0	45.9 ± 9.0	0.8 ± 0.3	23.6 ± 2.9	3904 ± 878	9 ± 1
12/30/2015	3/18/2016	5.0 ± 0.6	11.2 ± 0.3	2.6 ± 0.2	27.4 ± 2.8	0.2 ± 0.02	-	2557 ± 621	-

Average temperature (°C), salinity, ammonium (μM), nitrate + nitrite (μM), phosphate (μM), μg chlorophyll *a* L⁻¹, *H. rotundata* mL⁻¹, and copepod (*E. carolleae* + *Acartia tonsa*) L⁻¹ for 5 different winters. Eight samples were collected from 1/23/2012-3/13/2012, twelve samples were collected from 12/23/2012-3/10/2013, eleven samples were collected from 12/20/2013-3/10/2014 and 12/29/2014-3/9/2015, and thirty-two samples were collected from 12/30/2015-3/18/2016. Nutrient samples were not collected in winter 2012 and samples for chlorophyll *a* concentration and copepod abundance was not collected in winter 2016. Error = SE.

Chapter 2: Top-down control of micro- and mesozooplankton on winter dinoflagellate blooms of *Heterocapsa rotundata*

Introduction

In estuaries, dinoflagellates are known to form winter blooms (Marshall et al. 2005; Litaker et al. 2002a; Sellner et al. 1991) but winter is generally under-sampled and the aquatic food web-dynamics during this time are poorly understood. Winter productivity is often assumed to be low compared with the remainder of the year, and this period is not often the focus of research. However, Litaker et al. (2002a) and Sellner et al. (1991) have suggested that winter blooms of dinoflagellate species, *Heterocapsa triquetra* and *Heterocapsa rotundata*, respectively, can account for ~50% of annual phytoplankton carbon production within an estuary, suggesting an important role for winter blooms in the annual productivity of estuarine systems.

Past research on winter dinoflagellate blooms on the east coast of the United States has focused on the physical changes to the environment that initiate blooms (Cohen 1983, Sellner et al. 1991, Litaker et al. 2002b). High rainfall and increased river flow have been shown to trigger such blooms by creating a stratified water column (Cohen 1985) and causing a large influx of nutrients (Litaker et al. 2002b). However, few studies have addressed the influence of zooplankton grazers in the formation and maintenance of winter dinoflagellate blooms. Studies have explored the role of grazing on the decline of a winter dinoflagellate blooms. Sellner et al. (1991) calculated that the copepod, *Eurytemora carolleeae* (*cf. E. affinis*, Alekseev & Souissi 2011), removed 67% of the daily bloom biomass through grazing at the height of a *H. rotundata* bloom in the Patuxent River, a tributary of Chesapeake Bay, MD, USA and postulated that grazing

controlled the dissipation of the bloom. Litaker et al. (2002a) estimated that at peak winter abundance, the copepod *Acartia tonsa* removed only ~1% of *H. triquetra* standing stock during a bloom in the Newport Estuary, NC, USA. However in both these studies, the initiation of the bloom was attributed to bottom-up forcing based on river flow.

In the past decade the role of reduced grazing pressure in phytoplankton bloom formation, specifically from microzooplankton, has gained acceptance (Irigoiien et al. 2005, Stoecker et al. 2008). Irigoien et al. (2005) suggests that physical or chemical perturbations can breakdown strong predator – prey links in ‘mature systems’ to allow a ‘loophole’ that phytoplankton can exploit to form a bloom. Stoecker et al. (2008) suggested that in the Chesapeake Bay, eutrophication caused by land run-off can result in trophic cascades that produce negative feedback to microzooplankton grazing pressure and a ‘window of opportunity’ opens that allows small dinoflagellates to bloom.

Winters with high rainfall create optimum conditions for blooms (Cohen 1983, Litaker et al. 2002a, Sellner et al. 1991), and I focused my research on understanding how grazers impact and/or control winter dinoflagellate blooms. The removal of dinoflagellates by grazing can serve as an important top-down control on winter blooms. Therefore, I hypothesized that a reduction in zooplankton grazing rates is required for an increase in *H. rotundata* abundance. Reduced grazing pressure allows a bloom to form and increased grazing pressure leads to the collapse of the bloom (Irigorien et al. 2005). To test this hypothesis, I measured phytoflagellate, microzooplankton, and mesozooplankton abundances and the grazing rates by both zooplankton groups on the dominant microplankton in winters of 2012-2013 and 2013-2014 in the Choptank River, a tributary of Chesapeake Bay. Winters 2012-2013 and 2013-2014 will be referred to as

winter 2013 and winter 2014, respectively. I also compared the environmental conditions from the two years to confirm that relaxation in top-down controls was important to winter bloom formation, and that winter bloom formation was not driven by environmental conditions.

Methods

Setting and Sampling: I collected water weekly from December 23, 2012 – March 10, 2013 and December 30, 2013 – March 10, 2014 from a fishing pier on the Choptank River in Cambridge, MD USA (38°34'24" N 76°4'6" W). The Choptank River is a tributary that feeds into the mesohaline section of the Chesapeake Bay. Each week I collected 30 - 40 L of surface water with a bucket and immediately filtered it through 200 µm mesh to remove larger plankton. I then conducted two vertical net tows to collect mesozooplankton samples with a plankton ring net fitted with 200 µm mesh. The sample from one of these tows was immediately preserved in 4% formalin and the sample from the other tow was decanted into glass jars and kept alive to be sorted for copepods used in grazing experiments once I returned to the lab. Temperature and salinity were measured with a hand-held YSI-30 conductivity and temperature meter immediately after the bucket was retrieved. Samples for nutrients (dissolved nitrate + nitrite, ammonium, and phosphorous) were filtered through a Whatman's 0.45 µm nylon sieve with glass microfiber (model number: 4552) and immediately frozen for subsequent analysis at Horn Point Laboratory Analytical Services. Water and plankton for grazing and primary production experiments were transported to UMCES Horn Point Laboratory in Cambridge, MD and maintained in an incubator at ambient water temperature until all experiments were set up, always within 3 hours of sample collection.

Primary Production: Each week I incubated six 30 ml glass vials of unfiltered seawater (3 light, 3 dark) for 24 h to estimate the primary production rate using the oxygen evolution method (Howarth & Michaels 2000), similar to recent winter research in the Chesapeake Bay (Lee et al. 2012)

The vials were placed in mesh bags that allowed in 55% of natural light, and incubated in floats in a small, protected cove of the Choptank River. Gross primary production was quantified from the change in dissolved O₂ in the light and dark bottles. Samples were analyzed with a mass spectrometer to measure O₂ and Ar ratio; argon is an unreactive noble gas, and a change in the dissolved O₂:Ar ratio between the initial and final samples is assumed to be the result of changes in O₂ and not Ar (Kana et al. 1994). The coefficient of variation for the membrane inlet mass spectrometer is <0.5% for O₂ and <0.05% for O₂/Ar ratio (Kana et al. 1994). I converted the change in O₂ concentration to carbon, assuming that for every mole of carbon fixed, one mole of O₂ is produced (Howarth & Michaels 2000). I then converted the change in carbon concentration (μM C) over time to change in biomass per unit volume over time to estimate primary production (g C m⁻³ day⁻¹) at the surface at my sample site.

Microzooplankton grazing- Dilution experiments, as described by Landry & Hassett (1982), were used to measure community grazing coefficients (day⁻¹) for microzooplankton on phytoflagellates and intrinsic phytoflagellate growth rate (day⁻¹). The filtered water for the dilution experiments was made using a 0.2 μm pleated filter in a capsule from Life Sciences (model number: FW3846). Triplicate 1 L bottles were used for each of four treatments, 100%, 20%, 10%, and 5% whole water. These dilution treatments were chosen because the higher the proportion of filtered water, the greater the

decoupling between microzooplankton grazing and phytoflagellate growth, due to the reduced microzooplankton grazing pressure in diluted water (Landry & Hasset 1982).

Each week I estimated the microzooplankton grazing coefficient on phytoplankton biomass and on the dominant phytoflagellate species/groups, *Heterocapsa rotundata* (a dinoflagellate) and cryptophytes. Dominant phytoflagellates were defined as $\geq 25\%$ of the $>10\mu\text{m}$ phytoflagellate community. *H. rotundata*, a dominant species, and cryptophytes, a dominant group, were the only ones to fit this description (Table 1). Diatoms were present at abundances between 250 – 3500 cells mL^{-1} (data not shown) but were not included in analysis because of the focus on phytoflagellates.

As a proxy for phytoplankton biomass, I measured chlorophyll *a* from all the dilution bottles at the start and end of my experiments. Three samples from each initial treatment bottle and one sample from each triplicate final bottle, whole sea water and dilutions, were filtered onto 25mm GF/F glassfiber filters, extracted in 90% acetone for 24 hours in the freezer (Arar & Collins 1997). The chlorophyll fluorescence of the acetone extract was measured with a Turner Designs AU-10 fluorometer. To determine $>10\mu\text{m}$ phytoflagellate species and abundances, I preserved 10 to 12 mL from each bottle in acid Lugol's solution. Samples were counted and identified with a Nikon Eclipse E800 microscope at 20x magnification on a Sedgewick rafter slide (Sherr & Sherr 1993). A minimum of 300 cells were counted per sample. Chlorophyll *a* concentrations and abundances of phytoflagellates in the initial 100% whole water bottles were used to estimate *in situ* concentrations in the surface water.

I used the equation for exponential growth to estimate the apparent growth rate of the phytoplankton biomass, *H. rotundata*, and cryptophytes at each dilution (Landry &

Hasset 1982). In order to eliminate the potential to have non-linear regression curves in the dilution experiments caused by non-limiting concentrations of prey, I used the 2-point dilution method to estimate the microzooplankton community grazing coefficient (g) and the apparent phytoplankton growth rate (μ) (Worden and Binder 2003). The estimated phytoflagellate growth rate at 5% whole water was used to calculate μ and the difference between the estimated phytoflagellate growth rate at 100% whole water and 5% whole water was used to calculate g . The 2-point dilution method provides a conservative estimation of μ and g (Worden and Binder 2003). I calculated the ingestion rate of *H. rotundata* and cryptophytes by the microzooplankton community according to Strom et al. (2001).

Chlorophyll *a* concentrations and species abundances were both converted to carbon for comparison. Living algal carbon ($\mu\text{g L}^{-1}$) was estimated using the conversion of $50 \times \text{chlorophyll } a$ (Strickland 1965). The average cell volume for individual species was determined by measuring length and diameter of 30 individual organisms using a calibrated ocular micrometer, and cell volumes were estimated from the equation for a rotational ellipsoid ($\text{volume} = (\pi/6) \times (\text{diameter}^2) \times \text{height}$). The volume of an individual *H. rotundata* and cryptophyte cell was converted to carbon using the equation for dinoflagellates and the equation for other plankton excluding diatoms, respectively (Menden-Deuer & Lessard 2000).

Mesozooplankton Grazing: To estimate mesozooplankton grazing, I used prey removal experiments. Two triplicate sets of 1L containers with 200 μm filtered water were incubated along with the dilutions experiments. One set was enriched with 10 to 20 copepods from the vertical tows and one set was without copepods. I used the copepod *E.*

carolleeae because it is the dominant species in the estuary in winter (Kimmel et al. 2006) and also dominant in my mesozooplankton samples. Another copepod, *Acartia tonsa*, was present early in the time series in both years and a few individuals may have inadvertently been included in my experiments despite my best efforts to only pick *E. carolleeae*. I chose larger copepods (a mixture of copepodites and adults) with both of their antennae intact for each experiment.

I calculated the change in chlorophyll *a* biomass and abundances of *H. rotundata* and cryptophytes over the duration of the experiments (24 hours) for each of the bottles in the experiment each week. At the end of each experiment, the live copepods in each bottle were counted and this number was used to calculate the per capita clearance (ml copepod⁻¹ d⁻¹) and ingestion rates (cells copepod⁻¹ day⁻¹) according to calculations from Frost (1972). The percent of prey standing stock removed by copepods (SS_r, day⁻¹) in the surface water was estimated as:

$$SS_r = ((I * A_c) / A_p) * 100$$

where *I* is the ingestion rate of an individual copepod, *A_c* is the abundance of copepods in the water column (copepods L⁻¹), and *A_p* is the abundance of the prey in the water column (cells L⁻¹).

I counted a minimum of 200 copepods from a subsample of the preserved sample to estimate *in situ* abundances. The sample was counted with a dissecting microscope at 2x magnification on a gridded petri dish. I combined *E. carolleeae* and *A. tonsa* abundances to estimate total copepod abundance, but in general *E. carolleeae* accounted for 81% of all copepods counted. There were only three weeks when *E. carolleeae* accounted for <50% of the copepod population and those weeks were at the start of the

winter seasons when copepod abundances were low (data not shown). No attempt was made to separate the different copepodite stages. In the third week of winter 2013 my sample of copepods to estimate *in situ* abundances was lost, and I estimated copepod abundance for that week as the average of copepod abundance from the two previous and two subsequent weeks (7.25 ± 4.9 copepods L^{-1} , N=4).

Most the prominent phytoflagellate prey items measuring $>10 \mu m$ were identified to the species level, including *H. rotundata*, *Heterocapsa triquetra*, and *Prorocentrum minimum*. Diatom's had low abundances and were counted as a group. Microzooplankton abundances were pooled from abundances of non-loricate ciliates, tintinnids, and heterotrophic dinoflagellates; my experiments could only estimate community grazing coefficient of microzooplankton, not grazing by individual taxa.

Data Analysis: Similar to findings in previous studies (Worden and Binder 2003; Strom and Fredrickson 2008) there was not a significant difference between my analysis of dilution experiments using the 2 point method and the standard linear regression method, based on paired t-tests, $P=0.857(\mu)$ and $P=0.952(g)$ for *H. rotundata* and $P=0.402(\mu)$ and $P=0.249(g)$ for cryptophytes. Therefore, all subsequent data manipulation was done based on the data from the 2-point method. A paired t-test was used to compare the estimated growth rate of phytoplankton (Chlorophyll *a* concentration) or growth rates of individual target phytoplankton taxa (*H. rotundata* and cryptophytes abundances) between the 100% and 5% whole water treatments. The microzooplankton community grazing coefficient was considered significantly different from zero for each experiment when $P<0.05$ for these analyses. A one sample t-test was used to determine whether copepod ingestion rates were significantly different from zero

($P < 0.05$). Any negative grazing values were changed to zero for subsequent analysis of amount or proportion of standing stocks removed by grazers (Strom et al 2001). 17 of 46 copepod grazing rates and eighteen of forty – six microzooplankton community grazing rates were changed to zero.

I used two sample equal variance t-tests to determine statistically significant differences ($P < 0.05$) between my 2 sampling years. All of my averaged values are presented \pm standard deviation throughout the results.

Results

Environmental Conditions and Standing Stocks: The average water temperature in winter 2013 ($4.2 \pm 1.4^\circ\text{C}$) was not significantly different than the average water temperature in winter 2014 ($3.0 \pm 2.0^\circ\text{C}$) (two-sample T-test, $p = 0.103$, Figure 2.1). Between weeks 5 – 7 in 2014 the water temperature was below 1.0°C and the river was ice covered (Figure 2.1). In 2013 the minimum water temperature was 1.9°C . Salinity in winter 2013 was not significantly different than in winter 2014 ($p = 0.093$), averaging 10.1 ± 1.1 in 2013 and 9.1 ± 1.4 in 2014 (Figure 2.1). There was little variation in salinity from week to week in both winters (Figure 2.1a,b).

The average nitrate + nitrite, ammonium, and phosphate concentrations were not significantly different from each other between the two winters ($P = 0.09$, $P = 0.05$, and $P = 0.93$, respectively), and concentrations ranged from 0-100 μM for nitrate + nitrite (NO_x), from 0-10 μM for ammonium (NH_4^+), and from 0-1 μM phosphate (PO_4^{3-}) in the winter (Figure 2.1c,d). The average nutrient concentrations were $39.87 \pm 15.00 \mu\text{M}$ of NO_x , $2.29 \pm 1.33 \mu\text{M}$ of NH_4^+ , and $0.18 \pm 0.21 \mu\text{M}$ of PO_4^{3-} (Figure 2.1c) in the winter of 2013. In the winter of 2014 the average nutrient concentrations were $55.27 \pm 25.66 \mu\text{M}$

of NO_x , $4.63 \pm 3.67 \mu\text{M}$ of NH_4^+ , and $0.18 \pm 0.07 \mu\text{M}$ of PO_4^{3-} (Figure 2.1d). The standard deviations for the equipment used by Analytical Services are $<0.1 \mu\text{M}$ for NO_x and PO_4^{3-} and $0.06 \mu\text{M}$ for NH_4^+ .

I defined “bloom” abundances as $>10,000 \text{ cells L}^{-1}$ for both *H. rotundata* and cryptophytes or chlorophyll *a* concentrations $>45 \mu\text{g L}^{-1}$, and using this criteria there was no winter bloom at my station in the Choptank River in the winter of 2013. Total chlorophyll *a* concentrations averaged $20.5 \pm 6.4 \mu\text{g L}^{-1}$, *H. rotundata* averaged $1,330 \pm 970 \text{ cells mL}^{-1}$, and cryptophytes averaged $2,125 \pm 1032 \text{ cells mL}^{-1}$. For all but one week (week 3) cryptophytes were the dominant group of $>10 \mu\text{m}$ phytoflagellates (Figure 2.2a). From January to the middle of March 2013, *H. rotundata* and cryptophytes accounted for an estimated 50% of the total phytoplankton carbon each week (Figure 2.2a). *H. triquetra* and *P. minimum* were only present in background concentrations (Table 2.2)

In winter 2014, a *H. rotundata* bloom occurred in the last three weeks of sampling. Total chlorophyll *a* concentrations averaged $27 \pm 21.1 \mu\text{g L}^{-1}$, *H. rotundata* averaged $7,236 \pm 7,731 \text{ cells mL}^{-1}$, and cryptophytes averaged $993 \pm 968 \text{ cells mL}^{-1}$. *H. rotundata* accounted for an estimated 54% and cryptophytes for estimated 11% of the total phytoplankton carbon (Figure 2.2b). In the last four weeks of sampling in 2014, *H. rotundata* accounted for over 80% of the estimated phytoplankton carbon (Figure 2.2b). Abundances of *H. rotundata* and cryptophytes were initially $10,431 \text{ cells mL}^{-1}$ and $3,483 \text{ cells mL}^{-1}$ respectively, but abundances of both taxa declined to $<100 \text{ cells mL}^{-1}$ by week 3 (Figure 2.2b). Starting in week 4 *H. rotundata* grew exponentially each week until they reached $19,942 \text{ cells mL}^{-1}$ in week 9 (Figure 2.2b). cryptophytes abundance grew to 1208

cells mL⁻¹ in week 9 (Figure 2.2b). In week 9, chlorophyll *a* reached 61 µg L⁻¹. Similar to 2013, *H. triquetra* and *P. minimum* were only present in background concentrations (Table 2.2).

There was no difference in the mean abundance of copepods (adults and copepodites of *E. carolleae* and *A. tonsa*) between the two years (two-sample T-test, p=0.615). Abundance averaged 10 ± 7 L⁻¹ in 2013 and 8 ± 6 L⁻¹ in 2014 (Figure 2.2d). Mean abundance of microzooplankton was $8,781 \pm 5268$ cells L⁻¹ in 2013 and $12,111 \pm 6400$ cells L⁻¹ in 2014, with no difference between the two years (two-sample t-test, p=0.187, Figure 2.2d).

Proportion of *H. rotundata* and cryptophytes Consumed: I estimated the percent of standing stock for each species that was removed by each type of grazer to quantify the impact grazers had on the phytoflagellate abundances. In winter 2013, an average of 128.1 ± 144.8 *H. rotundata* µg carbon L⁻¹ d⁻¹ and an average of 118.3 ± 146.4 cryptophytes µg carbon L⁻¹ d⁻¹ were removed by grazers (Table 2.2). An average of 66.7% of *H. rotundata*'s standing stock was removed from grazing, 30.3% by copepods and 36.4% by microzooplankton. An average of 35.5% of cryptophyte's standing stock was removed from grazing, 18.2% by copepods and 17.3% by microzooplankton.

Similar to 2013, the amount of specific prey removed by different grazers in 2014 varied from week to week (Table 2.2). An average of 97.9 ± 205.2 *H. rotundata* µg carbon L⁻¹ d⁻¹ and 23.4 ± 30.5 cryptophytes µg carbon L⁻¹ d⁻¹ were removed by grazers in the 2014 winter (Table 2.2). A higher concentration of *H. rotundata* was removed by grazers than cryptophytes but a smaller percentage of *H. rotundata*'s standing stock was removed by grazers compared to cryptophytes (Figure 2.3b,d). On average, copepods

removed 5% and microzooplankton removed 17% of *H. rotundata*'s daily standing stock for a total of 22%. A smaller percentage of *H. rotundata*'s standing stock was removed compared to 2013 even though there is not a difference in concentration of carbon removed by grazers between the two years (Table 2.2). Copepods removed an average of 7% of cryptophyte's daily standing stock and microzooplankton removed 21% for a total of 28% cryptophytes removed by grazers (Figure 2.3d). A similar percentage of cryptophytes standing stock was removed by grazers in 2013, although a higher concentration of cryptophytes carbon was removed by grazers in 2013 than 2014.

Consumption of Primary Production by Copepods and Microzooplankton: I

compared how much carbon from *H. rotundata* and cryptophytes was consumed daily by microzooplankton and copepods to how much carbon was produced daily by gross primary production (GPP) (Figure 2.4). Similar average rates of GPP occurred between the two years but a smaller percentage of surface GPP was removed by zooplankton grazers in 2014 compared to 2013. The average estimated gross surface primary production in winter 2013 was $0.268 \pm 0.215 \text{ g C m}^{-3} \text{ d}^{-1}$ and $0.288 \pm 0.299 \text{ g C m}^{-3} \text{ d}^{-1}$ in 2014. In 2013 grazers removed at least $0.246 \pm 0.231 \text{ g C m}^{-3} \text{ d}^{-1}$ of the estimated gross daily primary production for the entire winter which accounts for 91% of the GPP. In 2014 grazers removed $0.121 \pm 0.199 \text{ g C m}^{-3} \text{ d}^{-1}$ of average gross daily primary production over the winter, which was 42% of the GPP.

Discussion

A bloom formed in winter 2014 but not winter 2013, not because the GPP was higher in 2014 but because grazing was lower. The average amount of carbon removed by copepods and microzooplankton grazing on *H. rotundata* and cryptophytes was

similar to the estimated amount of carbon produced by gross daily primary production during winter 2013. In the winter of 2014 grazers removed substantially less carbon than was produced by daily gross primary production; as a result the standing stock of the phytoplankton community reached higher concentrations compared to 2013. The decrease in grazing pressure in late winter 2014 played a large role in achieving high abundances of *H. rotundata* by the end of winter. As observed by Sellner et al. (1991), grazing played a large role in controlling the winter standing stock of *H. rotundata*.

I substituted GPP for growth rates, as Behrenfeld (2010) did, because my method for measuring GPP was more precise than my method for measuring growth rates; the change in O₂ as measured with the O₂:Ar ratio was less variable than my estimated growth rates from the dilution experiments. GPP only estimates the amount of new carbon added by the total photosynthesizing community and not individual phytoplankton species. However, *H. rotundata* and cryptophytes accounted for at least 50% of the total chlorophyll *a* in fifteen of the twenty - three samples. I used GPP as a proxy for *H. rotundata* or cryptophytes growth rates, assuming their growth accounted for the majority of primary productivity I measured. Indeed, for winter 2014 *H. rotundata* abundance strongly correlates with primary production.

I used the canonical value of 50 as the C:Chl *a* ratio (Strickland 1965) to convert between my measured chlorophyll *a* concentration to carbon concentration, however this ratio is highly variable depending on the environment, the season, and the phytoplankton community composition (Sathyendranath et al. 2009). If the actual ratio is lower or higher than 50, then I will have overestimated or underestimated, respectively, the contribution of *H. rotundata* and cryptophytes to the total phytoplankton biomass. The

combined biomass of cryptophytes and *H. rotundata*, estimated from my cell counts, measurements of cell size, and published carbon: volume relationships, was higher than total phytoplankton biomass estimated from chlorophyll *a* for two weeks out of twenty - three, suggesting that I may have underestimated the total phytoplankton biomass for those two weeks.

For the past 30 years the dilution method has been the most common and effective way to measure *in situ* microzooplankton grazing rates on primary producers (Schmoker et al. 2013), though scientists continue to improve application of the method (Gallegos 1989; Dolan et al. 2000; Calbet et al. 2008; Calbet et al. 2012; Latsa 2014). Average microzooplankton community grazing may be overestimated when negative and non-significant data points are removed from bulk analyses of the data (Latsa 2014). I included non-significant positive results but changed negative grazing rates to zero in my mean analyses, which is consistent with previous work (Strom et al. 2001; Calbet & Landry 2004; Sherr et al. 2009; Lawrence & Menden-Deuer 2012). The two-point dilution method, which I used for my calculations of growth and grazing rate, is a conservative estimate of microzooplankton grazing rates (Worden and Binder 2003) that reduces the potential for over-estimation of the microzooplankton community grazing rate coefficient. Recent research in Narragansett Bay successfully used dilution experiments in a similar approach to my research to measure microzooplankton community grazing rates on the phytoplankton community at single station throughout the year (Lawrence & Menden-Deuer 2012).

This study provides insight into what factors allow winter blooms to occur, but it does not address the full impact of winter blooms on the entire ecosystem because my

sampling was restricted to one station. Litaker et al (2002b) showed that winter blooms of *H. triquetra* in North Carolina were patchy and usually confined to specific areas of the estuary. Sellner et al (1991) also found patchy *H. rotundata* blooms in the Paxtuent River, with *H. rotundata* usually aggregated downriver of a steep salinity gradient. I conducted a 72 hour experiment to examine the influence of tides on *H. rotundata* abundance every three hours and found no relationship between tidal height and abundance (data not shown). To fully understand the impact of winter blooms, future research will need to explore the extent of these blooms and their overall productivity.

My data shows that higher abundances of *H. rotundata* occurred in winter 2014 than winter 2013, in part because grazers removed less of the standing stock in winter 2014 than in winter 2013. Mean grazer population size did not differ between years, but the temporal pattern of grazers abundances differed between years and average grazing rates were lower in winter 2014 than in 2013. In winter 2014 the water temperature was below 1.0°C for three weeks, which coincided with a decrease in microzooplankton and copepod abundances, and in their grazing pressure. An exponential increase in abundance of *H. rotundata* occurred during the period of low grazing. Grazing on cryptophytes was also reduced but this species did not bloom. It is most likely that *H. rotundata* is adapted for high growth rates in winter but cryptophytes are not, thus allowing *H. rotundata* populations to increase faster than cryptophytes when grazing is reduced. *H. rotundata* is known to bloom in the winter (Cohen. 1983; Sellner et al. 1991; Marshall et al. 2005; Seong et al. 2006), but there are no reports of cryptophytes forming a winter bloom.

Water temperatures below 1.0°C may have had a negative impact on zooplankton survival and grazing rates. The Chesapeake Bay is located in a temperate climate and

experiences a wide range of temperatures annually, with average water temperature 15°C in the Choptank River and monthly means that range from a minimum of 3°C in January to a maximum of 28°C in July (Maryland Department of Natural Resources 2013). Zooplankton grazing rates are reduced under cold temperatures (Caron et al. 2000), and my observations at temperatures <1.0°C suggest this may have had a negative impact on zooplankton. By the time zooplankton populations recovered following the anomalously cold weather, the *H. rotundata* population had reached bloom abundances, illustrating the complexities involved in bloom formation. Environmental conditions supporting phytoplankton growth are required, but low grazing pressure is also necessary for a bloom to initiate. The bloom I observed in winter 2014 may not have formed if the grazer population had recovered sooner or if *H. rotundata* growth was slower and they did not reach high abundances before recovery of the copepod population.

In winter 2014, the majority of fixed carbon produced was not consumed by zooplankton during the winter; however the fate of that carbon is unclear. Litaker et al. (2002a) measured low zooplankton grazing rates on a *H. triquetra* bloom in the Newport Estuary and they proposed that production from the bloom was primarily recycled in the microbial loop. However it is possible that the phytoplankton carbon is consumed by zooplankton in the spring. In spring 2014, when water temperatures increased, the *E. carolleae* populations increased (unpublished data, Millette) and probably grazed the *H. rotundata* bloom. *E. carolleae* peaks in abundance in late March and April in the Chesapeake Bay region (Martino & Houde 2010; North & Houde 2004; Kimmel & Roman 2004). Wet winters have been shown to result in high abundances and wide distribution of the copepod *E. carolleae* in spring in Chesapeake Bay (Kimmel et al.

2006). It is plausible that high copepod abundances in springs following wet winters can be partly attributed to the winter dinoflagellate blooms that occur in wet winters (Cohen 1983; Sellner et al. 1991) and persist into early spring, providing food for the copepods.

The link between *H. rotundata* and *E. carolleae* in winter and early spring may be important in understanding variations in survival and growth of fish larvae in the Chesapeake estuary. High abundances and the timing of the peak abundance of *E. carolleae* are correlated with striped bass (*Morone saxatilis*) larval recruitment in spring (Shoji et al 2005; Martino & Houde 2010). Timing of the bloom, of copepod population development, and fish spawning will all affect the trophic transfer between winter – spring dinoflagellate blooms and larval fish.

I suggest that a reassessment of the importance of the winter dinoflagellate blooms in ecosystems, especially in estuarine and coastal areas, is warranted, particularly in regard for their effects on population dynamics of zooplankton and fish larvae in the following spring.

References

- Alekseev, V.R. and A. Souissi (2011) A new species within the *Eurytemora affinis* complex (Copepoda: Calanoida) from the Atlantic Coast of USA, with observations on eight morphologically different European populations. *Zootaxa* 2767:41-56.
- Arar, E.J. and G.B. Collins (1997) In vitro determination of chlorophyll a and pheophytin a in marine and freshwater algae by fluorescence. Method 445.0, National Exposure Research Laboratory, EPA. Cincinnati, OH.
- Behrenfeld, M.J. (2010) Abandoning Sverdrup's Critical Depth Hypothesis on phytoplankton blooms. *Ecology* 91:977-989.
- Calbet, A. and M.R. Landry (2004) Phytoplankton growth, microzooplankton grazing, and carbon cycling in marine systems. *Limnol Oceanogr* 49:51-57.
- Calbet, A., I. Trepas, R. Almeda et al. (2008) Impact of micro- and nanograzers on phytoplankton assessed by standard and size-fractionated dilution grazing experiments. *Aquat Microb Ecol* 40: 145-156.
- Calbet, A., R.A. Martinez, S. Isari et al. (2012) Effects of light availability on mixotrophy and microzooplankton grazing in an oligotrophic plankton food web: Evidences from a mesocosm study in Eastern Mediterranean waters. *J Exp Mar Biol Ecol* 424: 66-77.
- Caron, D.A., M.R. Dennett, D.J. Lonsdale, D.M. Moran, and L. Shalapyonok (2000) Microzooplankton herbivory in the Ross Sea, Antarctica. *Deep-Sea Research II* 47: 3249-3272.
- Cohen, R.R.H. (1983) Physical processes and the ecology of a winter dinoflagellate bloom of *Katodinium rotundatum*. *Mar Ecol Prog Ser* 26:135-144.
- Dolan, J.R., C.L. Gallegos, and A. Moigis (2000) Dilution effects on microzooplankton in dilution grazing experiments. *Mar Ecol Prog Ser* 200:127-139.
- Frost, B.W. (1972) Effects of size and concentration of food particles on the feeding behavior of the marine planktonic copepod *Calanus pacificus*. *Limnol Oceanogr* 17:805-815.
- Gallegos, C.L. (1989) Microzooplankton grazing on phytoplankton in the Rhode River, Maryland: nonlinear feeding kinetics. *Mar. Ecol. Prog. Ser.* 57:23-33.
- Kana, T.M., C. Darkangelo, M.D. Hunt, J.B. Oldham, G.E. Bennett, and J.C. Cornwell (1994) Membrane Inlet Mass Spectrometer for Rapid High-Precision Determination of N₂, O₂, and Ar in Environmental Water Samples. *Anal Chem* 66:4166-4170.

Kimmel, D.G. and M.R. Roman (2004) Long-term trends in mesozooplankton abundance in Chesapeake Bay, USA: influence of freshwater input. *Mar Ecol Prog Ser* 267:71-83

Kimmel, D.G., W.D. Miller, and M.R. Roman (2006) Regional scale climate forcing of mesozooplankton dynamics in Chesapeake Bay. *Estuar Coast* 29:375-387.

Howarth, R.W., and A.F. Michaels (2000) The Measurement of Primary Production in Aquatic Ecosystems. In: Sala OE, Jackson RB, Mooney HA, and Howarth RW(eds) *Methods in Ecosystem Science*. Springer-Verlag New York, Inc., New York, p 72-85.

Irigoiien, X., K.J. Flynn, and R.P. Harris (2005) Phytoplankton blooms: a 'loophole' in microzooplankton grazing impact? *J Plankton Res* 27:313-321.

Landry, M.R., and R.P. Hassett (1982) Estimating the grazing impact of marine microzooplankton. *Mar Biol* 67:283-288.

Latasa, M. (2014) Comment: A potential bias in the databases of phytoplankton growth and microzooplankton grazing rates because of the improper formulation of the null hypothesis in dilution experiments. *Limnol Oceanogr* 59: 1092-1094.

Lawrence, C., and S. Menden-Deuer (2012) Drivers of protistan grazing pressure: seasonal signals of plankton community composition and environmental conditions. *Mar Ecol Prog Ser* 459: 39-52.

Lee, D.Y., D.P. Keller, B.C. Crump, and R.R. Hood (2012) Community metabolism and energy transfer in the Chesapeake Bay estuarine turbidity maximum. *Mar Ecol Prog Ser* 449:65-82

Litaker, R.W. et al (2002a) Seasonal niche strategy of the bloom-forming dinoflagellate *Heterocapsa triquetra*. *Mar Ecol Prog Ser* 232:45-62.

Litaker, R.W. et al (2002b) Effect of diel and interday variations in light on the cell division pattern and in situ growth rates of the bloom-forming dinoflagellate *Heterocapsa triquetra*. *Mar Ecol Prog Ser* 232:63-74.

Marshall, H.G., L. Burchardt, and R. Lacouture (2005) A review of phytoplankton composition within Chesapeake Bay and its tidal estuaries. *J Plankton Res* 27(11):1083-1102.

Martino, E. J., and E.D. Houde (2010) Recruitment of striped bass in Chesapeake Bay: spatial and temporal environmental variability and availability of zooplankton prey. *Mar Ecol Prog Ser* 409: 213-228.

Maryland Department of Natural Resources (2013) Eyes on the Bay. www.eyesonthebay.net (accessed 17 Dec 2014)

Menden-Deuer, S. and E.J. Lessard (2000) Carbon to volume relationships for dinoflagellates, diatoms, and other protist plankton. *Limnol Oceanog* 45:569-579.

North, E.W. and E.D. Houde (2004) Distribution and transport of bay anchovy (*Anchoa mitchilli*) eggs and larvae in Chesapeake Bay. *Estuar Coast Shelf S* 60:409-429.

Sathyendranath, S., V. Stuart, A. Nair et al. (2009) Carbon-to-chlorophyll ratio and growth rate of phytoplankton in the sea. *Mar Ecol Prog Ser* 383:73-84.

Schmoker, C., S. Hernandez-Leon, and A. Calbet (2013) Microzooplankton grazing in the oceans: impacts, data variability, knowledge gaps and future directions. *J Plankton Res* 35: 691-706.

Sellner, K.G. et al. (1991) Importance of a winter dinoflagellate-microflagellate bloom in the Patuxent River Estuary. *Estuar Coast Shelf S* 32:27-42.

Seong, K.A., H.J. Jeong, S. Kim, G.H. Kim, and J.H. Kang (2006) Bacterivory by co-occurring red-tide algae, heterotrophic nanoflagellates, and ciliates. *Mar Ecol Prog Ser* 322:85-97.

Sherr, E.B. and B.F. Sherr (1993) Preservation and storage of samples for Enumeration of Heterotrophic Protists. In: Kemp PF, Sherr BF, Sherr EB, Cole JJ(eds) *Aquatic Microbial Ecology*. Lewis Publishers, Boca Raton, p 207-212.

Shoji, J., E.W. North, and E.D. Houde (2005) The feeding ecology of *Morone americana* larvae in the Chesapeake Bay estuarine turbidity maximum: the influence of physical conditions and prey concentrations. *J Fish Biol* 66:1328-1341.

Stoecker, D.K., A.E. Thessen, and D.E. Gustafson (2008) "Windows of opportunity" for dinoflagellate blooms: reduced microzooplankton net growth coupled to eutrophication. *Harmful Algae* 8: 158-166.

Strickland, J.D.H. (1965) Production of organic matter in the primary stages of the marine food web chain. In: Riley JP, Skirrow G (eds) *Chemical oceanography*, vol. 1. Academic Press, New York, p 477-610.

Sherr, E.B., B.F. Sherr, and A.J. Hartz (2009) Microzooplankton grazing impact in the Western Arctic Ocean. *Deep-Sea Res II* 56: 1264–1273.

Strom, S.L., M.A. Brainard, J.L. Holmes, and M.B. Olson (2001) Phytoplankton blooms are strongly impacted by microzooplankton grazing in coastal North Pacific waters. *Mar Biol* 138:355-368.

Strom, S.L. and K.A. Fredrickson (2008) Intense stratification leads to phytoplankton nutrient limitation and reduced microzooplankton grazing in the southeastern Bering Sea. *Deep-Sea Res PT II* 55:1761-1774

Worden, A.Z. and B.J. Binder (2003) Application of dilution experiments for measuring growth and mortality rates among *Prochlorococcus* and *Synechococcus* population in oligotrophic environments. *Aquat Microb Ecol* 30:159-174.

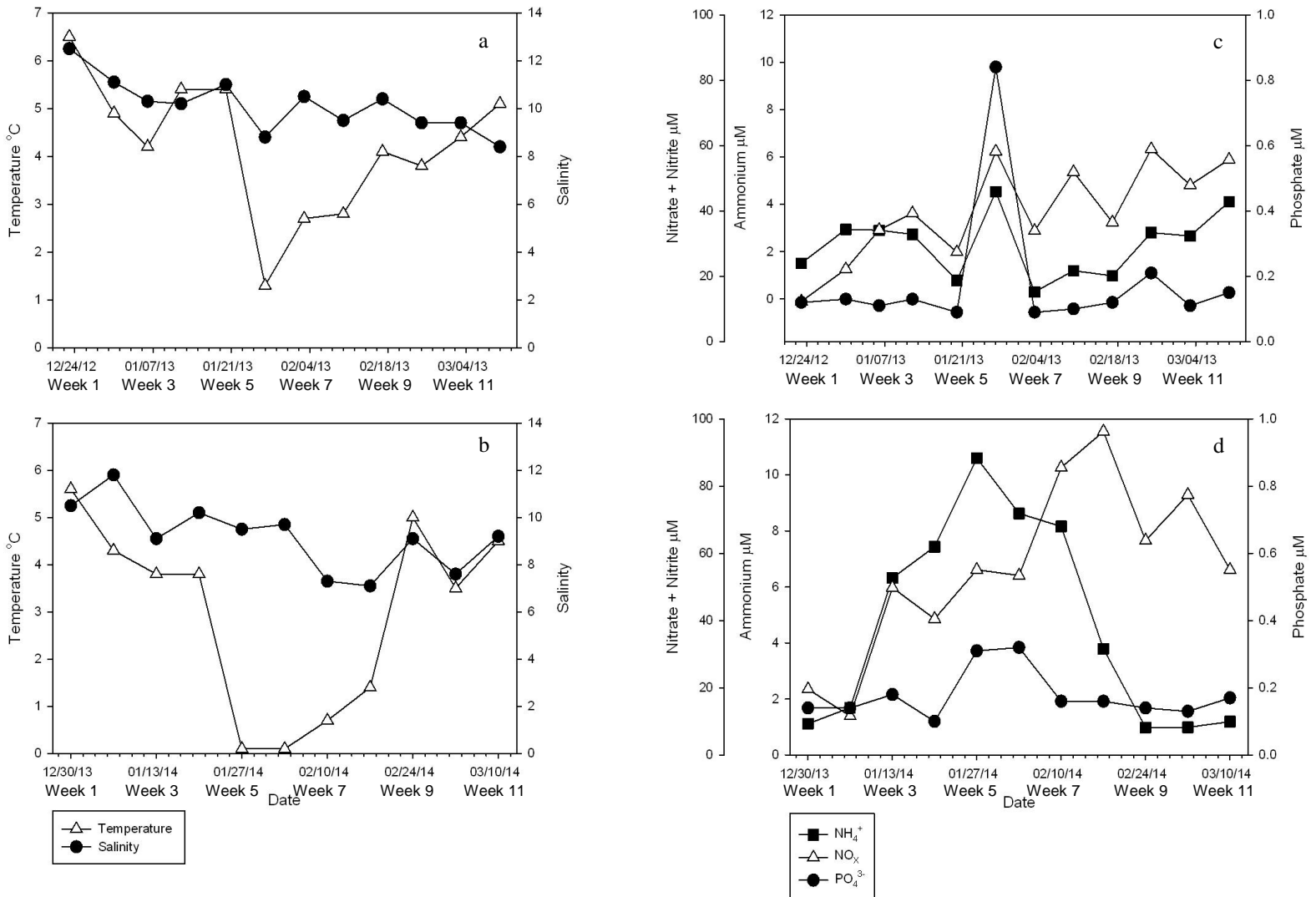
Tables and Figures

Table 2.1

Year	<i>H. rotundata</i>	Cryptophytes	<i>P. minimum</i>	<i>H. triquetra</i>
2012-2013	34.99 ± 10.25%	59.23 ± 12.47%	5.23 ± 7.81%	0.55 ± 0.98%
2013-2014	72.79 ± 20.95%	25.19 ± 18.08%	0.77 ± 1.48%	1.25 ± 2.66%

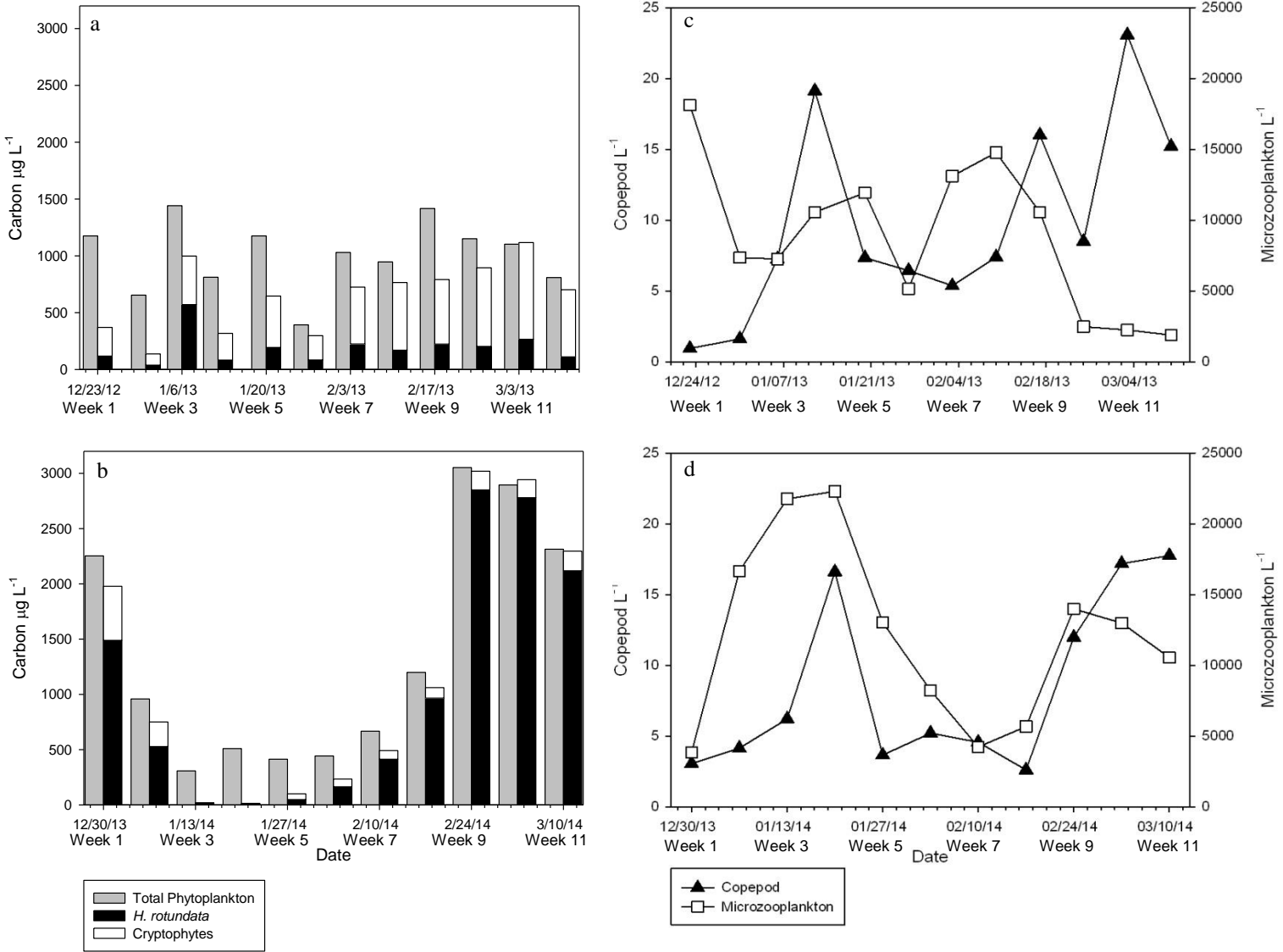
Average percentage of the total >10µm phytoflagellate community that *H. rotundata*, cryptophytes, *P. minimum*, and *H. triquetra* accounted for in winter of 2013 and 2014.

Figure 2.1



The water temperature (°C) and salinity in the Choptank River, MD, winter of 2013(a) and 2014(b). The ammonium, nitrate + nitrite, and phosphate concentration in Choptank River, MD, winter of 2013(c) and 2014(d).

Figure 2.2



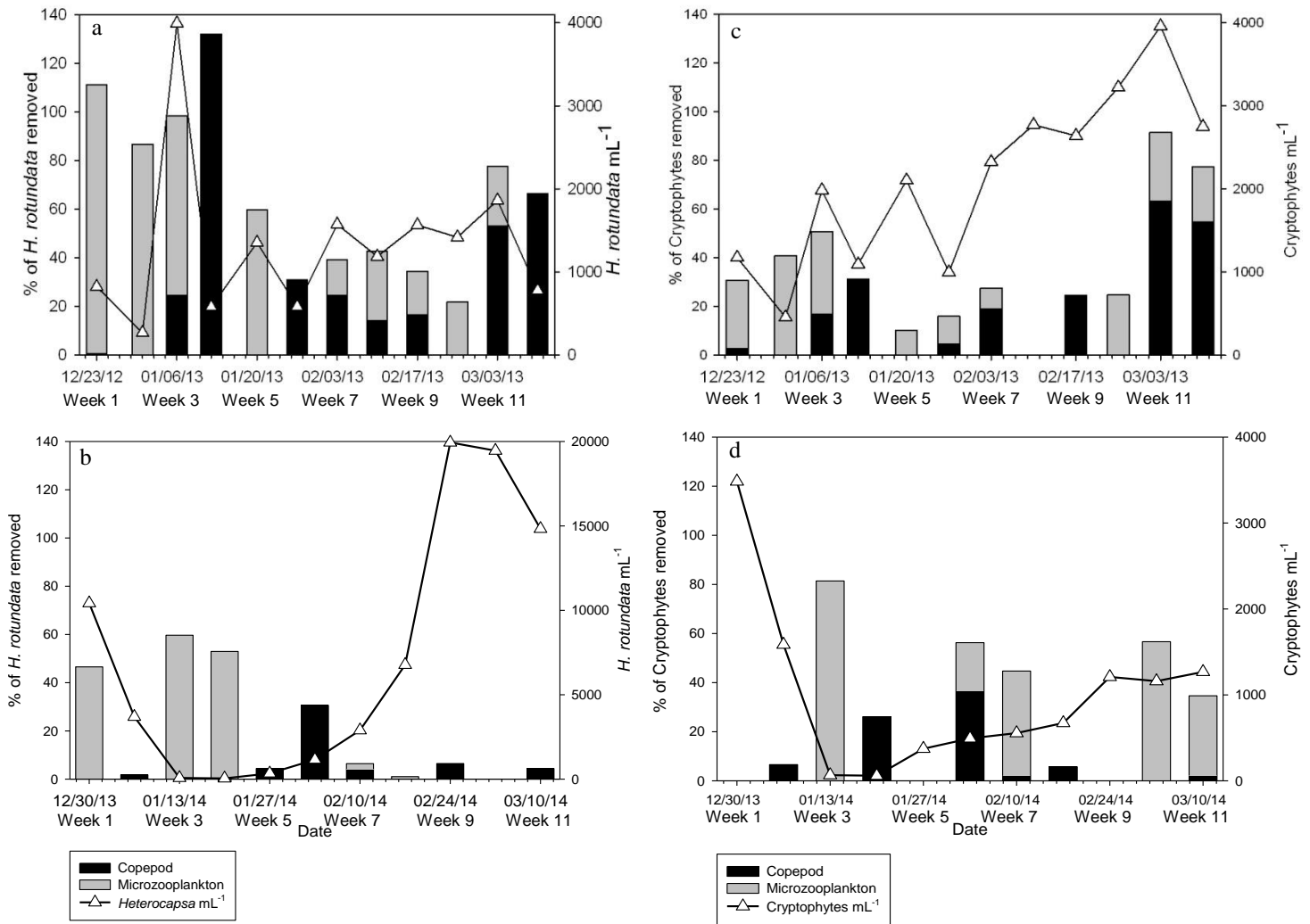
Estimated carbon content of total phytoplankton based on chlorophyll *a*, *Heterocapsa rotundata*, and cryptophytes in surface waters, Choptank River, MD, winters of 2013 (a) and 2014 (b). Estimate abundance of the copepod *E. carolleae* + *Acartia tonsa* and microzooplankton in surface waters, Choptank River, MD, winters of 2013(c) and 2014(d).

Table 2.2

Date	<i>H. rotundata</i>		Cryptophytes	
	Copepod ($\mu\text{g Carbon L}^{-1}$)	Microzooplankton ($\mu\text{g Carbon L}^{-1}$)	Copepod ($\mu\text{g Carbon L}^{-1}$)	Microzooplankton ($\mu\text{g Carbon L}^{-1}$)
12/23/2012	0.70	129.94	4.61	46.17
12/31/2012	0	33.16	0	26.30
1/6/2013	141.24	419.72	47.88	93.83
1/12/2013	109.20	0	48.02	0
1/20/2013	0	115.64	0	30.01
1/27/2013	25.68	0	6.68	15.69
2/3/2013	55.85	32.33	62.81	27.25
2/10/2013	24.57	47.60	0	0
2/17/2013	37.58	39.44	91.46	0
2/24/2013	0	44.33	0	112.15
3/3/2013	141.60	64.79	353.43	154.91
3/10/2013	73.87	0	212.61	86.07
Average	50.86 \pm 54.05	77.24 \pm 115.58	68.96 \pm 108.72	49.37 \pm 50.68
12/30/2013	0	693.36	0	0
1/6/2014	9.25	0	14.65	0
1/13/2014	0	6.27	0	7.53
1/20/2014	0	3.05	2.15	0
1/27/2014	2.11	0	0	0
2/3/2014	50.33	0	25.30	13.64
2/10/2014	17.25	9.21	1.57	33.22
2/17/2014	0	9.71	5.37	0
2/24/2014	183.91	0	0	0
3/3/2014	0	0	0	92.09
3/10/2014	92.84	0	3.80	57.71
Average	32.34 \pm 58.19	65.60 \pm 208.24	4.80 \pm 8.07	18.56 \pm 30.61

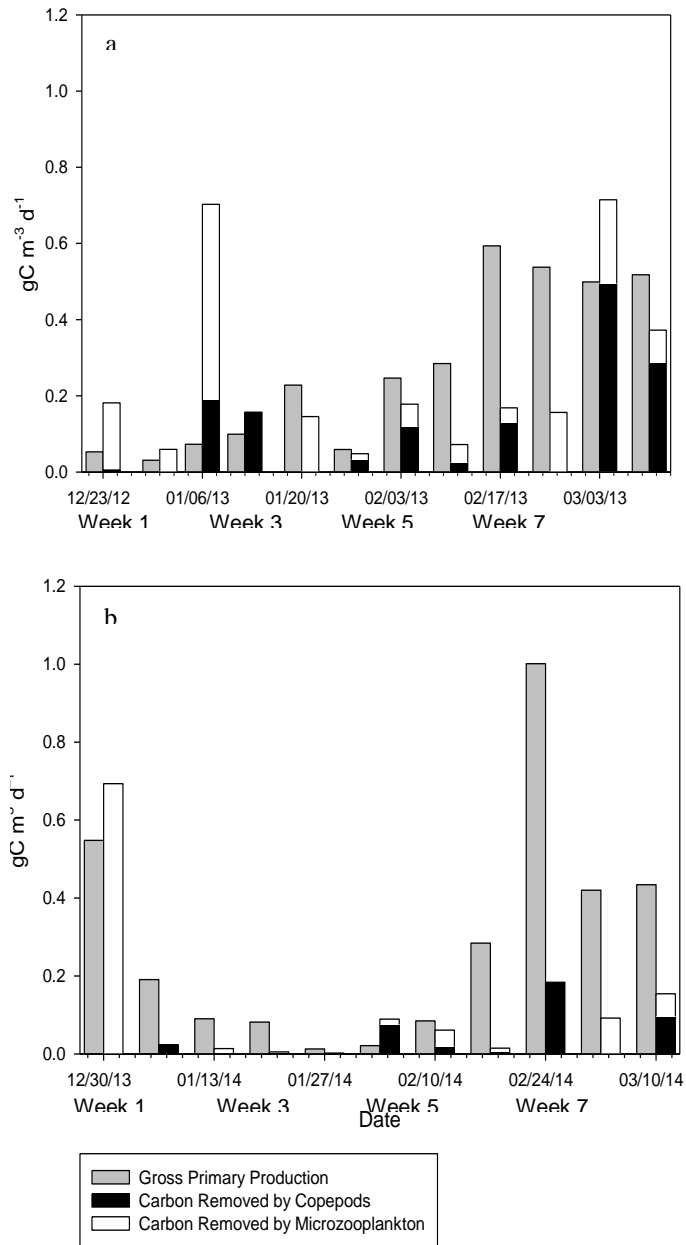
omparison of the concentration of *H. rotundata* and cryptophytes carbon L^{-1} removed by copepods and microzooplankton through grazing in winter of 2013 and 2014. Values in bold are based on grazing rates that are statistically different from zero ($P < 0.05$).

Figure 2.3



Comparison of the abundance of phytoplankton species (cells mL⁻¹) to the percent of standing stock of that species removed by copepods and microzooplankton ingestion. *Heterocapsa rotundata* 2013 (a) *Heterocapsa rotundata* 2014 (b) cryptophytes 2013 (c) cryptophytes 2014 (d). Note difference in right y-axis in graph b.

Figure 2.4



Comparison of the estimated amount of carbon removed by copepod consumption and microzooplankton consumption of *Heterocapsa rotundata* and cryptophytes in the surface Choptank River, MD, winter of 2013(a) and winter of 2014 (b).

Chapter 3: Mixotrophy in *Heterocapsa rotundata*: a mechanism for dominating the winter phytoplankton

Introduction

Heterocapsa is a genus of dinoflagellates that contains numerous bloom forming and toxic species (Salas et al. 2014). One particular species, *Heterocapsa rotundata* (Lohmann) Loeblich (Hansen, 1995), is ubiquitous and occasionally forms large blooms. *H. rotundata* has been reported in a range of environments all over the world including Chesapeake Bay, USA (Millette et al. 2015), Keum Estuary, South Korea (Seong et al. 2006), Manori Creek and Manim Bay, India (Shahi et al. 2015), Baltic Sea, Germany (Jaschinaski et al. 2015), and Kangaroo Island, Australia (Balzano et al. 2015). *H. rotundata* tends to either dominate or be a prominent part of the phytoplankton community for at least part of the year in some of these areas (Seong et al. 2006; Balzano et al. 2015; Millette et al. 2015). Yet, relatively few studies have focused on the ecology of *H. rotundata*.

Some studies have focused on the formation and decline of *H. rotundata* winter blooms in Chesapeake Bay, USA tributaries (Cohen 1985; Sellner et al. 1991; Millette et al. 2015). This research found *H. rotundata* blooms in wet, cold winters when salinity is low (Cohen 1985) and when there is a release in grazing pressure from microzooplankton and copepods (Millette et al. 2015). Although wet, cold winters and a release in grazing pressure are factors that impact every phytoplankton species, it is unknown how *H. rotundata* can take advantage of these conditions over other species to bloom.

H. rotundata may use mixotrophy to overcome light limitation, giving *H. rotundata* an advantage over other phytoplankton in the winter. *H. rotundata* has been

shown to consume heterotrophic bacteria, cyanobacteria such as *Synechococcus*, and small diatoms (Seong et al. 2005; Jeong et al. 2010). Their bacterial ingestion rate is known to increase with increasing bacteria abundances (Seong et al. 2006), but their phagotrophic response to changes in environmental factors has never been examined. Their maximum bacterial ingestion rate has been calculated to be 11.2 bacteria *H. rotundata*⁻¹ hr⁻¹, which is equivalent to ingestion of 76% of their body carbon per day (Seong et al. 2006).

Many phagotrophic phototrophs use mixotrophy to acquire limiting nutrients. In some nutrient limited mixotrophs, grazing increases with irradiance levels because at higher irradiance more nutrients are required to keep up with increased photosynthetic rates (Stoecker 1998). Other phagotrophic phototrophs use mixotrophy to acquire organic carbon when light is limited, and their grazing rates increase as irradiance levels decrease (Stoecker 1998). Light is the primary factor limiting phototrophic growth in the Chesapeake Bay during winter when inorganic nutrient limitation is rare (Fisher et al. 2003; Kemp et al. 2005). If *H. rotundata* is using phagotrophy to compensate for light limitation of photosynthesis, then I would expect their ingestion rates to increase as irradiance levels decrease.

I used a combination of laboratory and field experiments to measure *H. rotundata*'s phagotrophic and cellular response to changes in light and nutrients to understand how it can bloom during temperate winters in a coastal plain estuary. I hypothesize that as light decreased, *H. rotundata*'s ingestion on bacteria would increase, giving the dinoflagellate an advantage over other phytoplankton and allow them to dominate the nanoplankton community in the winter. If this is the case, the impact of *H.*

rotundata's grazing may keep bacteria and small phytoplankton populations at low abundances during the winter bloom (Seong et al. 2006).

Methods

Our overall approach combined laboratory and field experiments to determine how the ingestion of *H. rotundata* was affected by changes in irradiance levels and nutrients. I conducted two sets of laboratory experiments to identify how changes in irradiance and nutrients impacted *H. rotundata*'s ingestion rate and cellular content under controlled conditions. I then conducted high frequency field sampling and *in situ* experiments to track how natural variation in environmental factors impacted *H. rotundata*'s ingestion rate *in situ* and compared it to my laboratory data. The field experiments also allowed me to estimate the impact of grazing by these mixotrophs on the bacterial population.

Laboratory experiments: A culture of *H. rotundata* (K-0483) from the Scandinavian Culture Collection of Algae and Protozoa at the University of Copenhagen in Denmark was used in all laboratory experiments. *H. rotundata* was reared at the Horn Point Laboratory in Cambridge, MD, USA on enriched f/2 – Si medium (Guillard and Ryther, 1962) in autoclaved Choptank River water at 10.8 salinity and 4°C on an 8:16 light:dark cycle at 85 $\mu\text{mol photons m}^{-2} \text{sec}^{-1}$. The culture conditions were the same conditions used for the laboratory experiments unless otherwise noted. The culture was non-axenic and unidentified bacteria in the culture were used as prey for the laboratory experiments. The bacteria in the culture had an average length (\pm SE) of 0.725 (\pm 0.04) μm and average width (\pm SE) of 0.251 (\pm 0.01) μm (N=30). The average volume of the bacterial cells was estimated with the equation for a cylindrical rod (Lee 1993) and

converted to carbon biomass with the equation $\text{pg C cell}^{-1} = 0.12 \times V^{0.7}$ (Norland 1993), with volume expressed in μm^3 . The average volume of the bacterial cells was $0.032 \pm 0.004 \mu\text{m}^3$ and average carbon content per cell was $11.0 \pm 0.9 \text{ fg C cell}^{-1}$.

Laboratory Experiment 1: effect of irradiance and ammonium on grazing coefficient

The cultured *H. rotundata*'s community grazing coefficient (g) was measured at three different ammonium concentrations and at five different light levels. Ammonium was chosen as the form of nitrogen to examine in this experiment because during a large 2014 winter bloom of *H. rotundata* there was a strong negative correlation between ammonium concentration and *H. rotundata* abundance and no correlation between nitrate and *H. rotundata* (unpublished data, Millette). Different light levels were achieved by incubating containers without mesh ($300 \mu\text{mol photons m}^{-2} \text{ s}^{-1}$, I_0), with 1 (~58% I_0), 2 (~15% I_0), or 4 (~4% I_0) layers of black nylon mesh, or one layer of black electric tape covering the container (completely dark). The three different ammonium (NH_4^+) concentrations of 0 (none), 5 (average) and 50 (extreme) μM were tested at each irradiance level, for a total of 15 treatments. An ammonium concentration of 5 μM was picked as the average based on winter ammonium concentration in the Choptank River (Millette et al. 2015). Each treatment consisted of four 20 mL scintillation vials with 10 mL of f/2-Si media, with one bottle for a control (only bacteria) and three bottles for experimental replicates (bacteria + *H. rotundata*). Ammonium was added to the f/2-Si media, which already contains nitrate but not ammonium, to represent the natural environment where ammonium and nitrate are present. Bacterial cells in controls were isolated from the *H. rotundata* culture through gentle reverse filtration using a 3 μm nuclepore filter.

The experiment ran for 72 hr with vials strapped to a plankton wheel (1 rpm). At 0, 24, 48, and 72 hr I took samples for bacterial abundance. 1 mL aliquots from each vial were preserved in 4% buffered paraformaldehyde (PFA) and then stored in cryovials at -80 °C. The bacteria were then stained with SYBR green (Van Nevel et al. 2013) and counted using a BD Accuri C6 flow cytometer within a week after preservation.

H. rotundata's community grazing coefficient ($g\ d^{-1}$) on bacteria was calculated every 24 hr using the Frost (1972) equations. Recently, the equations by Frost (1972) have been used by Kang (2011) and Lee (2014) to measure the ingestion and prey removal rates of various mixotrophic dinoflagellate species. I applied a 2-way ANOVA to test the effect of irradiance level and NH_4^+ concentration on the community grazing coefficient on bacteria.

Laboratory Experiment 2: effect of irradiance on ingestion rates and H. rotundata

Based on the results from the previous set of experiments, the methods were adjusted in order to measure individual ingestion rates and collect additional data on how changes in irradiance affects *H. rotundata*. To measure *H. rotundata* ingestion rates on bacteria I had to measure their abundance over the experiment. These experiments were conducted in 250 mL Nalgene polycarbonate bottles and I increased the volume of the f/2-Si medium from 10 mL to 100 mL in order to collect samples for *H. rotundata* counts and cellular carbon and chlorophyll *a* concentrations. In addition, I did not place the bottles on a plankton wheel but instead gently bubbled air into the containers, similar to culture conditions used to maintain the cells in suspension. There were no ammonium treatments and I only tested irradiance levels below $50\ \mu\text{mol photons m}^{-2}\ \text{s}^{-1}$.

The experiments ran for 48 hr, the first 24 hr were used as an adaptation period to experimental conditions during which *H. rotundata* division and grazing rates were not measured. Bacteria samples of 1 mL were taken at 24 and 48 hrs and 5 mL of water was collected at 0, 24, and 48 hrs to estimate *H. rotundata* abundance. Bacteria samples were preserved and analyzed as described in the previous experiment. *H. rotundata* samples were preserved in Lugol's solution and counted with a Nikon Eclipse E800 microscope at 20x magnification on a Sedgewick rafter slide (Sherr & Sherr 1993). A minimum of 300 cells were counted per sample, resulting in < 11.5% counting error (Lund et al. 1958).

I calculated the geometric mean *H. rotundata* concentration in each bottle throughout the run of the experiment (Båmsted et al. 2000) to estimate per capita ingestion rate with the following equation,

$$n = (n_t - n_0) / \ln(n_t/n_0)$$

where n is the mean *H. rotundata* concentration throughout the experimental run and n_0 and n_t are the initial and final concentrations of *H. rotundata*. Calculated average concentrations of *H. rotundata* were used to estimate the amount of bacteria consumed per *H. rotundata* in laboratory experiments.

To measure cellular concentration of chlorophyll *a* and carbon in *H. rotundata*, 15 – 30 mL of water was filtered onto 25mm GF/F (glassfiber filters) at 0 and 48 hr. Filters used to estimate chlorophyll *a* were extracted in 90% acetone for 24 hr in the freezer (Arar & Collins 1997). The chlorophyll fluorescence of the acetone extract was measured with a calibrated Turner Designs AU-10 fluorometer. Carbon samples were filtered onto pre-combusted GF/Filters and stored in the freezer. The filters were then dried at 60°C

and analyzed on an Exeter Analytical CE-440 Elemental Analyzer at Horn Point Laboratory Analytical Services.

Linear regressions were used to analyze the data from this experiment to look for relationships between irradiance levels, *H. rotundata* bacterial ingestion rates, division rates, cellular carbon concentration, cellular chlorophyll *a* concentration, and carbon:chlorophyll *a*.

Winter field experiments: I estimated *in situ* ingestion rates of *H. rotundata* on bacteria at natural nutrient concentrations and irradiance levels throughout winter using water collected at the field sampling site. I collected water at 08:00 twenty times from January 27, 2016 – March 18, 2016 from a fishing pier on the Choptank River in Cambridge, MD USA (38°34'24" N 76°4'6" W) (Figure 3.1). At this location *H. rotundata* is known to dominate the winter phytoplankton community and form large winter blooms (Millette et al. 2015). On each sampling date I collected 10 L of surface water with a bucket, and immediately filtered it through 20 µm mesh to remove larger plankton. Temperature and salinity were measured with a hand-held YSI-30 immediately after the bucket was retrieved. Samples for nutrients (dissolved nitrate + nitrite (NO_x), ammonium, and ortho-phosphate) were filtered through a Whatman's 0.45 µm nylon sieve with a glass microfiber filter and frozen until analyzed. Nutrient samples were analyzed at Horn Point Laboratory Analytical Services with a Technicon AutoAnalyzer II. PAR data were recorded with a hand-held 4π LI-COR light sensor and day length was downloaded from the website <http://www.sunrisesunset.com/usa/Maryland.asp>. Water for ingestion experiments was transported to the UMCES Horn Point Laboratory in Cambridge, MD.

I used fluorescent microspheres to estimate *H. rotundata* ingestion rates. Three 250 mL Nalgene polycarbonate bottles were filled with 100 mL of 20 μm filtered Choptank water. Fluorescent microspheres (0.5 μm diameter, Fluoresbrite® YG Carboxylate Microspheres from Polysciences, Inc.) were added to each bottle at a concentration of $2.5 \times 10^5 \text{ mL}^{-1}$, equivalent to approximately 25% of the mean natural bacterial abundance (unpublished data), and bottles were gently rotated to mix them. At the start of experiments 12-15 mL of water was collected from each bottle and preserved with acid Lugol's solution to estimate phytoplankton abundance, and 1 mL of water was collected and preserved with 4% buffered PFA to estimate bacterial and microsphere abundance. These samples were analyzed as described for the laboratory experiments.

The bottles were placed in black mesh bags that allowed 55% of natural light exposure, and were then incubated in floats in a small, protected cove of the Choptank River. Based on preliminary experiments (see appendix B), the *H. rotundata* culture linearly up took microspheres for 60 minutes, so I incubated the bottles for each experiment for 30 minutes, typically starting experiments between 08:30 and 09:00. After 30 minutes, 50 mL of water were fixed using the Lugol's/formaldehyde/ $\text{Na}_2\text{S}_2\text{O}_3$ method to prevent regurgitation of microspheres (Sherr & Sherr, 1993). Samples were filtered onto 2 μm membrane polycarbonate filters (Poretics Corp.) and mounted with immersion oil and cover slips on glass slides. To eliminate loss of microsphere fluorescence, specimens were frozen until counted. A Zeiss epifluorescence microscope at 1000x using a 43 HE Red Fluorescent filter was used to count the microspheres within a *H. rotundata* cell. When a cell was located, the number of microspheres cell^{-1} was counted inside the

cell; at least 100 individual cells were examined for each sample to count ingested microspheres.

The ingestion rate of microspheres (I_m) was calculated by dividing the total number of microspheres ingested by the number of *H. rotundata* counted for each replicate. Using these ingestion rates, I calculated the actual ingestion rate on bacteria (I_b) based on equations from Domaizon et al. (2003). These equations calculate a cell's clearance rate on microspheres to estimate how much of the available bacteria a cell could ingest at that clearance rate:

$$I_b = (I_m/MS) B$$

Where MS is the abundance of microspheres mL^{-1} and B is the abundance bacteria mL^{-1} .

I assumed that *H. rotundata* had no preference for bacteria or microspheres and their clearance rates on microspheres were the same as on bacteria.

I fitted a logarithmic curve to the response of *H. rotundata* ingestion rates from both field and laboratory experiments to irradiance.

Results

Effect of irradiance and ammonium on grazing coefficient: Results of a two-way ANOVA with data from the first experiment collected at 24-48 hr showed irradiance and ammonium have an interactive effect on *H. rotundata*'s community *g* on bacteria (Table 3.1). At high irradiance levels there is a difference between *H. rotundata*'s community *g* at varying ammonium concentrations, with the lowest *g* observed for 5 μM . At low irradiance levels, *H. rotundata* showed no response to the ammonium concentrations (Figure 3.2). Overall, as irradiance decreased, *H. rotundata*'s community *g* increased and the difference between ammonium treatments decreased (Figure 3.2). Although I detected

significant differences in grazing using the 24-48 hr data, I detected no effects of irradiance or ammonium on grazing using the 0-24 hr and 48-72 hr data (see appendix).

Effect of irradiance on ingestion rates and *H. rotundata*: In the second laboratory, I used five different treatments with three replicates per treatment, but because of the experimental design each bottle received slightly different irradiance levels. Some of the replicates in a treatment had irradiance levels that were closer to other treatments (Table 3.2). As a result, I treated each replicate as an individual data point and did not group data by treatments, and analyzed the data using regression techniques.

The minimum and maximum hourly ingestion rates on bacteria were 4.7 and 15.4 bacteria cell⁻¹ hr⁻¹, respectively (Table 3.2). As irradiance decreased, ingestion rates increased (linear regression, df = 11, r² = 0.419, p = 0.009) (Figure 3.3). The *H. rotundata* minimum and maximum population division rates were -0.31 and 0.24 d⁻¹, respectively (Table 3.2). *H. rotundata* division rates were positively correlated to irradiance (linear regression, df = 11, r² = 0.292, p = 0.04) but not correlated to ingestion rates (linear regression, df = 11, r² = 0.177, p = 0.12).

The mean (\pm SE) initial cellular content of cultured *H. rotundata* raised at 85 $\mu\text{mol photons m}^{-2} \text{s}^{-1}$ was 1.28 (\pm 0.12) pg Chl *a* cell⁻¹ and 84.77 (\pm 1.18) pg carbon cell⁻¹, with a carbon:chlorophyll *a* (C:Chl) ratio of 67.07 (\pm 5.44) (Figure 3.4). *H. rotundata* cellular chlorophyll *a* concentration was negatively correlated with irradiance levels (linear regression, df = 12, r² = 0.576, p = 0.004) (Figure 3.4). C:Chl ratio was positively correlated to irradiance levels (linear regression, df = 12, r² = 0.810, p < 0.001) (Figure 3.4). *H. rotundata* cellular carbon concentration was not related to irradiance levels (linear regression, df = 12, r² = 0.046, p = 0.39) (Figure 3.4).

Winter field experiments: During the winter in the Choptank River between 1/27/2016 to 3/18/2016 the mean (\pm SE) temperature and salinity was 4.9 (\pm 0.8) °C and 10.4 (\pm 0.3), respectively (Table 3.3). Average ammonium concentration was 2.5 (\pm 0.2) μ M-N, average NO_x concentration was 35.6 (\pm 3.0) μ M-N, average phosphate concentration was 0.1 (\pm 0.01) μ M-P, and average N:P ratio of NH₄⁺ + NO_x: PO₄³⁻ was 345 (\pm 38) (Table 3.3). The average *H. rotundata* abundance was 3924 (\pm 865) cells mL⁻¹ and range from 297 to 11475 cells mL⁻¹.

The average calculated *H. rotundata* ingestion rate was 4.1 (\pm 0.6) bacteria h⁻¹ and ranged from 1.17 to 12.34 bacteria h⁻¹. I fitted a logarithmic equation (MATLAB Statistics Toolbox) to the field and laboratory *H. rotundata* ingestion rates at different irradiance levels (Figure 3.5, $r^2 = 0.64$):

$$I_b = -1.37 \log_e (P+1) + 12.1$$

where I_b is *H. rotundata* bacterial ingestion rates and P is irradiance. In the laboratory experiments I measured the level of irradiance each treatment received but in the field I measured the amount of available irradiance reaching the water surface (Table 3.3). Experimental bottles were incubated in mesh bags that allowed 55% of the light to reach the bottles, so I multiplied my surface irradiance measurements (Table 3.3) by 0.55.

Above 400 μ mol photons m⁻² sec⁻¹ changes in irradiance resulted in negligible changes in bacterial ingestion by *H. rotundata* (Figure 3.5). Below 400 μ mol photons m⁻² sec⁻¹ decreases in irradiance levels result in significantly higher ingestion rates (Figure 3.5). A comparison of field ingestion rates above (2.5 (\pm 0.9) bacteria hr⁻¹) and below (5.3 (\pm 0.3) bacteria hr⁻¹) 400 μ mol photons m⁻² sec⁻¹ showed that *H. rotundata* bacterial

ingestion was significantly higher at irradiance levels below $400 \mu\text{mol photons m}^{-2} \text{ sec}^{-1}$ (unequal variance t-test, $p=0.006$).

There was no relationship between bacteria concentration and either *H. rotundata* clearance rate (linear regression, $df = 19$, $r^2 = 0.08$, $p = 0.19$) or ingestion rate (linear regression, $df = 19$, $r^2 = 0.09$, $p = 0.22$) (Figure 3.6). There was also no relationship between *H. rotundata* ingestion rate and ammonium, NO_x , phosphate, and N:P ratio (Table 3.4).

Between 1/27/2016 - 2/19/2016 the average *H. rotundata* abundance ($\pm\text{SE}$) was $1021 (\pm 211) \text{ cells mL}^{-1}$ and I estimated they consumed of $4.8 (\pm 0.5) \%$ of bacteria's standing stock d^{-1} at $I=55\% I_0$ (Figure 3.7). Between 2/29/2016 - 3/18/2016 the average *H. rotundata* abundance ($\pm\text{SE}$) was $7472 (\pm 967) \text{ cells mL}^{-1}$ and I estimated they consumed $52.9 (\pm 12.0) \%$ of bacteria's standing stock d^{-1} at $55\% I_0$ (Figure 3.7).

Discussion

I ran two laboratory experiments and a series of 20 *in situ* experiments which all suggested that *H. rotundata* uses phagotrophy as a primary means to partially compensate for light limitation. As light levels decreased *H. rotundata*'s ingestion rate on bacteria increased. *H. rotundata* phagotrophic response to decreasing irradiance levels likely gives them an ecological advantage over other phytoplankton in the winter that allows them to survive and sometimes bloom under light limited conditions. A similar use of phagotrophy to overcome light limitation has been demonstrated in other mixotrophs that dominate in low light conditions (Czypionka et al. 2011; McKie-Krisberg et al. 2015). There was no relationship between *in situ* *H. rotundata* ingestion rates and nutrients (nitrate + nitrite, ammonium, and phosphate) in the field experiments. Average nitrate +

nitrite and ammonium concentrations in the Choptank River were high in winter, thus it is unlikely that nitrogen limitation was an important factor regulating bacterivory in my field experiments. Based on high N:P driven by low phosphate concentrations phosphorus limitation was possible, but I saw no evidence that phosphate concentrations effected ingestion rates.

H. rotundata's cellular chlorophyll *a* concentrations increased as irradiance decreased. Cohen (1985) also found *H. rotundata* responded to low light by increasing chlorophyll *a* concentrations. Phytoplankton are known to increase their concentrations of chlorophyll *a* in order to trap more light energy and maintain photosynthesis as light becomes limiting (Perry et al. 1981). This response to a decrease in irradiance suggests autotrophy is *H. rotundata*'s preferred method to acquire energy.

Our data suggest that below approximately $400 \mu\text{mol photons m}^{-2} \text{sec}^{-1}$ light becomes limiting to *H. rotundata* and it responds by increasing ingestion of bacteria. There was a weak negative relationship between irradiance levels and growth and no relationship between growth and ingestion rates. Ingestion of bacteria does not appear to support *H. rotundata*'s growth in the absence of phototrophy, but it likely reduces the rates at which growth decreases as irradiance levels decrease. At some critical light level, even with the ingestion of bacteria, it appears that *H. rotundata* cannot maintain positive division rates because more energy is required for cell maintenance than is produced by photosynthesis and derived from phagotrophy. Based on my laboratory experiments, this critical light level for *H. rotundata* appears to be $\sim 10 \mu\text{mol photons m}^{-2} \text{sec}^{-1}$. I propose that *H. rotundata* uses phagotrophy to partially compensate for light limitation to improve its winter survival and growth compared to other cold adapted estuarine

phytoplankton species. Future research identifying the critical light levels of other winter phytoplankton species and how quickly *H. rotundata* and other winter phytoplankton species recover from exposure to subcritical light levels is necessary to confirm whether or not *H. rotundata* is better adapted to low light compared to other co-occurring species.

Our estimates of *H. rotundata* ingestion rates are similar to rates reported in other studies. The minimum and maximum ingestion rate measured in the field was $1.2 (\pm 0.4)$ and $12.3 (\pm 2.9)$ bacteria hr^{-1} , respectively. In my laboratory experiments, I assumed that bacterial growth rates (μd^{-1}) in the experimental treatments were the same as the rates I measured in the control treatment at 24-48 hr. It is possible that bacterial growth rates were higher in experimental treatments than I assumed as a result of stimulation of growth by DOM released by *H. rotundata*. If this was the case, then my ingestion rates would be underestimates; however, my indirect measurements of *H. rotundata*'s ingestion rate were similar to direct measurements that I made in the field and estimates that other scientists have made in the laboratory. The minimum and maximum ingestion rates measured in the laboratory in this study were 4.7 and 15.4 bacteria hr^{-1} , respectively. Seong et al. (2006) estimated that *H. rotundata*'s maximum ingestion rate was 11.2 bacteria hr^{-1} at saturating bacteria concentrations, illumination of $30 \mu\text{mol photons m}^{-2} \text{sec}^{-1}$, and $20 \text{ }^\circ\text{C}$, and they measured ingestion rates of $2.2 (\pm 0.1)$ bacteria hr^{-1} in Kuem Estuary, South Korea in May at $21.5 \text{ }^\circ\text{C}$. The *H. rotundata* ingestion rates reported here are similar to those reported in Seong et al. (2006)'s, this is unexpected given the $17.5 \text{ }^\circ\text{C}$ difference in temperature. Seong et al. (2006) did not test for environmental factors controlling the dinoflagellate's ingestion rate, so different factors may be impacting the *H. rotundata* ingestion rates in South Korea.

Prey concentration has been identified as an important factor in controlling plankton clearance and ingestion rates, with clearance rates decreasing and ingestion rates increasing as prey concentration increases until a saturating concentration is reached (Frost 1972). This relationship with prey has also been shown for mixotrophic protists, including *H. rotundata* (Seong et al. 2006), but I did not see this response with *H. rotundata* and bacteria (Figure 3.5). Laboratory experiments by Seong et al. (2006) were run at a constant irradiance level as bacteria concentrations varied, in my field experiments bacteria concentration and irradiance both varied. The range of bacterial concentrations Seong et al. (2006) tested was $>1.0 \times 10^6$ to $21.0 \times 10^6 \text{ mL}^{-1}$, while bacteria concentrations in the Choptank River during my experiments ranged from 0.9×10^6 to $2.9 \times 10^6 \text{ mL}^{-1}$. Based on Seong and colleague's results I would have expected to see a linear relationship between *H. rotundata* ingestion rates and bacteria concentration but I did not. It is possible that if irradiance levels were constant, I could have seen the functional response of ingestion rate to increased bacteria concentrations. Nonetheless, my findings suggest that irradiance likely has a stronger effect on *H. rotundata* ingestion rates than bacterial concentrations *in situ*.

The benefits and drawbacks of using fluorescent microspheres to measure ingestion rates have been addressed previously in the literature (McManus and Okubo 1991; Vaqué et al. 1994; Domaizon et al. 2003). Some studies have found discrimination against (Sherr et al. 1987; Sanders et al. 1989) and preference for microspheres (Sanders and Gast 2012) compared to fluorescently labeled bacteria, which would underestimate or overestimate ingestion, respectively. Size selectivity appears to be the most important factor in determining which particles are preferentially grazed by nanoflagellates

(Domaizon et al. 2003; Sanders and Gast 2012). I selected 0.5 μm diameter microspheres because they were the easiest to see and count inside cells and rarely stuck to the outside of cells, therefore providing the most accurate counts.

H. rotundata can form large blooms (Seong et al. 2006; Balzano et al. 2015; Millette et al. 2015). Now that I have robust estimates of how many bacteria an individual *H. rotundata* cell is capable of ingesting per hour and what controls their ingestion rates, the next step is to understand how *H. rotundata* blooms impact the bacteria community and nutrient cycling in the microbial loop. My data show when *H. rotundata* reached elevated (3000 cells mL^{-1}) or bloom (10^4 cells mL^{-1}) abundances they were capable of ingesting up to 100% of the bacteria standing stock daily. Future research comparing *H. rotundata* ingestion rates and bacterial division rates is necessary to know if *H. rotundata* blooms are capable of controlling field bacteria populations.

H. rotundata is a mixotroph that increases its ingestion rate when light is limiting (below 400 $\mu\text{mol photons m}^{-2} \text{sec}^{-1}$). This likely allows them to out-compete other phytoplankton species and form winter blooms under the low light conditions. Under bloom abundances, the *H. rotundata* population is estimated to ingest >50% of the bacterial standing stock, however the impact on bacterial population's dynamics is not known. Future research should address if blooms of *H. rotundata* are capable of controlling or reducing the *in situ* bacterial population and how this affects the DOM pool and microbial loop in winter.

Reference

- Balzano, S., A.V. Ellis, C. Le Lan, and S.C. Leterme (2015) Seasonal changes in phytoplankton on the north-eastern shelf of Kangaroo Island (South Australia) in 2012 and 2013. *Oceanologia* 57:251-262.
- Båmsted, J., D.J. Gifford, X. Irigoien, A. Atkinson, and M. Roman (2000) In: R. Harris, P. Wiebe, J. Lenz, H.R. Skjoldal, and M. Huntley (eds) ICES zooplankton methodology manual. Academic, London. P. 297-399.
- Cohen, R. R. H (1985) Physical processes and the ecology of a winter dinoflagellate bloom of *Katodinium rotundatum*. *Mar Ecol Prog Ser* 26:135-144.
- Czypionka, T., C.A. Vargas, N. Silva, G. Daneri, H.E. González, and J. L. Iriarte (2011) Importance of mixotrophic nanoplankton in Aysén Fjord (Southern Chile) during austral winter. *Cont Shelf Res* 31: 216-224.
- Domaizon, I., S. Viboud, and D. Fontvieille (2003) Taxon-specific and season variation in flagellates grazing on heterotrophic bacteria in the oligotrophic Lake Annecy – importance of mixotrophy. *FEMS Microbiol Ecol* 46:317-329.
- Fisher, T.R., A.B. Gustafson, K. Sellner, R. Lacouture, L.W. Haas, R.L. Wetzel, R. Magnien, D. Everitt, B. Michaels, and R. Karrh (1999) Spatial and temporal variation of resource limitation in Chesapeake Bay. *Mar Biol* 133:763-778.
- Fisher, T.R., A.B. Gustafson, G.M. Radcliffe, K.L. Sundberg, and J.C. Stevenson (2003) A long-term record of photosynthetically available radiation (PAR) and total solar energy at 38.6°N, 78.2°W. *Estuaries* 26:1450-1460.
- Flynn, K.J., D.K. Stoecker, A. Mitra, J.A. Raven, P.M. Glibert, P.J. Hansen, E. Granéli, and J.M. Burkholder (2013) Misuse of the phytoplankton-zooplankton dichotomy: the need to assign organisms as mixotrophs within plankton functional types. *J Plankton Res* 35(1): 3-11.
- Frost, B.W (1972) Effects of size and concentration of food particles on the feeding behavior of the marine planktonic copepod *Calcanus pacificus*. *Limnol Oceanogr* 17:805-815.
- Guillard, R.R.L (1975) Culture of phytoplankton for feeding marine invertebrates. In W. L. Smith and M. H. Chanley. [eds.], Culture of marine invertebrate animals. Plenum.
- Hansen, G (1995) Analysis of the thecal plate pattern in the dinoflagellate *Heterocapsa rotundata* (Lohmann) comb. nov. (= *Katodinium rotundatum* (Lohmann) Loeblich). *Phycologia* 34:166-170.

Jeong, H.J., Y.D. Yoo, K.A. Seong, J.H. Kim, J.Y. Park, S. Kim, S.H. Lee, J.H. Ha, and W.H. Yih (2005) Feeding by the mixotrophic red-tide dinoflagellate *Gonyaulax polygramma*: mechanisms, prey species, effects of prey concentration, and grazing impact. *Aquat Microb Ecol* 38:249-257.

Jeong, H.J., Y.D. Yoo, J.S. Kim, K.A. Seong, N.S. Kang, and T.H. Kim (2010) Growth, feeding and ecological roles of the mixotrophic and heterotrophic dinoflagellates in marine planktonic food webs. *Ocean Sci J* 45:65-91.

Jaschinski, S., S. Flöder, T. Petenati, and G. Göbel (2015) Effects of nitrogen concentration on the taxonomic and functional structure of phytoplankton communities in the Western Baltic Sea and implications for the European water framework directive. *Hydrobiologia* 745: 201-210.

Kang, N.S., H.J. Jeong, Y.D. Yoo, E.Y. Yoon, K.H. Lee, K. Lee, and G. Kim (2011) Mixotrophy in the newly described phototrophic dinoflagellate *Woloszynskia cincta* from Western Korean waters: feeding mechanism, prey species and effect of prey concentration. *J Euk Microbio* 58:152-170.

Kemp, W.M., W.R. Boynton, J.E. Adolf, D.F. Boesch, et al (2005) Eutrophication of Chesapeake Bay: historical trends and ecological interactions. *Mar Ecol Prog Ser* 303:1-29.

Laybourn-Parry, J., W.A. Marshall, H.J. Marchant (2005) Flagellate nutritional versatility as a key to survival in two contrasting Antarctic saline lakes. *Freshwater Biol* 50: 830-838.

Lee, S.H. (1993) Measurement of carbon and nitrogen biomass and biovolume from naturally derived marine bacterioplankton. In: Kemp, P.F., B.F. Sherr, E.B. Sherr, J.J. Cole (eds) *Aquatic Microbial Ecology*. Lewis Publication, Boca Raton, FL, p. 319-325.

Lee, S.K., H.J. Jeong, S.H. Jang, K.H. Lee, N.S. Kang, M.J. Lee, and Éric Potvin (2014) Mixotrophy in the newly described dinoflagellate *Ansanella granifera*: feeding mechanism, prey species, and effect of prey concentration. *Algae* 29:137-152.

Legrand, C., E. Granéli, and P. Carlsson (1998) Induced phagotrophy in the photosynthetic dinoflagellate *Heterocapsa triquetra*. *Aquat Microb Ecol* 15: 65-75.

Litaker, R.W., P.A. Tester, C.S. Duke, B.E. Kenney, J.L. Pinckney, and J. Ramus (2002) Seasonal niche strategy of the bloom-forming dinoflagellate *Heterocapsa triquetra*. *Mar Ecol Prog Ser* 232: 45-62.

Lund, J.W.G, C. Kipling, and E.D. LeCren (1958) The inverted microscope method of estimating algal numbers and the statistical basis of estimation by counting. *Hydrobiologia* 11:143-169.

McKie-Krisberg, Z.M., R.J. Gast, and R.W. Sanders (2015) Physiological responses of three species of Antarctic mixotrophic phytoflagellates to changes in light and dissolved nutrients. *Microbiol Aquat Syst* 70: 21-29.

McManus, G.B. and A. Okubo (1991) On the use of surrogate food particles to measure protistan ingestion. *Limnol Oceanogr* 36:613-617.

Millette, N.C., J.J. Pierson, and D.K. Stoecker (2015a) Top-down control of micro- and mesozooplankton on winter dinoflagellate blooms of *Heterocapsa rotundata*. *Aquat Microb Ecol* 76: 15-25.

Perry, M.J., M.C. Talbot, and R.S. Alberte (1981) Photoadaptation in marine phytoplankton: response of the photosynthetic unit. *Mar Biol* 62: 91-101.

Salas, R., U. Tillmann, and S. Kavanagh (2014) Morphological and molecular characterization of the small armoured dinoflagellate *Heterocapsa minima* (Peridinales, Dinophyceae). *Europ J Phycol* 49: 413-428.

Sanders, R.W., K.G. Porter, S.J. Bennett, and A.E. DeBiase (1989) Seasonal patterns of bacterivory by flagellates, ciliates, rotifers, and cladocerans in a freshwater planktonic community. *Limnol Oceanogr* 34:673-687.

Sanders, R.W. and R.J. Gast (2012) Bacterivory by phototrophic picoplankton and nanoplankton in Arctic waters. *FEMS Microbiol Ecol.* 82:242-253.

Sellner, K. G., R.V. Lacouture, S.J. Cibik, A. Brindley, and S.G. Brownlee (1991) Importance of a winter dinoflagellate-microflagellate bloom in the Patuxent River estuary. *Estuar Coast Shelf S* 32: 27-42.

Seong, K.A., H.J. Jeong, S. Kim, G.H. Kim, and J.H. Kang (2006) Bacterivory by co-occurring red-tide algae, heterotrophic nanoflagellates, and ciliates. *Mar Ecol Prog Ser* 322: 85-97.

Shahi, N., A. Godhe, S.K. Mallik, K. Härnström, and B.B. Nayak (2015) The relationship between variation of phytoplankton species composition and physico-chemical parameters in northern coastal waters of Mumbai, India. *Indian Journal of Geo-Marine Sciences* 44.

Stoecker, D.K., A. Li, D.W. Coats, D.E. Gustafson, and M.K. Nannen (1997) Mixotrophy in the dinoflagellate *Prorocentrum minimum*. *Mar Ecol Prog Ser* 152: 1-12.

Stoecker, D.K (1999) Mixotrophy among dinoflagellates. *J Eukaryot Microbiol* 45: 397-401.

Tyler, M.A. and H.H. Seliger (1981) Selection for a red tide organism: physiological responses to the physical environment. *Limnol Oceanogr* 26: 310-324.

Van Nevel, S. S. Koetsch, H.U. Weilenmann, N. Boon, and F. Hammes (2013) Routine bacterial analysis with automated flow cytometry. *J Microbiol Meth* 94:73-76.

Vaqué, D., J.M. Gasol, and C. Marrasé (1994) Grazing rates on bacteria: the significance of methodology and ecological factors. *Mar Ecol Prog Ser* 109:263-274.

Tables and Figures

Table 3.1

Source of variance	df	MS	<i>F</i>	<i>P</i>
Irradiance	4	0.0003	16.70	<0.0001
NH ₄ ⁺	2	0.0002	8.95	0.0009
Irradiance x NH ₄ ⁺	8	<0.0001	4.84	0.0007

Laboratory Experiment 1-Results of two-way ANOVA with replication for community grazing coefficient experiments. Dependent variable is *H. rotundata* community grazing coefficient (d^{-1}) on bacteria. Data are shown in Figure 3.1.

Table 3.2

Treatment	Replicate	PAR	I	Chl <i>a</i>	μ	Carbon	C:Chl
L	A	44	5.35	1.81	0.20	55.9	30.9
	B	28.9	8.32	2.18	-0.24	84.1	38.6
	C	43.8	6.77	1.49	0.24	53.9	36.2
	Average	38.9 \pm 6.12	6.81 \pm 0.62	1.83 \pm 0.24	0.07 \pm 0.19	64.6 \pm 11.9	35.2 \pm 2.8
L1	A	37.3	4.72	1.68	0.21	53.6	31.9
	B	34.3	5.14	n/a	0.05	54.3	n/a
	C	10.8	10.57	2.28	0.04	66.2	29.0
	Average	27.47 \pm 10.26	6.81 \pm 1.97	1.98 \pm 0.42	0.10 \pm 0.07	58.0 \pm 5.0	30.5 \pm 1.4
L2	A	10.8	9.79	2.27	0.14	58.3	25.7
	B	21.1	6.86	3.1	-0.14	76.7	24.7
	C	13.3	8.01	3.1	0.22	64.1	20.7
	Average	15.07 \pm 3.80	8.22 \pm 0.52	2.82 \pm 0.34	0.07 \pm 0.13	66.3 \pm 6.7	23.7 \pm 1.9
L4	A	6.3	5.55	2.09	0.02	59.0	28.2
	B	4.8	12.13	2.43	0	76.1	31.3
	C	1.2	4.93	3.17	-0.27	100.2	31.6
	Average	4.11 \pm 4.11	7.54 \pm 2.58	2.56 \pm 0.55	-0.08 \pm 0.11	78.4 \pm 14.6	30.4 \pm 1.3
D	A	0	13.93	2.92	-0.28	72.5	24.8
	B	0	12.25	1.67	0.07	40.3	24.1
	C	0	15.40	2.92	-0.31	85.7	29.4
	Average	0 \pm 0.00	13.86 \pm 1.11	2.50 \pm 0.51	-0.17 \pm 0.15	66.2 \pm 16.5	26.1 \pm 2.0

Laboratory Experiment 2-*Heterocapsa rotundata* ingestion rates (I, bacteria *H. rotundata*⁻¹ hr⁻¹), cellular chlorophyll *a* concentration (Chl *a*, pg chlorophyll *a* *H. rotundata*⁻¹), population growth rate (μ , d⁻¹), cellular carbon concentration (pg carbon *H. rotundata*⁻¹), and cellular carbon:chlorophyll *a* at the different irradiance levels (PAR, $\mu\text{mol photons m}^{-2} \text{s}^{-1}$) for each treatment. The average (\pm SE) of each factor in each treatment is given.

Table 3.3

Date	Temperature	Salinity	NH ₄ ⁺	NO _x	PO ₄ ³⁻	N:P	PAR	(h:m)
1/27	1.1	13.3	2.8	16.7	0.14	140	480	10:4
1/29	1.3	12.5	3.1	15.2	0.15	122	520	10:8
2/1	2.5	12.8	2.0	17.3	0.12	160	1250	10:14
2/3	4	11.1	4.9	32.0	0.23	160	260	10:18
2/5	4.5	10.6	4.5	36.6	0.16	257	240	10:22
2/8	4.3	10.3	3.1	42.0	0.13	347	440	10:29
2/10	4.1	11.9	2.6	20.4	0.12	192	720	10:33
2/12	2.1	11.6	1.7	25.6	0.12	227	2000	10:38
2/15	-0.1	10.6	2.8	36.1	0.10	389	620	10:44
2/17	1.6	9.5	3.4	50.3	0.08	672	2000	10:49
2/19	1.7	8.6	3.1	66.0	0.10	691	1400	10:54
2/29	5.2	10.4	1.9	36.7	0.14	276	425	11:18
3/2	6.5	10.9	1.9	28.7	0.13	235	1500	11:23
3/4	5.9	7.9	1.8	57.5	0.11	539	630	11:28
3/7	5.7	9.5	1.6	41.0	0.11	387	2150	11:35
3/9	7.3	9.3	1.5	42.7	0.09	492	2200	11:40
3/11	9.1	10.4	1.7	31.9	0.10	336	270	11:45
3/14	9.8	9.6	2.1	37.7	0.09	442	225	11:53
3/16	10.3	9.3	2.3	39.5	0.11	380	1750	11:58
3/18	11.2	8.8	1.5	38.8	0.09	447	1900	12:3
Average	4.9 ± 0.8	10.4 ± 0.3	2.5 ± 0.2	35.6 ± 3.0	0.1 ± 0.01	345 ± 38	1049 ± 169	11:1

Temperature (°C), salinity, NH₄⁺ (μM-N), NO₃⁻ + NO₂⁻ (NO_x) (μM-N), PO₄³⁻ (μM-P), NH₄⁺ + NO_x: PO₄³⁻ (N:P), Irradiance at 0900 h (PAR) (μmol photons sec⁻¹ m⁻²), and day-length (hour:minute) in the Choptank River each day an experiment was set-up between 1/27/2016 and 3/18/2016.

Table 3.4

Factor	df	r²	p-value
NH ₄ ⁺	19	0.001	0.92
NO _x	19	0.02	0.55
PO ₄ ³⁻	19	0.01	0.69
N:P	19	0.03	0.44

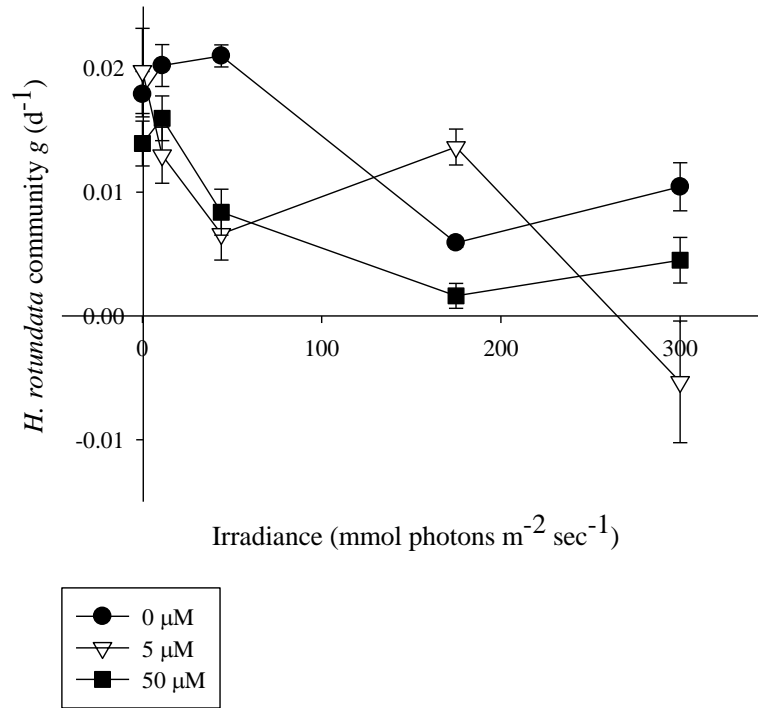
Linear regression analysis of *H. rotundata* bacterial ingestion rates collected in the Choptank River during the 2016 winter compared to ammonium (μM-N), nitrate + nitrite (μM-N), and phosphate (μM-P) concentrations and N:P. All r² were non-significant.

Figure 3.1



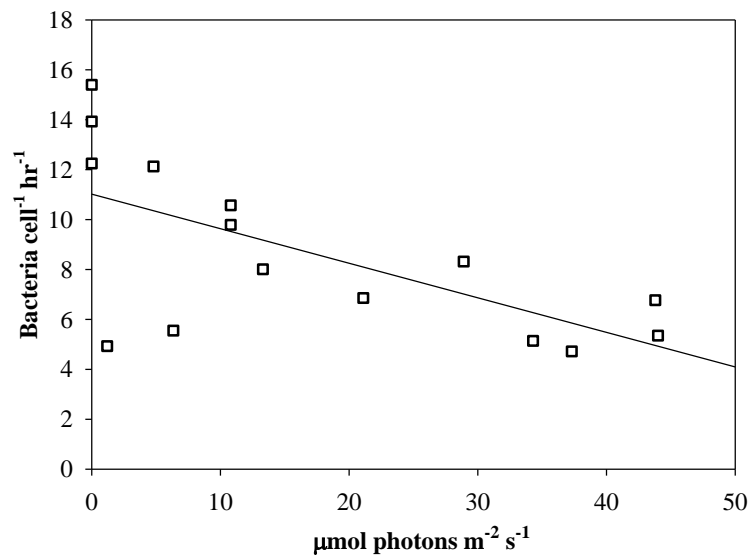
Location of sampling site in Choptank River, MD on the Bill Burton Fishing Pier.

Figure 3.2



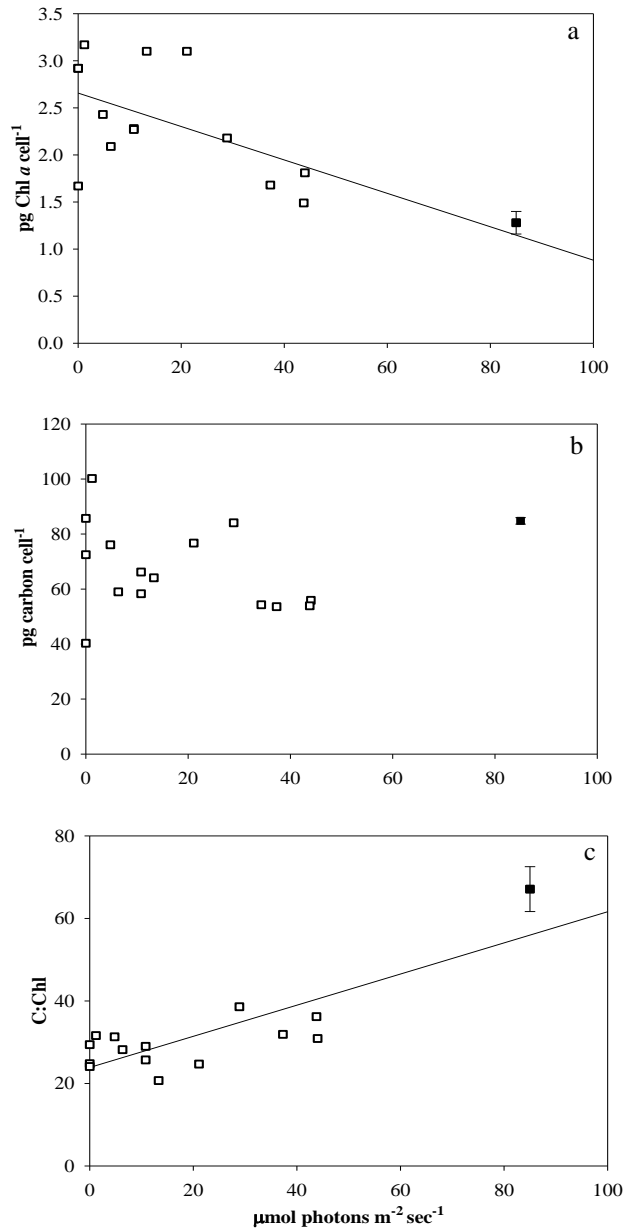
Laboratory Experiment 1: *Heterocapsa rotundata* community grazing coefficient g (d⁻¹) at different irradiance levels ($\mu\text{mol photons m}^{-2} \text{s}^{-1}$) for three different ammonium concentrations (μM). Bars indicate SE.

Figure 3.3



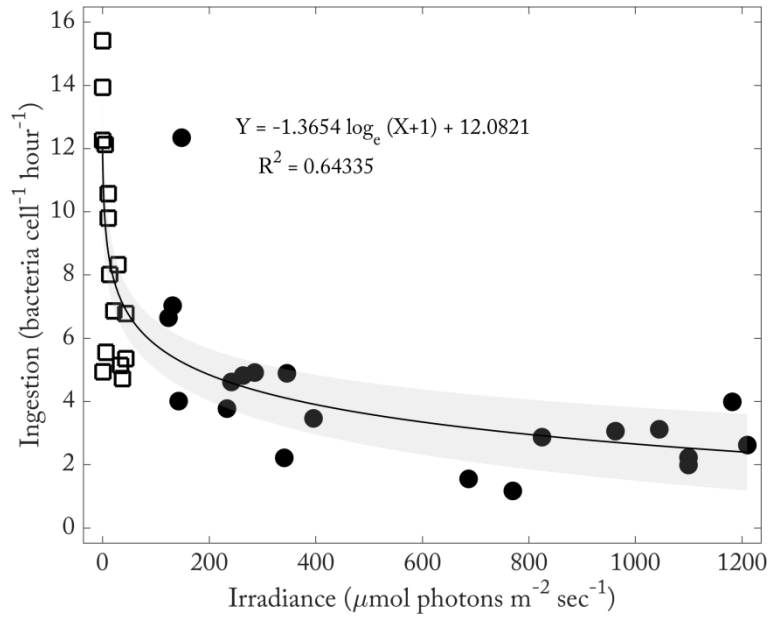
Laboratory Experiment 2. *Heterocapsa rotundata* ingestion rates (bacteria cell⁻¹ hr⁻¹) at different irradiance levels (μmol photons m⁻² s⁻¹).

Figure 3.4



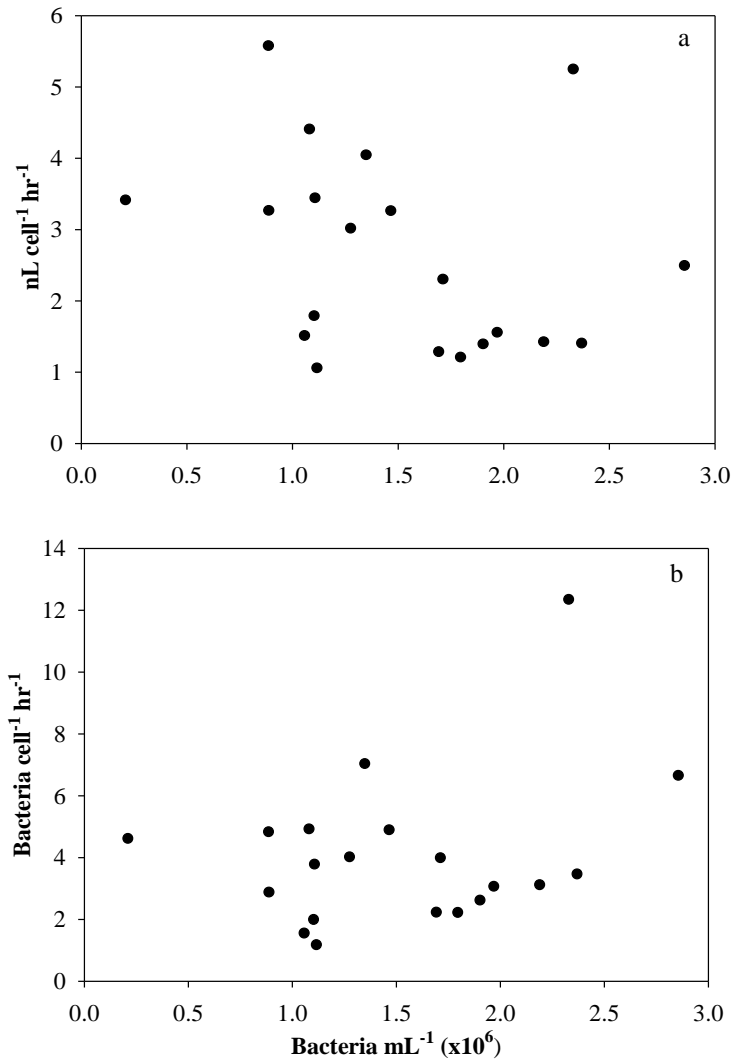
Variation of *H. rotundata*'s cellular chlorophyll *a* concentration (pg Chl. *a* cell⁻¹) (a), carbon concentration (pg carbon cell⁻¹) (b), and C:Chl ratio (c) at different irradiance levels. Filled squares are the initial values of the *H. rotundata* culture and the open squares are experimental values after 48 hrs at treatment irradiance levels. Bars = SE for initial values.

Figure 3.5



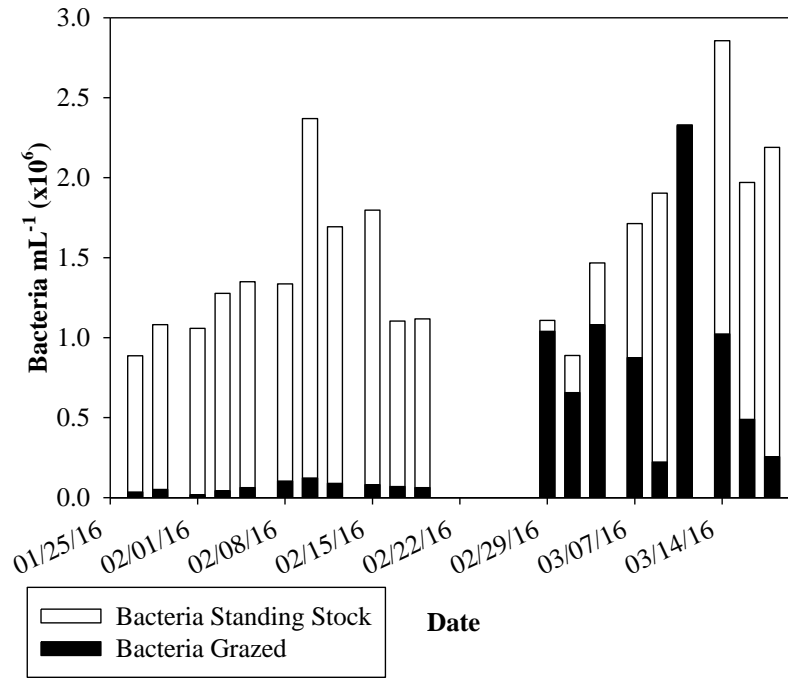
Ingestion rates of *H. rotundata* (bacteria hr⁻¹) collected from the Choptank River in winter 2016 (□) and in culture (●) at different irradiance levels (μmol photons m⁻² s⁻¹) with a log functional response curve. Grey area denotes 95% confidence intervals.

Figure 3.6



The clearance rates (nL *H. rotundata*⁻¹ hr⁻¹) (a) and ingestion rates (bacteria cell⁻¹ h⁻¹) (b) of *H. rotundata* measured at various bacterial concentrations (mL⁻¹)

Figure 3.7



Estimated bacterial standing stock (open bars) and the bacteria ingested by the *H. rotundata* population (black bars) in the Choptank River during winter 2016.

Chapter 4: Impact of winter temperature and *Heterocapsa rotundata* abundance on the production and survival of winter *Eurytemora carolleeae* eggs and nauplii

Introduction

In Chesapeake Bay *Eurytemora carolleeae* (cf. *E. affinis*, Alekseev and Souissi, 2011) dominates the zooplankton in winter and early spring (Devreker et al., 2012; Kimmel et al., 2004) and is an important prey item for striped bass (*Morone saxatilis*) larvae hatched in spring (Shoji et al., 2005). Kimmel et al. (2006) showed that wet winters resulted in high abundances and wide distribution of the copepod *E. carolleeae* in spring in Chesapeake Bay. The wide distribution is most likely due to high river input that transports copepods farther down the bay and lowers the salinity, which provides suitable habitat for *E. carolleeae*. There is a lack of a suitable mechanistic explanation for the increase in *E. carolleeae* abundance (Kimmel et al. 2006). Wet winters also cause *H. rotundata* blooms (Cohen 1985; Sellner et al 1991), and it may follow that high spring copepod abundances can be mechanistically attributed to the winter through these blooms.

In my first chapter I showed that large winter blooms of *Heterocapsa rotundata* are grazed on by *E. carolleeae* but *E. carolleeae* copepodite abundance does not appear to increase in response to these blooms (Millette et al., 2015). Copepod development rate is proportional to ambient water temperatures, and at winter temperatures in the Chesapeake Bay *E. carolleeae* requires nearly two months to develop from egg to adult (Heinle and Flemer, 1975). Thus, eggs hatched in winter would remain nauplii for

approximately one month before metamorphosing into the copepodite stages (Heinle and Flemer, 1975). 5.5°C is the coldest temperature at which *E. carolleae*'s developmental rate has been estimated but winter water temperatures in the Chesapeake Bay can get as low as 0.1 °C (Millette et al., 2015). Given the slow development time of *E. carolleae* in the winter, egg production rate and subsequent nauplii survival in winter could be impacting spring copepodites abundance, not winter abundance. Investigating egg production rates and naupliar survival rate on *H. rotundata* is relevant because *H. rotundata* experience a large range of abundance in winter and dominate the phytoplankton community (Millette et al., 2015). *H. rotundata* is likely the prey to have the largest impact on egg production rate and nauplii survival.

If food is limiting, then copepod egg production rate may be reduced (Kimmerer et al., 2005). During some winters the abundance of >10µm phytoplankton never exceeds 500 mL⁻¹ and other winters the phytoplankton abundance can fluctuate from 100 mL⁻¹ to 20,000 mL⁻¹ over the course of five weeks (Millette et al., 2015). It is unknown if ranges in phytoplankton abundances causes food limitation in *E. carolleae* during winter, or what impact it has on egg production rates and egg hatching success.

If *E. carolleae* are not food limited, then temperature is likely important in determining egg production rate of *E. carolleae* (Devreker et al. 2012; Lloyd et al. 2013). Temperature is positively related to clutch size (CS) and inter-clutch time (ICT) (Devreker et al. 2012). Lloyd et al. (2013) devised an equation to estimate clutch size at different temperatures (T, °C):

$$\text{Clutch Size} = 112 - 3.76 * T$$

Based on this equation for clutch size *E. carolleae* should be producing ~100 eggs per clutch between 3-4 °C.

Devreker et al. (2012) created a temperature (T, °C) dependent equation to measure ICT, which is the time from when a clutch is laid to when a new clutch is laid:

$$ICT = 30.31*(T^{-0.378})-7.637$$

Inter-clutch time increases at a faster rate compared to clutch size as temperature decreases. Thus egg production rate decreases as temperature increases because even though copepods are producing more eggs per clutch, the eggs are taking longer to hatch. To calculate egg production rate (EPR) clutch size is divided by inter-clutch time:

$$EPR = CS/ICT$$

There is an alternate equation that could be used that breaks up the ICT into two parts, the egg development time (EDT) and the latency time (LT). Both EDT and LT can be predicted separately and added together with temperature dependent equations to equal ICT (Devreker et al., 2012). This approach tends to overestimate LT and as a result underestimate EPR (Devreker et al., 2012).

I investigated the egg production rate of adult *E. carolleae*, the hatching success rate of eggs produced, and the survivorship of *E. carolleae* nauplii in the winter (Dec 21st-March 19th) to address the cause of high *E. carolleae* copepodite abundance in the spring (March 20th-June 19th). I specifically tested for a significant relationship between *H. rotundata* abundance and all these factors in order to assess if *H. rotundata* blooms have any impact of spring *E. carolleae* abundances. If the population of *E. carolleae* in

the winter is not food limited, then egg production rate should be related to temperature. Therefore, I also tested for a significant relationship between *E. carolleae* egg production rate and temperature to compare my results to published relationships.

Methods

Field Experiments: On five separate occasions between December 21, 2013 and March 21, 2014 I conducted egg production experiments on *in situ* *E. carolleae*. I collected 10-15 L of water from the Bill Burton Fishing Pier and filtered the water through 20 µm mesh to remove all micro- and mesozooplankton. I also collected live copepods for the experiments with a 50 cm diameter ring net fitted with 200 µm mesh.

Copepod egg production experiments were set up according to Vehmaa et al. (2012) with the goal to test whether *in situ* egg production is limited by food quantity. This experimental design uses the *in situ* phytoplankton community as the control group with treatment groups using the same community spiked with cultured phytoplankton. Triplicate 1L bottles of the control and treatment groups were used, with 10,000 cells mL⁻¹ of cultured *H. rotundata* added to treatment bottles from a culture reared at 5°C on a 12:12 light cycle. Five egg bearing females and one mature male *E. carolleae* were sorted from the plankton tow and added to each control and treatment bottle.

The bottles were placed on a plankton wheel in an environmental chamber at 5°C with a 12:12 light cycle for seven days under dim light conditions. After seven days all the *E. carolleae* nauplii in each bottle were filtered onto a 64 µm mesh sieve and preserved in 5% Lugol's solution. Any females with eggs sacs still attached were placed in individual wells in a 6-well tissue culture plate with 15 ml filtered water. These plates with females in them were placed back in the environmental chamber for seven days to

allow viable eggs to hatch. I incubated the females for seven days because that is how many days it takes for eggs to hatch at 5°C according to the Devreker et al. (2012) and Lloyd et al. (2013) equations. After seven days the nauplii and eggs were preserved in Lugol's and counted with a Zeiss stereo dissecting microscope.

Egg production rate (eggs female⁻¹ d⁻¹) calculated by dividing the total number of nauplii (N) and loose, unhatched eggs (E) in each single bottle by the number of females without an egg sac in that bottle (F) and the number of days the experiment ran (t) (7).

$$EPR=(N+E)/F/t$$

There were two potential experimental lengths, 7 days for first time point and 14 days for second time point. Hatching success rate for the first seven days was calculated by dividing the number of nauplii in a bottle by the total amount of nauplii and loose, unhatched eggs in the same bottle. Hatching success rate for the second seven days was calculated by dividing the number of nauplii in a well by the total amount of nauplii and loose, unhatched eggs in the same well.

I calculated the average and standard error for egg production and hatching success rate for the control treatments and experiment treatments each week. Differences in egg production rate between the control and experiment treatments were tested for each week with a two sample t-test assuming equal variation (P<0.05). To test whether *H. rotundata* abundance or temperature is related to egg production rate or hatching success rate, I fit a linear regression equation to the data. If the slope of the linear model was significantly different from zero (P<0.05), it suggests that there is a relationship between the tested factor and egg production rate.

Laboratory Experiments: *E. carolleae* nauplii and *H. rotundata* were reared in batch cultures at 4°C and 10.8 salinity on a 12:12 light cycle at 85 $\mu\text{mol photons m}^{-2} \text{sec}^{-1}$. The *H. rotundata* culture was kept in f/2-Si medium made from 0.2 μm filtered and autoclaved Choptank River water, while *E. carolleae* was kept in 0.2 μm filtered Choptank River water. *E. carolleae* were isolated from the Choptank River in April 2014 and *H. rotundata* were obtained from the culture collection at Scandinavian Culture Collection of Algae and Protozoa (Strain # K-0483). *E. carolleae* used in the experiments were in the third to sixth naupliar stages, which are known to feed (Merrell and Stoecker, 1998). I performed two separate experiments to measure grazing rates and survival rates. Both experiments were conducted in f/2-Si medium made with 0.2 μm filtered and autoclaved Choptank River water at ambient salinity (8-12), 4°C, and 12:12 light cycle at 85 $\mu\text{mol photons m}^{-2} \text{sec}^{-1}$.

Naupliar Grazing: Twenty-two grazing experiments were conducted in the summer of 2014. For each experiment, five nauplii in various feeding stages were randomly selected and placed in each of three 20 mL scintillation vials, each containing 10 mL of filtered seawater and a predetermined concentration of *H. rotundata*. These, along with three control vials containing only *H. rotundata*, were incubated for 24 hours. At the beginning and end of the experiments (t_0 and t_{24}) I preserved 2.5 mL samples from each of the vials in 5% Lugol's solution. *H. rotundata* concentration was counted from each sample with a 1mL Sedgewick-Rafter Counting Cell on a Nikon Eclipse E800 microscope at 10x magnification. I calculated the clearance ($\text{mL copepod}^{-1} \text{d}^{-1}$) and ingestion ($\text{cells eaten copepod}^{-1} \text{d}^{-1}$) rates of the nauplii using equations from Frost (1972). The full equations can be found in chapter 1.

Survival Experiments: Nauplii in survival experiments were subjected to six concentrations of *H. rotundata*, 300, 500, 1,000, 3,000, 5,000, and 10,000 cells mL⁻¹, with a control group in filtered media without *H. rotundata*. Experiments ran for 15 days in 60mL wide mouth jars with 10 nauplii and 30mL of water per jar. The containers were kept on a rotating plankton wheel (1 rpm) to keep *H. rotundata* in suspension. Every three days, nauplii were gently collected on a sieve to record mortality and the number of individuals that moulted to copepodite stage. Copepodites and dead nauplii were removed and remaining nauplii were returned to vials with fresh media containing the initial concentration of *H. rotundata*. Based on the ingestion rate I calculated from the grazing experiments, the nauplii would not be able to remove *H. rotundata* at a higher rate than *H. rotundata* growth; *H. rotundata*'s average growth rate in the culture is 0.5 d⁻¹ (data not shown).

I estimated the volume of individual *H. rotundata* cells in the culture using the equation for a rotational ellipsoid, volume = $\pi/6 * \text{diameter}^2 * \text{height}$. Average measured length (\pm SE) was 10.17 (\pm 0.91) μm and average measured width (\pm SE) was 6.67 ± 0.78 μm based on 30 randomly selected cells. Cellular carbon content *H. rotundata* was calculated using the equation to convert cell volume to carbon content for dinoflagellates, $\text{pg C cell}^{-1} = 0.760 * \text{volume}^{0.819}$, from Menden-Deuer and Lessard (2000). Average carbon concentration (\pm SE) was 68 (\pm 15) pgC cell^{-1} . The cultured *H. rotundata* were about half the size of field collected *H. rotundata* measured in chapter one.

Results

Egg Production Rates: I conducted five different egg production experiments with 10 different concentrations of *H. rotundata*, from <100 cells mL⁻¹ to 25,000 cells mL⁻¹

(Table 4.1). There was no significant difference between the control group and experimental group for any of the experiments (Table 4.1). The average EPR among *E. carolleae* for different treatments ranged from 3.2 ± 0.5 to 4.6 ± 1.0 eggs copepod⁻¹ d⁻¹ with an overall average of 3.9 ± 0.2 eggs copepod⁻¹ d⁻¹ (Table 4.1). There is no relationship between the abundance of *H. rotundata* and the EPR of *E. carolleae* ($r^2 = 0.05$, $p = 0.53$, linear regression, Figure 4.1a). There was a significant, positive relationship between the estimated EPR and the *in situ* temperature that copepods were collected ($r^2 = 0.44$, $p = 0.04$, linear regression, Figure 4.2a).

There was no relationship between hatching success and *H. rotundata* abundances ($r^2 = 0.04$, $p = 0.56$, linear regression, Figure 4.1b) or temperature and *H. rotundata* abundance ($r^2 = 0.25$, $p = 0.14$, Figure 4.2b). The average hatching success rate among *E. carolleae* for different treatments ranged from 55 ± 17 to $94 \pm 3\%$ with an overall average of $77\% \pm 4$.

Nauplii Experiments: I compared the *E. carolleae* naupliar clearance and ingestion rates to the *H. rotundata* concentrations to characterize the relationship between *H. rotundata* concentration and naupliar grazing. I fitted the ingestion (*I*) data to a Holling type II grazer functional response for different *H. rotundata* concentrations (*P*) using nonlinear curve estimation (MATLAB Statistics Toolbox) to estimate the maximum ingestion rate (I_{max}) and the half saturation constant (*K*) of the curve:

$$I = \frac{I_{max}P}{K+P}$$

Both coefficients for the Holling type II curve were significantly different from zero ($P < 0.05$), with values (\pm SE) of *K* and I_{max} calculated to be $245 (\pm 154) \mu\text{g C L}^{-1}$ and $0.22 (\pm 0.07) \mu\text{g copepod}^{-1} \text{ day}^{-1}$, respectively (Figure 4.3).

I fitted a logarithmic equation (MATLAB Statistics Toolbox) to the nauplii mortality data at different *H. rotundata* concentrations (Figure 4.4):

$$N_m = 89.6 - 7.6 \log_e (A_{Hr} + 1)$$

where N_m is naupliar mortality after 15 days expressed as percent and A_{Hr} is the abundance of *H. rotundata*. Using this relationship, 50% mortality after 15 days (LD_{50}), occurs at 182 cells L^{-1} , or 12.4 $\mu g L^{-1}$.

Discussion

Heterocapsa rotundata abundance does not impact the number of *E. carolleae* nauplii produced in winter, but they can increase the survival rate of the nauplii once they start feeding. *Eurytemora carolleae* egg production rates were not impacted by *H. rotundata* abundance but there was a correlation between temperature and egg production rates. If *E. carolleae*'s egg production rate is not impacted by *H. rotundata* abundance but is impacted by water temperature, this suggests *E. carolleae* are not food limited in the winter, even at low abundances of phytoplankton. The survival experiments demonstrated that higher *H. rotundata* abundances can support higher nauplii abundances, as hypothesized.

The data suggests that regardless of prey abundance in the water column, copepods will continue to produce the expected amount of eggs based on the temperature of the water with a high hatching success rate. There was a week when abundance of *H. rotundata* was 31 cells mL^{-1} and other prey abundance was low but *E. carolleae* egg production rate remained high (Table 4.1). I propose two possibilities for high egg production rates under low prey abundance: (1) *E. carolleae* stores up lipids they can live off of when prey abundance is low. I have photographic evidence of lipid storages in

E. carolleae collect in the 2014 winter (Figure 4.5). (2) There is a delay between when food is consumed by *E. carolleae* and that energy is turned into eggs. Egg production rate is not effected by the current prey availability but by prey they consumed earlier, maybe up to a month. Both of these hypotheses are equally plausible and not mutually exclusive but require further testing.

While egg production rate decreased with water temperature, as expected, the production rates were rarely accurately predicted by the Lloyd et al. (2013) and Devreker et al. (2012) equations. When I calculated the ICT directly with water temperature, the predicted EPR values were always higher than EPR I measured, sometime over 50% higher (Table 4.1). When I calculated the ICT by adding up calculated values of EDT and LT, the predicted EPR values were slight close to the EPR I measured. Using this method, when the temperature was $>4^{\circ}\text{C}$ the predicted EPR was the same as measured EPR (Table 4.1). Although, $<4^{\circ}\text{C}$, as water temperature decreased, the predicted EPR decreased at a higher rate compared to the measured rates. This questions the accuracy of those equations to predict *E. carolleae* egg production rates at winter temperatures. The lowest temperature experimental test to create the Lloyd et al. (2013) and Devreker et al. (2012) equations was 7°C and the highest temperature I tested was 4.8°C . Replicating Lloyd and Devreker's experiments at temperatures between $0-4^{\circ}\text{C}$ will create more accurate models to predict *E. carolleae*'s egg production rate.

I compared the ingestion rates for *E. carolleae* nauplii that I estimated at winter temperatures to nauplii ingestion rates reported for other copepod species (Table 3.2). In my experiments I did not differentiate between the different feeding stages of nauplii and this may account for the large variability in the ingestion rate measurements. Measured

ingestion rates of copepod nauplii appear to be species specific (Table 3.2). My estimated maximum ingestion rate on *E. carolleae* nauplii is comparable to estimated ingestion rates of other copepod nauplii, especially other *E. carolleae* nauplii. Stoecker and Merrell (1998) measured ingestion rates of *E. carolleae* nauplii on natural populations of microzooplankton and phytoplankton. Similar to my methods, they did not distinguish between the feeding stages of nauplii and found ingestion rates ranged from 0.001 – 0.050 $\mu\text{g C ind}^{-1} \text{d}^{-1}$ (Table 3.2). The range of ingestion rates observed by Stoecker and Merrell (1998) is due to the range of natural prey abundances on their five different sample dates. My estimate of *E. carolleae* ingestion rates on a laboratory culture is within the range of values they measured on a field population, suggesting that my ingestion rates may be representative of the ingestion rate of *E. carolleae* nauplii in an *in situ* community.

I estimated that 50% naupliar mortality after 15 days (LD_{50}) occurs at 182 cells mL^{-1} , or 12.4 $\mu\text{g C mL}^{-1}$ using the fitted logarithmic equation. This equation does not include mortality from other factors that could affect naupliar survival in the wild, such as predation, but it does provide an estimate of the potential mortality of nauplii under different abundances of *H. rotundata*. Some nauplii moulted to the copepodite stage C1 during the experimental period and were removed, but I assume this had no impact on mortality. Nauplii mortality at low concentrations was most likely caused by nauplii expending more energy capturing prey compared to higher concentrations, not because nauplii were competing for food. It is worth noting there was a significant difference between the number of nauplii that moulted into copepodites in the different treatments (One-way ANOVA, $F(6, 14)=4.593$, $P=0.009$). The lowest fraction of nauplii (0.3/10)

moulted into copepodites in the 0 and 500 *H. rotundata* mL⁻¹ treatments and the highest number (5/10) molted in the 10,000 *H. rotundata* mL⁻¹ treatment. This suggests that low prey concentration decreases developmental rate (Campbell et al., 2001).

Slow developmental rates of *E. carolleae* at low temperatures means nauplii hatched in the winter will likely spend most of the winter as nauplii and then develop into copepodites in the spring. This would explain why Millette et al. (2015) did not see an increase in copepodite abundance in response to a *H. rotundata* bloom and Kimmel et al. (2006) saw a positive relationship between wet winters and *E. carolleae* abundances in spring. The potential impact of winter *H. rotundata* abundances on copepodite abundances would not be seen until one or two months later, in the spring.

Naupliar survival in the wild can be crucial to sustaining commercially and recreationally important fish populations. The match/mismatch hypothesis suggests that for optimal recruitment to occur, abundant food must be available for fish larvae during the “critical period” when they begin feeding (Cushing, 1990). In the Chesapeake Bay, high abundance of *E. carolleae* copepodites is positively correlated with striped bass larval recruitment in spring (Shoji et al., 2005; Martino and Houde, 2010). Striped bass spawn in April and May and it takes their eggs 2 to 3 days to hatch and 5 to 10 days after that for larvae start feeding (Secor and Houde, 1995). The copepodites that striped bass larvae feed upon most likely came from nauplii that were produced in winter, due to slow develop time in low temperatures. Therefore, the more *E. carolleae* nauplii that are produced and survive winter in the Chesapeake Bay, the more striped bass larvae that will likely survive.

A winter *H. rotundata* bloom improves the survival rate of *E. carolleae* nauplii, which spend up to two months in the nauplii stages in winter temperatures. There are two known factors that are important in causing a winter *H. rotundata* bloom, a wet winter (Cohen, 1985) and a reduction in zooplankton grazing (Millette et al. 2015). Zooplankton grazing is likely reduced by cold temperatures (<1.0 °C) (Millette et al. 2015) but these temperatures will also reduce the egg production rate of *E. carolleae*. Therefore, if temperatures are too high in winter, then there won't be enough food to sustain a large population of developing nauplii but if temperatures are too low, then *E. carolleae*'s egg production rate will be too low to produce a large abundance of nauplii.

Reference

- Alekseev, V.R. and A. Souissi (2011) A new species within the *Eurytemora affinis* complex (Copepoda: Calanoida) from the Atlantic Coast of USA, with observations on eight morphologically different European populations. *Zootaxa* 2767:41-56.
- Campbell, R.G., M.M. Wagner, G.J. Teegarden, C.A. Boudreau, and E.G. Durbin (2001) Growth and development rates of the copepod *Calanus finmarchicus* reared in the laboratory. *Mar Ecol Prog Ser* 221:161-183.
- Cohen, R.R.H. (1985) Physical processes and the ecology of a winter dinoflagellate bloom of *Katodinium rotundatum*. *Mar Ecol Prog Ser* 26:135-144.
- Cushing, D.H. (1990) Plankton production and year-class strength in fish populations: an update of the Match/Mismatch Hypothesis. *Adv Mar Biol* 26:249-293.
- Devreker, D., J.J. Pierson, S. Souissi, D.G. Kimmel, and M.R. Roman (2012) An experimental approach to estimate egg production and development rate of the calanoid copepod *Eurytemora affinis* in Chesapeake Bay, USA. *J Exp Mar Biol Ecol* 416-417:72-83.
- Durell, E.Q. and C. Weedon (2011) Striped Bass Seine Survey Juvenile Index Web Page. <http://dnr2.maryland.gov/fisheries/Pages/juvenile-index/index.aspx>. Maryland Department of Natural Resources, Fisheries Service.
- Frost, B.W. (1972) Effects of size and concentration of food particles on the feeding behavior of the marine planktonic copepod *Calanus pacificus*. *Limnol Oceanogr* 17:805-815.
- Heinle, D.R. and D.A. Flemer (1975) Carbon requirements of a population of the estuarine copepod *Eurytemora affinis*. *Mar Biol* 31:235-247.
- Katona, S.K. (1970) Growth characteristics of the copepods *Eurytemora affinis* and *E. herdmani* in laboratory cultures. *Helgoländer wiss Meeresunters* 20:373-384.
- Kimmel, D.G. and M.R. Roman (2004) Long-term trends in mesozooplankton abundance in Chesapeake Bay, USA: influence of freshwater input. *Mar Ecol Prog Ser* 267:71-83.
- Kimmerer, W.J., N. Ferm, M.H. Nicolini, and C. Penalva (2005) Chronic food limitation of egg production in populations of copepods of the genus *Acartia* in the San Francisco Estuary. *Estuaries* 28:541-550.
- Lloyd, S.S., D.T. Elliott, and M.R. Roman (2013). Egg production by the copepod, *Eurytemora affinis*, in the Chesapeake Bay turbidity maximum regions. *J Plankton Res* 35:299-308.

- Martino, E. J. and E.D. Houde (2010) Recruitment of striped bass in Chesapeake Bay: spatial and temporal environmental variability and availability of zooplankton prey. *Mar Ecol Prog Ser* 409:213-228.
- Menden-Deuer, S. and E.J. Lessard (2000) Carbon to volume relationships for dinoflagellates, diatoms, and other protist plankton. *Limnol Oceanogr* 45:569-579.
- Merrell, J.R. and D.K. Stoecker (1998) Differential grazing on protozoan microplankton by developmental stages of the calanoid copepod *Eurytemora affinis* Poppe. *J Plankton Res* 20:289-304.
- Millette, N.C., D.K. Stoecker, and J.J. Pierson (2015) Top-down control of micro- and mesozooplankton on winter dinoflagellate blooms of *Heterocapsa rotundata*. *Aquat Microb Ecol* 76:15-25
- Paffenhöfer, G.A. (1971) Grazing and ingestion rates of nauplii, copepodids, and adults of the marine planktonic copepod *Calanus helgolandicus*. *Mar Biol* 11:286-298.
- Pierson, J.J., D.G. Kimmel, and M.R. Roman (2016) Temperature impacts on *Eurytemora carolleeae* size and vital rates in the Upper Chesapeake Bay in winter. *Estuaries and Coasts* DOI 10.1007/s12237-015-0063-z
- Secor, D.H. and E.D. Houde (1995) Temperature effects on the timing of striped bass egg production, larval viability, and recruitment potential in the Patuxent River (Chesapeake Bay). *Estuaries* 18:527-544.
- Sellner, K.G., R.V. Lacouture, S.J. Cibik, A. Brindley, and S.G. Brownlee (1991) Importance of a winter dinoflagellate-microflagellate bloom in the Patuxent River Estuary. *Estuar Coast Shelf S* 32:27-42.
- Shoji, J., E.W. North, and E.D. Houde (2005) The feeding ecology of *Morone americana* larvae in the Chesapeake Bay estuarine turbidity maximum: the influence of physical conditions and prey concentrations. *J Fish Biol* 66:1328-1341.
- Vogt, R.A., T.R. Ignoffo, L.J. Sullivan, J. Herndon, J.H. Stillman, and W.J. Kimmerer (2013) Feeding capabilities and limitations in the nauplii of two pelagic estuarine copepods, *Pseudodiaptomus marinus* and *Oithona davisae*. *Limnol Oceanogr* 58:2145-2157.

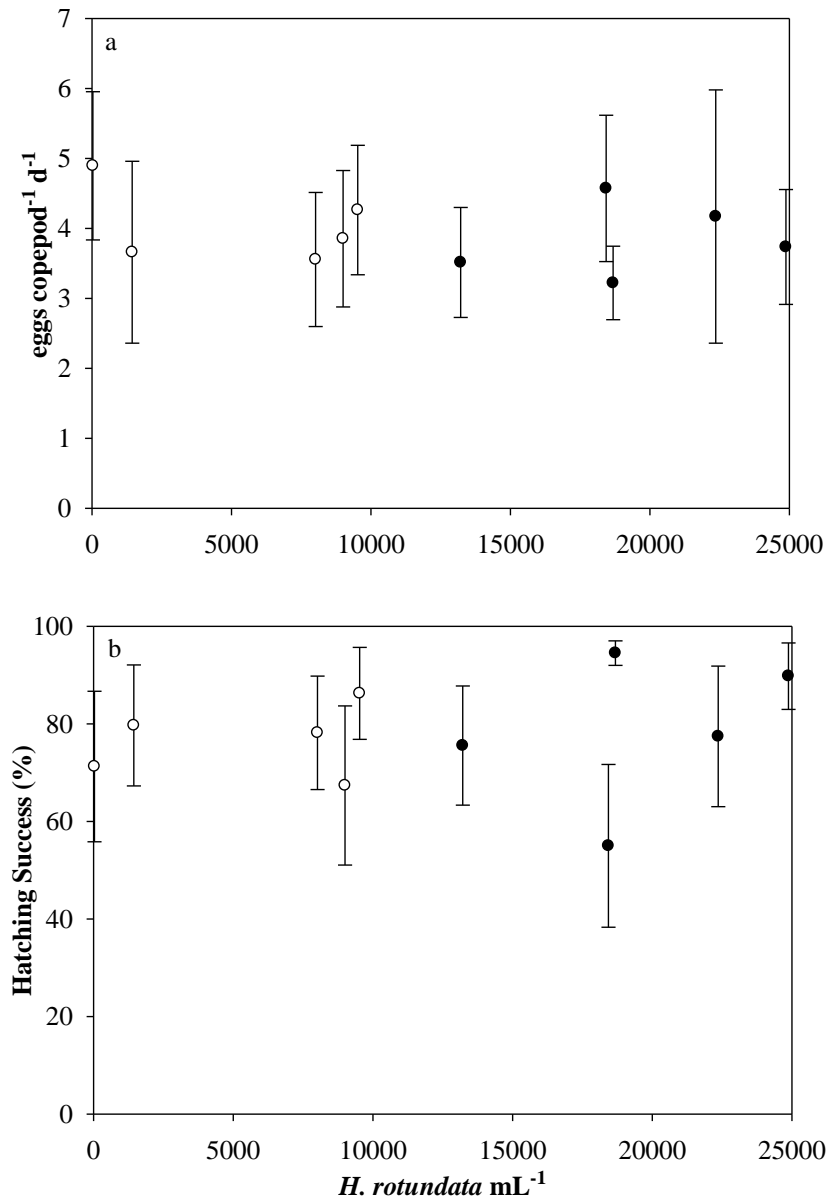
Tables and Figures

Table 4.1

Date	Temp (°C)	CS/ICT (egg production copepod ⁻¹ d ⁻¹)	CS/(EDT+LT) (egg production copepod ⁻¹ d ⁻¹)	<i>H. rotundata</i> con. abundance (mL ⁻¹)	Control (egg production copepod ⁻¹ d ⁻¹)	<i>H. rotundata</i> exp. abundance (mL ⁻¹)	Experiment (egg production copepod ⁻¹ d ⁻¹)	P-value
1/01/14	4.7	10.2	4.1	9525	4.3 ± 0.9	18433	4.6 ± 1.0	0.82
1/15/14	4.8	10.3	4.2	31	4.9 ± 1.1	13217	3.5 ± 0.8	0.27
2/05/14	0.9	4.5	0.5	1443	3.7 ± 1.3	18683	3.2 ± 0.5	0.74
2/18/14	2.5	7.4	1.9	9000	3.9 ± 1.0	24877	3.7 ± 0.8	0.92
3/05/14	3.1	8.3	2.5	8017	3.6 ± 1.0	22360	4.2 ± 1.8	0.78

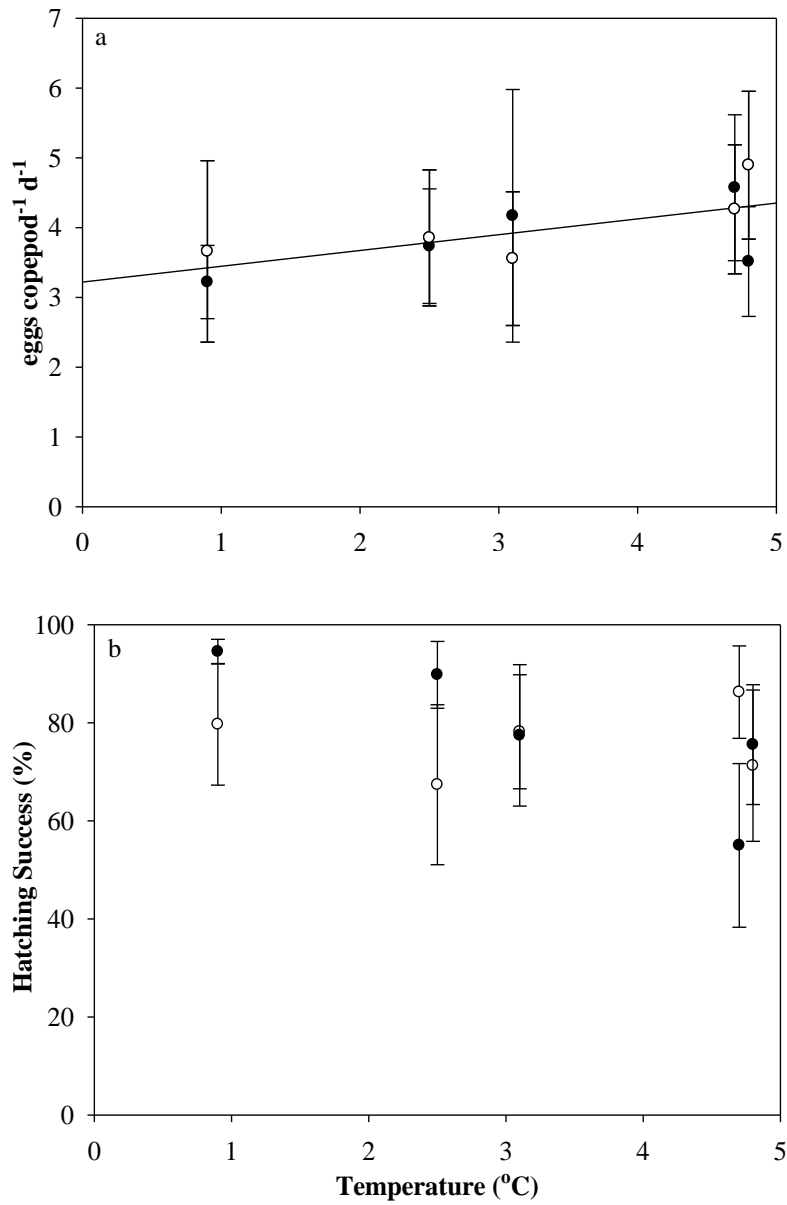
Comparison of calculated and experimentally tested *E. carolleae* egg production rate (eggs female⁻¹ day⁻¹ ±SE) at different *H. rotundata* abundances (cells ml⁻¹) in the control treatment and experimental treatment for five different weeks. *H. rotundata* abundance refers to their abundance at the start of the experiment and temperature (°C) is the temperature of the water the day the copepods and seawater were collected and experiments were set up. Calculated egg production rates were based on Lloyd et al. 2013 and Devreker et al. 2012 equations using water temperature. P-value compares the egg production rate in the control treatment to the experimental treatment each week.

Figure 4.1



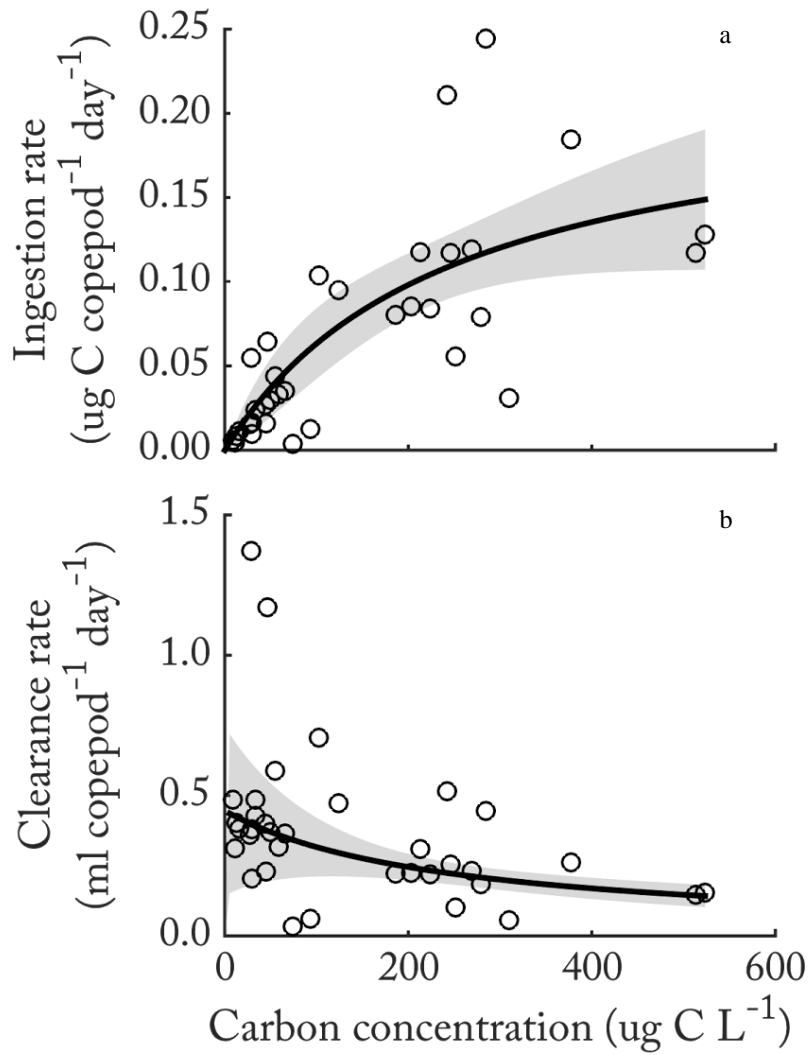
Individual *E. carolleae* (a) egg production rates (eggs female⁻¹ day⁻¹) and (b) hatching success rate (%) from control (white circle) and treatment (black circle) experiments compared to *H. rotundata* abundance (cells mL⁻¹). Error bars = SE.

Figure 4.2



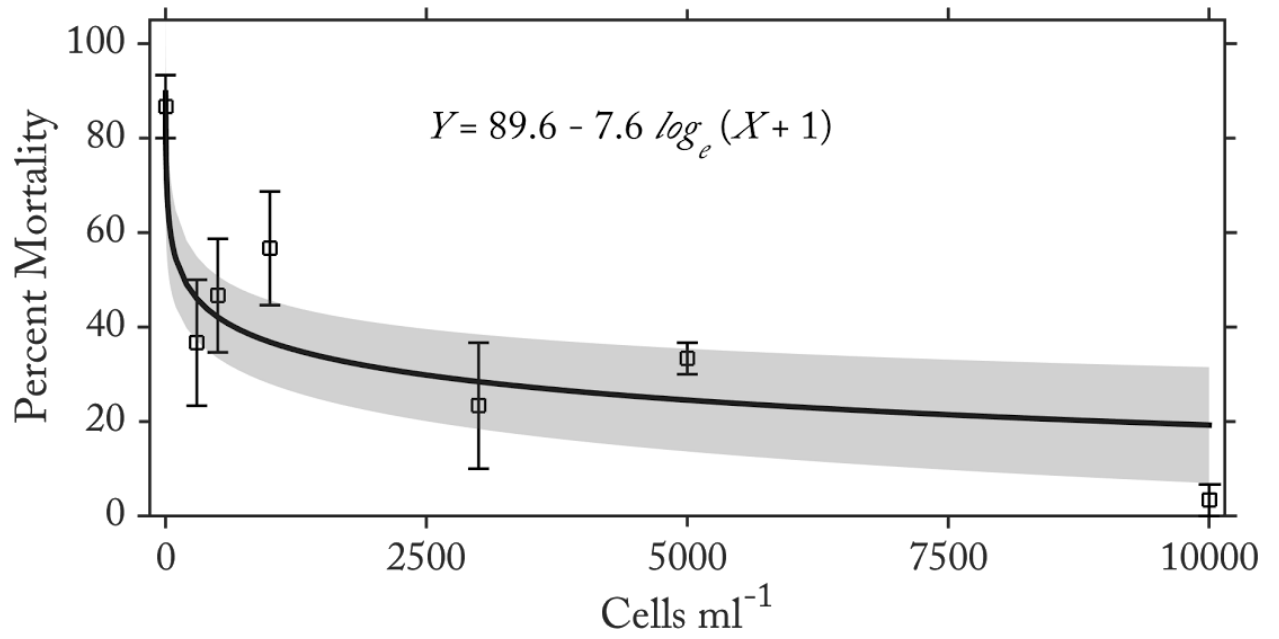
Individual *E. carolleae* (a) egg production rates (eggs female⁻¹ day⁻¹) and (b) hatching success rate (%) from control (white circle) and treatment (black circle) experiments compared to the *in situ* temperature (°C) when *E. carolleae* were collected. Error bars = SE.

Figure 4.3



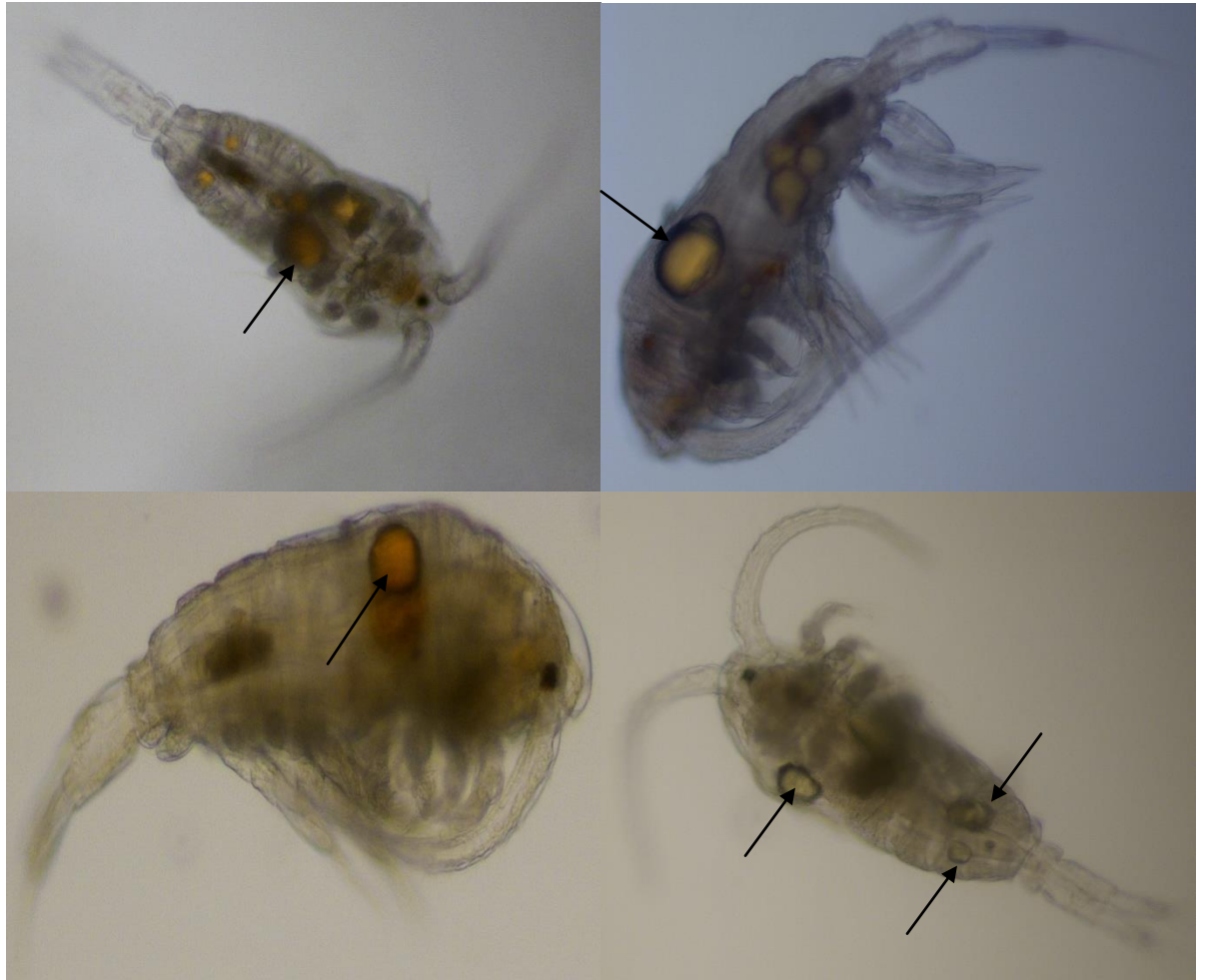
The ingestion rates (a, $\mu\text{g C copepod}^{-1} \text{ day}^{-1}$) and clearance rates (b, $\text{ml copepod}^{-1} \text{ day}^{-1}$) of *E. carolleae* nauplii measured at various carbon concentrations ($\mu\text{g C L}^{-1}$) of *H. rotundata* with a type II functional response curve. Grey area denotes 95% confidence intervals.

Figure 4.4



Percent mortality of nauplii at different *H. rotundata* concentrations. Error bars refer to standard error.

Figure 4.5



Lipid storages in *Eurytemora carolleae* collected from the Choptank River in the 2014 winter. Black arrows point to lipids.

Table 3.2

Copepod	Stage	Prey	Temperature (°C)	Ingestion Rate ($\mu\text{g C ind}^{-1} \text{d}^{-1}$)	References
<i>Eurytemora carolleeeae</i>	N3-N6	<i>Heterocapsa rotundata</i>	4	$0.022 \pm .007$	This paper
<i>Eurytemora carolleeeae</i>	N3-N6	Natural population	10-18	0.016 ± 0.006	Stoecker & Merrell 1998
<i>Pseudodiaptomus marinus</i>	N5	various	19	0.004 ± 0.0002	Vogt et al. 2013
<i>Oithona darisae</i>	N5	various	“	0.001 ± 0.001	“
<i>Calanus finmarchicus</i>	N/A	Total Chl <i>a</i>	10	0.066 ± 0.003	Meyer et al. 2002
<i>Calanus helgoladnicus</i>	N/A	“	15	0.039 ± 0.003	“
<i>Acartia tonsa</i>	N3	various	20	0.013 ± 0.009	Stoecker & Egloff 1987
<i>Calanus helgoladnicus</i>	N4	various	15	0.056 ± 0.014	Paffenhöfer 1971
<i>Calanus helgoladnicus</i>	N5	various	“	0.130 ± 0.022	“
<i>Calanus helgoladnicus</i>	N6	various	“	0.132 ± 0.019	“

Average species-specific ingestion rates ($\mu\text{g C ind}^{-1} \text{d}^{-1} \pm \text{SE}$) of copepod nauplii measured in different studies. All of the studies used the Frost (1972) equations to calculate ingestion rates except for Paffenhöfer (1971), and all reported data on a range of prey items or reported multiple measurements on the same prey. Ingestion rates from other studies were calculated or converted to standardize units.

Chapter 5: Impact of winter water temperature on timing of peak spring *Eurytemora carolleeae* abundances and implications for anadromous fish larvae survival

Introduction

In chapters 2-4 I have shown that winter water temperature and freshwater flow rate have the potential to indirectly affect spring *E. carolleeae* populations through winter *H. rotundata* abundances. Winters with high rainfall create a stratified water column by increasing freshwater flow, which is associated with *H. rotundata* blooms (Cohen 1985). In addition to high rainfall, water temperatures below 1 °C sustained for 2-3 weeks are necessary to reduce zooplankton grazing rates and allow a *H. rotundata* winter bloom to form (Millette et al. 2015a). High abundances of *H. rotundata* in winter increase the survival rate of *E. carolleeae* nauplii that are hatched in winter, supporting *E. carolleeae* copepodite abundance in spring (Millette et al. 2015b). In this chapter I address the hypothesis that variations in winter water temperature have a direct effect on the coupling between *E. carolleeae* populations and fish larvae in spring by determining the timing of peak spring *E. carolleeae* abundance.

Eurytemora carolleeae (cf. *E. affinis*, Alekseev and Souissi, 2011) is a common copepod species in Chesapeake Bay that dominates the zooplankton assemblage during winter and spring (Kimmel and Roman 2004). It has been suggested that physical conditions in winter can result in bottom-up control on spring copepod populations (Kimmel et al. 2006; Pierson et al., 2016). Cold, wet winters are associated with high abundance and wide distribution of *E. carolleeae* populations in spring in Chesapeake

Bay (Kimmel et al., 2006). The wide distribution is most likely due to high river input that transports copepods farther down the Bay and lowers the salinity, providing ample suitable habitat for *E. carolleae* (Kimmel et al. 2006). Large winter dinoflagellate blooms associated with cold, wet winters (Cohen 1985; Sellner et al. 1991; Millette et al. 2015a) increase the survival of *E. carolleae* nauplii that are hatched in winter, and it has been hypothesized these nauplii develop into the spring *E. carolleae* copepodite population (Millette et al. 2015b). The timing of peak spring *E. carolleae* abundance is important to the success of anadromous fish recruitment, and it has been shown that the later in spring that zooplankton reach peak abundances, the stronger anadromous fish recruitment is for that year (Fig. 8 in Martino and Houde 2010).

Striped bass (*Morone saxatilis*) and white perch (*Morone americana*) are important commercial and recreational fisheries along the eastern Atlantic coast. These species, and other anadromous fish, spawn in oligohaline and freshwater regions of estuaries such as Chesapeake Bay during April and May (Secor and Houde, 1995; Shoji et al., 2005). Striped bass spawn at 12 °C and (Secor and Houde, 1995) and peak white perch spawning occurs at 15 °C (Feiner et al. 2012). Once striped bass and white perch larvae start feeding, their preferred prey is the copepod *E. carolleae* (Shoji et al., 2005; Martino and Houde, 2010). When high *E. carolleae* abundances coincide with striped bass larvae in space and time (e.g. Match-Mismatch hypothesis, Cushing 1990), spring striped bass recruitment for that year is elevated (North and Houde, 2003; Martino and Houde, 2010).

In addition to the timing of peak prey abundance, prey density is also important to fish larvae when they begin to feed. High prey density results in higher encounter rates

and higher anadromous fish larval survival (Shoji et al., 2005). The number of larvae hatched each spring does not predict how successful recruitment is in a given year (North and Houde, 2003), but once larvae double in size and reach 8 mm they are considered potential recruits. The abundance of potential recruits positively correlates to increased recruitment (Secor and Houde, 1995). Thus, high prey density during the first-feeding stage helps larvae grow to 8mm quickly and increases the chance for successful recruitment (Martino and Houde, 2010).

Thus, the timing of high prey density is critical to survival of anadromous fish larvae. In order to understand what factors affect survival of fish larvae, we need to understand what factors affect the timing of the peak abundance of their prey. In the case of white perch and striped bass, this means understanding the timing of the peak of *E. carolleae* abundance. The generation time of *Eurytemora spp.* is temperature dependent, and in this chapter I examine how variations in winter temperature affect *E. carolleae*'s developmental rate under different temperature scenarios. At lower temperatures the generation time is longer, and the rate of change of development rate is larger at these low temperatures, meaning that a small change in temperatures at lower initial temperatures results in a large change in generation time compared than it would at higher initial temperatures (Heinle and Flemer; Heerkloss et al. 1990; Lee et al. 2007; Devreker et al. 2012; Pierson et al. 2016). Average winter temperature varies between years as does the pattern of temperature over the winter (Millette et al., 2105a; Pierson et al., 2016), and thus the developmental rate of *E. carolleae* must vary throughout and between winters. This variation in developmental rates likely has an impact on when *E. carolleae* reaches peak abundances in spring, with below average winter temperature

delaying the peak until later in spring. As noted previously, this delayed peak has been shown to correlate with strong striped bass recruitment (Martino and Houde 2010).

There is evidence to suggest that water temperature and rainfall in winter can increase spring *E. carolleae* distribution and abundance (Kimmel et al. 2006; Pierson et al. 2016). Thus, winter environmental conditions could indirectly affect fish larvae recruitment through effects on *E. carolleae* populations. My goal is to understand if and how winter conditions, specifically water temperature and discharge rates, affect the success of spring anadromous fish recruitment through impacts on the timing of peaks in *E. carolleae* abundance. To achieve this goal I addressed two specific questions, (1) is there a statistical relationship between anadromous fish recruitment and winter temperature and discharge rates? (2) How do variations in daily winter temperature affect the timing of peak spring *E. carolleae* abundances? To address the first question I obtained monitoring data from three regions in the Chesapeake Bay collected over several years and analyzed the relationships among water temperature, river discharge, and fish recruitment indices. For the second question I developed a temperature-based developmental model to explore how variations in winter water temperatures may affect the timing of peak spring *E. carolleae* abundances. My findings provide evidence that cold winters are most likely to support more successful recruitment of striped bass and white perch larvae due to a delay in the timing of *E. carolleae*'s peak abundance by up to three weeks.

Methods

I used historical monitoring data to investigate whether there was evidence for a relationship between anadromous fish recruitment and winter temperature and discharge.

From this analysis I identified a relationship between winter temperature and anadromous fish recruitment, and then I attempted to explain why winter temperature impacts fish recruitment through changes in the timing of their prey, *E. carolleeae*. I created a temperature-dependent developmental model to demonstrate how winter temperature influences the timing of when *E. carolleeae* reach the adult stage. This allowed me to develop an explanation as to how below average winter temperatures may favor high anadromous fish recruitment.

Anadromous fish larval recruitment: To investigate whether variations in winter conditions, specifically water temperature and discharge, are related to striped bass and white perch young of the year (YOY) recruitment, I examined winter water temperature and discharge rates, because they have been shown to increase the spring abundance and distribution of anadromous fish prey, *E. carolleeae* (Kimmel et al. 2006; Pierson et al. 2016). Three regions (Choptank River, Patuxent River, and Head of Chesapeake Bay) were selected based on availability of daily water temperature, daily discharge, and annual YOY recruitment data (Table 1), allowing for a statistical comparison among variables at each site.

Hourly temperature (°C) data was downloaded for the period January 1 to March 19 from NOAA Tides and Currents (<https://tidesandcurrents.noaa.gov/>) for weather monitoring stations near Cambridge, MD (station #8571892, Figure 5.1), Solomons Island, MD (station #8577330, Figure 5.1), and Tolchester Beach, MD (station #8573364, Figure 5.1). The hourly temperature data was averaged monthly for statistical analyses. The equipment used to collect temperature data periodically malfunctioned, and years with large gaps in daily temperature (>14 days) were excluded. Mean monthly

discharge data ($\text{m}^3 \text{sec}^{-1}$) were obtained from the USGS water data website (<http://waterdata.usgs.gov/nwis>) from monitoring stations near Greensboro, MD (station #01491000, Figure 5.1), Bowie, MD (station #01594440, Figure 5.1), and the Conowingo Dam (station #01578310, Figure 5.1). Annual young of the year (YOY) recruitment indices were obtained from the Maryland Department of Natural Resources (DNR, <http://dnr2.maryland.gov/fisheries/Pages/stripped-bass/juvenile-index.aspx>). The annual Maryland DNR YOY index for striped bass and white perch is based on the geometric mean catch per haul of YOY fish caught in seine surveys conducted between July and September (Durell and Weedon 2011). YOY recruitment indices for the Choptank River, Patuxent River, and Head of Bay were used in the analyses presented here. The number of years included in analysis varied from 14-17 among stations, depending on data availability (Table 5.1).

I employed a multiple linear regression approach to explore relationships in each region between monthly winter discharge rates and water temperature as independent variables and striped bass and white perch recruitment as dependent variable, using the “leaps” (Luneley 2009) and “car” (Fox and Weisberg 2016) packages in R. To determine the best multiple linear regression model I used two criteria. First, I collected the Bayesian information criterion (BIC) of all possible combinations of monthly average temperatures and discharge rates during each winter month (January, February, and March). The BIC takes into account how well the model fits the data and how many parameters are in the model, penalizing models for every additional parameter (Findley 1991). The range between BICs for all the combinations for all analyses was small (max. 17.18), so the lowest BIC for each region was selected as having the strongest influence

on the recruitment index. Second, I selected the combination of variables for the multiple linear regression analysis for each region that had the lowest BIC and also only identified one month for temperature and/or discharge as a factor. This means the combination selected would have, at most, only two factors, a temperature from a given month and a discharge from a given month. It was these combinations that were then used to develop the scenarios tested in the modeling (see Developmental Rate Model section).

For cases where both temperature and discharge in a given month were identified in the multiple linear regression analysis, I tested the interactive effect of these factors on the model. For this additional analysis I tested whether the slope of each factor (temperature, discharge, and the interactive effect of temperature and discharge) was significantly different from zero ($P < 0.05$). If the slope of a factor was not significantly different from zero, it was removed from the final model. For example, January temperature and March discharge were identified as the two most important factors affecting Striped Bass recruitment in the Choptank River, so I tested the significance of the slope for each factor (January temperature, March discharge, and the interactive effect of January temperature and March discharge) in the model. This analysis showed that January temperature and an interactive effect of January temperature and March discharge had slopes significantly different than zero, but March discharge did not. Therefore, March discharge, as a single factor, was removed from the multiple linear regression.

Developmental Rate Model: To test how variations in winter temperature affected the timing of when the *E. carolleae* that were hatched in winter reached the adult stage, I

created a temperature-dependent developmental model. The model was forced with climatologically averaged daily temperature data from each region as described in the previous section (Figure 5.2). In 2012 a large portion of daily temperature data were missing from the Cambridge station. To fill this gap, I used my own water temperature data collected weekly at the Bill Burton fishing pier with a hand-held YSI-30. The fishing pier is located within 0.8 km of the monitoring equipment used to collect water temperature data for NOAA. I linearly interpolated my water temperature data between each of my sampling time points, for a total of 27 interpolated data points. This accounted for 30% of the data in 2012. Linear interpolation was also used for smaller gaps (<7 days) in water temperature data from the NOAA site for some years.

In the model, a cohort of *E. carolleeae* nauplii was hatched each day throughout winter, and model output was the date that each of these nauplii cohorts reached the adult stage. There was no abundance associated with these daily cohorts, but each cohort of nauplii were followed through to metamorphosis into the adult stage as affected by temperature. For each model run, nauplii cohorts were hatched into the model from January 1 – March 19, for a total of 78 cohorts (Figure 5.3). The basis for the model was a fitted equation of generation time at a range of temperatures, compiled by Pierson et al. (2016):

$$G=14185*(T+8.95)^{-2.05}$$

where G (days) is the number of days for *Eurytemora spp.* to develop from the first nauplii stage (N1) stage to the adult stage (C6) at a given water temperature (T °C). *E. carolleeae* have 12 distinct developmental stages, six nauplii and six copepodite, with the sixth copepodite stage being the adult stage. The equation to calculate G assumes that

water temperature is constant during *Eurytemora* spp. entire developmental period, but water temperature is not constant in the environment. Here I use the reciprocal of G ($1/G$, in days^{-1}) to calculate the daily fractional developmental rate of copepods in the model for each daily temperature, and track the fractional generation of each cohort as it develops based on the temperature in the model (Figure 5.3). To do this, the cumulative sum of the fractional developmental rates was calculated daily (Figure 5.3). The date when $G = 1$ specifies the date when a cohort reached the adult stage, and I calculated the number of cohorts reaching the adult stage on each date. These model results are used to show how temperature affects the timing of when daily cohorts newly hatched nauplii transition to a generation of new adults.

To test how altered temperature may affect the timing and magnitude of these peaks, I ran the model using eight different simulations in which the climatologically averaged daily temperature for each region (Figure 5.2) was increased or decreased in specific months (Table 5.2). These scenarios were based on the results of the multiple linear regression analysis to determine factors that affected fish recruitment, as described in the previous section. For example, water temperature in January had the largest, statistically significant effect on striped bass and white perch YOY indices in the Choptank River. Therefore, I ran the model using Choptank River climatologically averaged daily temperature with January water temperature increased $3\text{ }^{\circ}\text{C}$ (simulation 1a) and decreased $3\text{ }^{\circ}\text{C}$ (simulation 1b). For the Head of the Chesapeake Bay, I ran the simulations with altered temperatures for February and March, and for the Patuxent River February altered temperatures were used in the simulations.

To examine the effects of altered temperatures, I compared the average generation time of nauplii cohorts hatched under each simulation and for each location, the daily proportional developmental rate in the months I altered for each simulation, and the number of daily cohorts hatched in winter forming the ‘peak’ in spring after lower winter temperatures to higher winter temperatures.

Results

Anadromous fish larvae recruitment: I tested the YOY index data for normality, and four of the six YOY indices failed a Lilliefors normality test, so all of the data were \log_{10} transformed to achieve normal distribution before calculating the multiple linear regressions (Table 5.3). Overall, the linear regression analysis showed that mean monthly temperatures were the primary factor shown to have a significant relationship to YOY indices in each system. These relationships were always negative; the annual YOY index increased as mean monthly winter temperatures decreased. Mean monthly discharge rates had an interactive effect with mean monthly water temperature in the Choptank River, and increased mean monthly discharge rates increased the annual YOY index at higher monthly water temperatures. At lower average monthly water temperatures, average monthly discharge rates did not have an impact on the YOY index.

For the Choptank River, mean water temperature in January and the interaction of mean water temperature and mean discharge rate in January both had a significant effect on white perch and striped bass recruitment indices (Table 5.4). For white perch recruitment, mean discharge in January was significantly related to the YOY index, while for the striped bass YOY index a significant relationship was found with mean discharge in March (Table 5.4). For the Head of Chesapeake Bay and the Patuxent River, mean

water temperatures in February and March showed significant relationships to striped bass and white perch recruitment indices, respectively (Table 5.4). For the Patuxent River, mean water temperature in February was significantly related to striped bass and white perch recruitment indices (Table 5.4). Monthly average discharge rates did not have significant relationship to recruitment in the Patuxent River and Head of Chesapeake Bay.

Developmental Rate Model: For a set of simulations for a given region, the daily fractional developmental rate of *E. carolleae* was the same every day except during the specific month that temperature was altered in a given scenario (Figure 5.4). The daily fractional developmental rate ($1/G$) was lower when temperature was reduced by 3 °C compared to when it was increased by 3 °C, corresponding to longer generation times at lower temperatures. Likewise, the mean generation time for daily cohorts of *E. carolleae* hatched in winter in each simulation was significantly higher when temperature was decreased for a specific month compared to when it was increased (Table 5.5).

Using the daily fractional developmental rate from each model simulation, I estimated the date on which *E. carolleae* cohorts that were hatched on each day in the winter reached the adult stage (Figure 5.5). When water temperature for a specific month was reduced by 3 °C, winter-hatched cohorts of *E. carolleae* reached the adult stage later in the year and over a shorter period of time compared to when water temperature was increased by 3 °C (Figure 5.5). The first *E. carolleae* cohort to reach the adult stage appeared 15-19 days later in simulation runs when the temperature was reduced (Figure 5.5).

When the average daily temperature was reduced in January in the Choptank River by 3 °C, 33% of the daily cohorts hatched in winter reached the adult stage over a six day period (Figure 5.5a), compared to 22% of the daily cohorts when temperature was increased by 3 °C. When the average daily temperature was reduced in February in the Head of Bay by 3 °C, 47% of the daily cohorts hatched in winter reached the adult stage over a six day period (Figure 5.5c), compared to 23% of the daily cohorts when temperature was increased by 3 °C. When the average daily temperature was reduced in February in the Patuxent River by 3 °C, 37% of the daily cohorts hatched in winter reached the adult stage over a six day period (Figure 5.5d), compared to 18% of the daily cohorts when temperature was increased by 3 °C.

Discussion

The relationship between striped bass and white perch YOY recruitment indices and both water temperature and discharge rates in winter suggests that winters with below average water temperatures had the highest likelihood of successful recruitment. Winter water temperature is likely affecting striped bass and white perch recruitment indirectly through changes in the timing of peaks of their preferred food source, *E. carolleae*. Cold winters delay the development of *E. carolleae* to the adult stage, increasing the chance of fish larvae survival during the first-feeding stage.

When peak spring *E. carolleae* abundance occurs later in the season striped bass recruitment for that year has been shown to be higher (Martino and Houde 2010). This model, based on the empirical relationship between temperature and *E. carolleae* generation time, showed that *E. carolleae* that were hatched in winter reached the adult stage over a shorter period of time that was later in spring when winter temperatures were

below average, compared to above average temperatures. Under warmer conditions in winter, typically, *E. carolleae* cohorts produced over 1-2 days reached the adult stage on a single day in spring. Alternatively, under colder conditions in winter *E. carolleae* hatched over 7 day separate days could reach the adult stage on a single day in spring. This would likely cause a sudden, rapid increase in *E. carolleae* abundance that could increase survival of fish larvae that started feeding during and after this time period.

The developmental model did not consider the number of nauplii hatched in a cohort on each day, only that *E. carolleae* nauplii would be hatching each day, and that cohort would reach adulthood on a given day. The number of nauplii hatching each day in the winter would depend on the abundance of adult female *E. carolleae* and the egg production rate, shown to be temperature-dependent (Devreker et al. 2012; Lloyd et al. 2013). Based on four years of winter sampling in the Choptank River, average winter *E. carolleae* copepodite (C1 – adult) abundance is typically stable between years, 8-10 L⁻¹ (Millette et al. 2015, chapter 1). An exception to this was winter 2012, when average winter *E. carolleae* copepodite abundance was lower, 2 L⁻¹ (Millette, chapter 1). I expect that winter 2012 copepodite abundances are an outlier. That winter was abnormally warm and dry in the Chesapeake Bay region (NOAA NCEI, 2013), and phytoplankton abundance was abnormally low (Millette, chapter 1). These are the same environmental conditions that are shown to result in poor anadromous fish recruitment in the Choptank River. The relatively stable *E. carolleae* copepodite abundances between winters suggest that the number of egg producing adult *E. carolleae* females in winter is relatively consistent, with warm and dry winters being the notable exception when abundance is lower.

Temperature is another factor that could affect the number of nauplii hatched each day. As temperature decreases the egg production rate of a single female copepod decreases (Deverker et al. 2012). This means that in winters with below average water temperature, the same conditions that delay developmental rates, *E. carolleae* will have low egg production rates. *E. carolleae* hatched over a large number of days in winter may be reaching the adult stage on a single day in spring, but the *E. carolleae* abundances associated with those days may be lower compared to warmer winters. Alternatively, survival of *E. carolleae* hatched in cold winters is likely to be higher compared to warm winters. Winter blooms of *Heteroapsa rotundata* that increase the survival *E. carolleae* nauplii need a reduction in temperature for a prolonged period of time to form a bloom (Millette et al. 2015b). Future work with this developmental model could be to track the abundances of *E. carolleae* hatched each day in winter as they develop. In order to accomplish this accurately, *in situ* data on *E. carolleae* developmental stage composition and mortality rates throughout multiple winters are needed.

Winter discharge rates were not as important as water temperature in predicting recruitment indices; discharge rates only had an effect in the Choptank River at above average water temperatures. Cold winter temperatures caused distinct peaks in *E. carolleae* cohorts reaching adult stage during spring, but warm temperatures did not. High discharge rates are known to concentrate *E. carolleae* at the estuarine turbidity maximum (ETM), causing a high abundance of *E. carolleae* in a specific region of the system (Shoji et al. 2005). This could be how high discharge rates improve the likelihood of successful recruitment even in warm winters. Any fish larvae located near the ETM

when they start feeding could encounter high concentrations of prey, despite a low peak in *E. carolleeae* abundance in the rest of the system, improving their chances of survival (Shoji et al. 2005).

This developmental model incorporates the daily variability of fractional developmental rates but assumes that temperature is the only factor that affects copepod developmental rate. Prey concentration has also been shown to have an impact on copepod nauplii development, with lower prey concentrations decreasing the rate (Campbell et al., 2001; Millette et al., 2015b). Millette et al. (2015b) showed that cultured *E. carolleeae* nauplii developed at a slower rate when their prey concentration (*Heterocapsa rotundata*) was reduced. *H. rotundata* forms large winter blooms in temperate estuaries and *E. carolleeae* are known to be a major grazer of *H. rotundata* blooms (Sellner et al., 1991; Millette et al., 2015a). If prey abundances are high enough in winter, then *E. carolleeae* development should solely depend on temperature, although research is needed to determine below what concentration prey abundance negatively affects *E. carolleeae* developmental rates.

The equation that forces the model presented here (Pierson et al. 2016) is compiled from developmental rates published in a range of different papers. The lowest temperature for which developmental rates were measured was 5.0 °C (Heerkloss et al. 1990); this means that most of the developmental rates that I calculated with the model have not been empirically determined. Experimental measurements of developmental rates at temperatures between 0-4 °C would improve the accuracy of this equation, but this does not negate the results from the model. Our results are theoretical, but they

suggest that winter temperature is important to the timing of peak *E. carolleae* spring abundances, and highlight the potential magnitude of those impacts on *E. carolleae*.

These findings point to three differing winter scenarios that affect fish recruitment through their zooplankton prey and the prey of the zooplankton: warm/dry, warm/wet, and cold. Warm/dry winters are the least likely to result in strong anadromous fish recruitment. In warm/dry winters, phytoplankton and zooplankton abundance is likely very low and as a result the number of nauplii hatched each day and their survival rate are both low (Figure 5.6a). Nauplii hatched in a warm winter start to reach the adult stage early in spring and there is a small peak in *E. carolleae* abundance (Figure 5.6a). When anadromous fish larvae hatch and start to feed, there is a low concentration of *E. carolleae* and their abundance is unlikely to increase during the critical period of the fish larvae (Figure 5.6a). This leads to low recruitment of striped bass and white perch.

In warm/wet winters phytoplankton and zooplankton abundance is higher compared to a wet/dry winter (Millette et al. 2015a; unpublished data, Figure 5.6b), leading to more nauplii hatched each day. Survival of nauplii hatched in winter would likely be higher compared to warm/dry winters because phytoplankton abundance is higher and can support survival of zooplankton nauplii (Millette et al. 2015b). *E. carolleae* nauplii hatched in warm/wet winter reach the adult stage around the same time as warm/dry winters but the peak is expected to be higher in warm/wet conditions because of higher nauplii abundances accumulated throughout winter (Figure 5.6b). Most of the *E. carolleae* will likely be concentrated at the ETM after wet winters (Shoji et al. 2005). When anadromous fish larvae start to feed, those located in the ETM will have a high concentration of prey and an increased likelihood of survival to the adult population.

This increases the overall recruitment to the YOY stage compared to warm/dry years (Figure 5.6b).

In cold winters, zooplankton abundance is similar to warm/wet winters but there is a higher chance of a winter dinoflagellate bloom forming (Millette et al. 2015a, Figure 5.6c). If a bloom does form, a higher portion of nauplii hatched in winter are likely to survive to the copepodite stages (Millette et al. 2015b). *E. carolleae* hatched in winter will reach the adult stage and form a large peak later in spring (Figure 5.6c). When anadromous fish start to feed, there is a better chance there will be a high concentration of prey available to them, and that their prey will also be well fed, increasing the likelihood of high recruitment to the YOY stage (Figure 5.6c).

By the end of the 21st century winter water temperatures are predicted to increase by up to 5 °C in the Chesapeake Bay (Najjar et al. 2011). This increase in average water temperature would likely have a negative impact on anadromous fish larval recruitment through the mechanisms described here. In warmer winters, *E. carolleae* reach the adult stage earlier in spring and there will be a reduced peak in spring abundance, which would reduce the chance of successful striped bass and white perch recruitment. Based on these findings, it is likely that with climate change, the current mean values of the YOY recruitment index for striped bass and white perch would become the new maximum recruitment indices, and there would be a reduction in mean YOY recruitment.

Striped bass and white perch larvae appear to benefit from cold winters that delay the development of *E. carolleae* and allow this key prey species to reach peak abundances later in spring, as shown in correlations published previously (Martino and Houde 2010). This has implications in the management of anadromous fish in temperate

estuaries and how we understand the impact of the winter ecosystem on the spring ecosystem. Future field research is necessary to confirm the direct mechanistic links between winter conditions and fish recruitment through trophic interactions suggested here. Tracking the abundance and development of *E. carolleae* from winter into spring in cold compared to warm winters to validate the findings of our developmental model and increased monitoring during winter are obvious starting points to address this.

References

- Alekseev, V.R. and A. Souissi (2011) A new species within the *Eurytemora affinis* complex (Copepoda: Calanoida) from the Atlantic Coast of USA, with observations on eight morphologically different European populations. *Zootaxa* 2767:41-56
- Campbell, R.G., M.M. Wagner, G.J. Teegarden, C.A. Boudreau, and E.G. Durbin (2001) Growth and development rates of the copepod *Calanus finmarchicus* reared in the laboratory. *Mar Ecol Prog Ser* 221:161-183
- Cohen, R.R.H. (1985) Physical processes and the ecology of a winter dinoflagellate bloom of *Katodinium rotundatum*. *Mar Ecol Prog Ser* 26:135-144
- Cushing, D.H. (1990) Plankton production and year-class strength in fish populations: an update of the Match/Mismatch Hypothesis. *Adv Mar Biol* 26:249-293
- Devreker, D., J.J. Pierson, S. Souissi, D.G. Kimmel, M.R. and Roman (2012) An experimental approach to estimate egg production and development rate of the calanoid copepod *Eurytemora affinis* in Chesapeake Bay, USA. *J Exp Mar Biol Ecol* 416-417:72-83
- Durell, E.Q. and C. Weedon (2011) Striped Bass Seine Survey Juvenile Index Web Page. <http://dnr2.maryland.gov/fisheries/Pages/juvenile-index/index.aspx>. Maryland Department of Natural Resources, Fisheries Service
- Findley, D.F. (1991) Counterexamples to parsimony and BIC. *Ann I Stat Math* 43: 505-514.
- Feiner, Z.S., D.D. Aday, and J.A. Rice (2012) Phenotypic shifts in white perch life history strategy across stages of invasion. *Biol Invasions* 14:2315-2329
- Fox, J. and S. Weisberg (2016) Companion to applied regression. R package version 2.1-3
- Heinle, D.R. and D.A. Flemer (1975) Carbon requirements of a population of the estuarine copepod *Eurytemora affinis*. *Mar Biol* 31:235-247
- Kimmel, D.G. and M.R. Roman (2004) Long-term trends in mesozooplankton abundance in Chesapeake Bay, USA: influence of freshwater input. *Mar Ecol Prog Ser* 267:71-83
- Kimmel D.G., W.D. Miller, and M.R. Roman (2006) Regional scale climate forcing of mesozooplankton dynamics in Chesapeake Bay. *Estuar Coast* 29:375-387
- Lee, C.E., J.L. Remfert, and Y.M. Chang (2007) Response to selection and evolvability of invasive populations. *Genetica* 129:179-192

- Lloyd, S.S., D.T. Elliott, and M.R. Roman (2013) Egg production by the copepod, *Eurytemora affinis*, in the Chesapeake Bay turbidity maximum regions. *J Plankton Res* 35: 299-308
- Luneley, T. (2009) Regression subset selection. R package version 2.9
27:187-200
- Martino, E.J. and E.D. Houde (2010) Recruitment of striped bass in Chesapeake Bay: spatial and temporal environmental variability and availability of zooplankton prey. *Mar Ecol Prog Ser* 409:213-228
- Millette, N.C., D.K. Stoecker, and J.J. Pierson (2015a) Top-down control of micro- and mesozooplankton on winter dinoflagellate blooms of *Heterocapsa rotundata*. *Aquat Microb Ecol* 76:15-25
- Millette, N.C., G.E. King, and J.J. Pierson (2015b) A note on the survival and feeding of copepod nauplii (*Eurytemora carolleeae*) on the dinoflagellate *Heterocapsa rotundata*. *J Plankton Res* 37:1095-1099
- NOAA National Centers for Environmental Information, State of the Climate: National Overview for Annual 2012, published online January 2013, retrieved on March 21, 2016 from <http://www.ncdc.noaa.gov/sotc/national/201213>
- Najjar, R.G., C.R. Pyke, M.B. Adams, D. Breitburg, C. Hershner, M. Kemp R. Howarth, et al. (2011) Potential climate-change impacts on Chesapeake Bay., *Estuar Coast Shelf S* 86:1-20
- North, E.W. and E.D. Houde (2003) Linking ETM physics, zooplankton prey, and fish early-life histories to striped bass *Morone saxatilis* and white perch *M. americana* recruitment. *Mar Ecol Prog Ser* 260:219-236
- Pierson, J.J., D.G. Kimmel, and M.R. Roman (2016) Temperature impacts on *Eurytemora carolleeae* size and vital rates in the Upper Chesapeake Bay in winter. *Estuaries and Coasts* DOI 10.1007/s12237-015-0063-z
- Secor, D.H. and E.D. Houde (1995) Temperature effects on the timing of striped bass egg production, larval viability, and recruitment potential in the Patuxent River (Chesapeake Bay). *Estuaries* 18:527-544
- Sellner, K.G., R.V. Lacouture, S.J. Cibik, A. Brindley, and S.G. Brownlee (1991) Importance of a winter dinoflagellate-microflagellate bloom in the Patuxent River Estuary. *Estuar Coast Shelf S* 32:27-42

Shoji, J., E.W. North, and E.D. Houde (2005) The feeding ecology of *Morone americana* larvae in the Chesapeake Bay estuarine turbidity maximum: the influence of physical conditions and prey concentrations. J Fish Biol 66:1328-1341

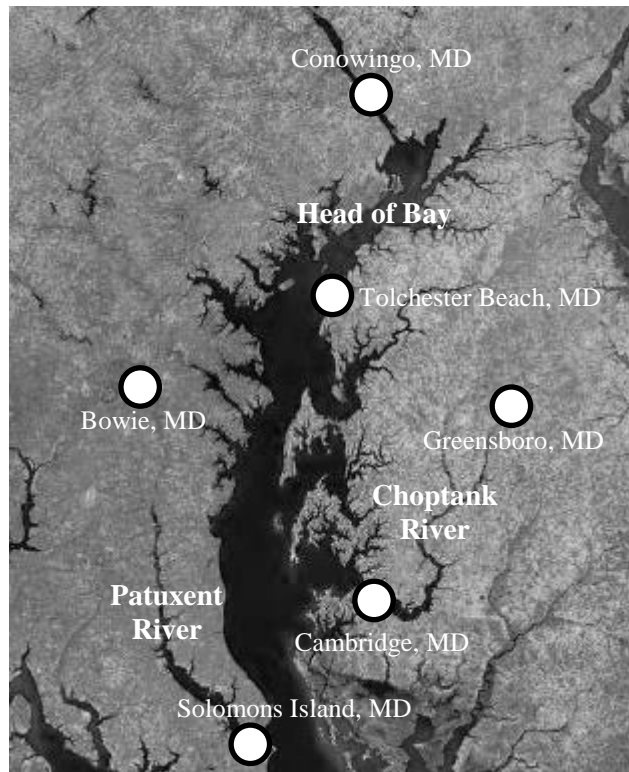
Figure and Table Legends

Table 5.1

Location	Temperature	Discharge	# of years	Years
Choptank River	Cambridge	Greensboro	14	1998 -2004, 2006-2008, 2011 -2012, 2014 -2015
Head of Bay	Tolchester Beach	Conowingo Dam	17	1996 -1997, 1999 -2003, 2005 -2006, 2008 -2015
Patuxent River	Solomons Island	Bowie	16	1995 -1996, 1998 -2003, 2007 -2012, 2014 -2015

The name of the stations where temperature ($^{\circ}\text{C}$) and discharge ($\text{m}^3 \text{sec}^{-1}$) data was collected in each system, number of years we had data for in each system, and a list of the years we data.

Figure 5.1



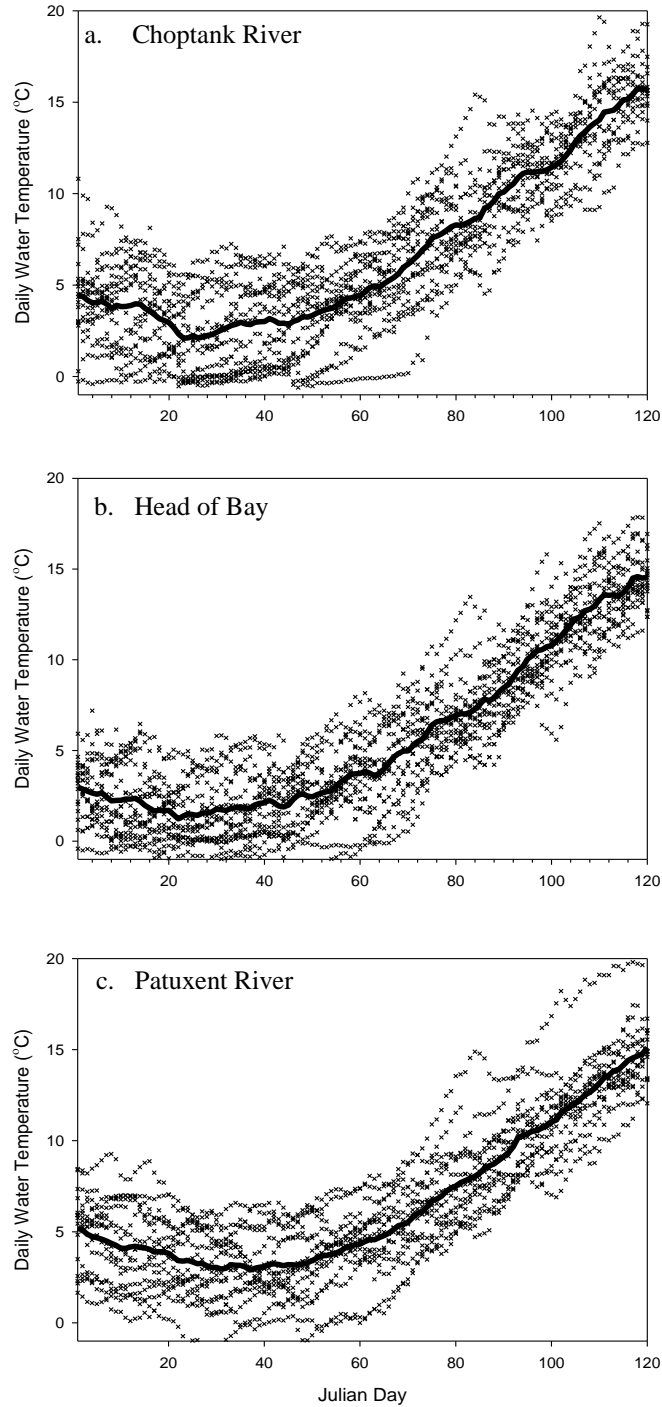
The location of the monitoring stations from which we obtained data. Temperature data was collected by NOAA at Cambridge, Solomons, and Tolchester Beach. Discharge data was collected by USGS at Greensboro, Bowie, and Conowingo. YOY indices were collected by Maryland DNR based off of seine surveys done throughout the Choptank River, Patuxent River, and head of Chesapeake Bay.

Table 5.2

Simulation	Location	Month altered	Temperature change
1	Choptank	January	a. +3 °C b. -3 °C
2	Head of Bay	February	a. +3 °C b. -3 °C
3	Head of Bay	March	a. +3 °C b. -3 °C
4	Patuxent	February	a. +3 °C b. -3 °C

The different simulations run in the temperature-dependent developmental model. Location refers to which system's (Choptank River, Head of Chesapeake Bay, or Patuxent River) the climatological daily averages of winter water temperature (°C) were used (See Figure 5.2). Month altered refers to the specific month in which temperature from the climatological daily average every day was increased or decreased by 3°C.

Figure 5.2



The daily water temperature (°C) for the first four months of the year in the (a) Choptank River for 14 different years, (b) head of Chesapeake Bay for 17 different years, and (c) Patuxent River for 16 different years. The black line is the average daily water temperature for all years.

Figure 5.3

	1	2	3	4	...	84	85
Date	1/1	1/2	1/3	1/4	...	3/25	3/26
Temp (°C)	3.0	2.9	2.8	2.7	...	7.3	7.5
Daily Development	0.011	0.011	0.011	0.011	...	0.023	0.024
Cohort 1	0.011	0.022	0.033	0.044	...	1.01	-
Cohort 2		0.011	0.022	0.033	...	1.00	-
Cohort 3			0.011	0.022	...	0.99	1.01
Cohort 4				0.011	...	0.97	1.00
...
Cohort 78						0.144	0.166

An example of the matrix for each simulation run used to calculate the daily fractional development rate and estimate the date each cohort of *E. carolleae* would reach the adult stage. The model calculated the daily fractional developmental rate using the daily temperature input into the model, and the cumulative fractional development was tracked for each cohort in its row. These daily cohorts had no abundance and only the fractional development was tracked for a given cohort. Once the cumulative development reached 1, the cohort was assumed to have reached the adult stage.

Table 5.3

Fish species	Location	Lilliefors test untransformed	Lilliefors test log transformed
Striped Bass	Choptank River	0.0088	0.2548
	Head of Bay	0.1467	0.1423
	Patuxent River	0.0009	0.1551
White Perch	Choptank River	0.1098	0.0885
	Head of Bay	0.0019	0.5731
	Patuxent River	<0.0001	0.3129

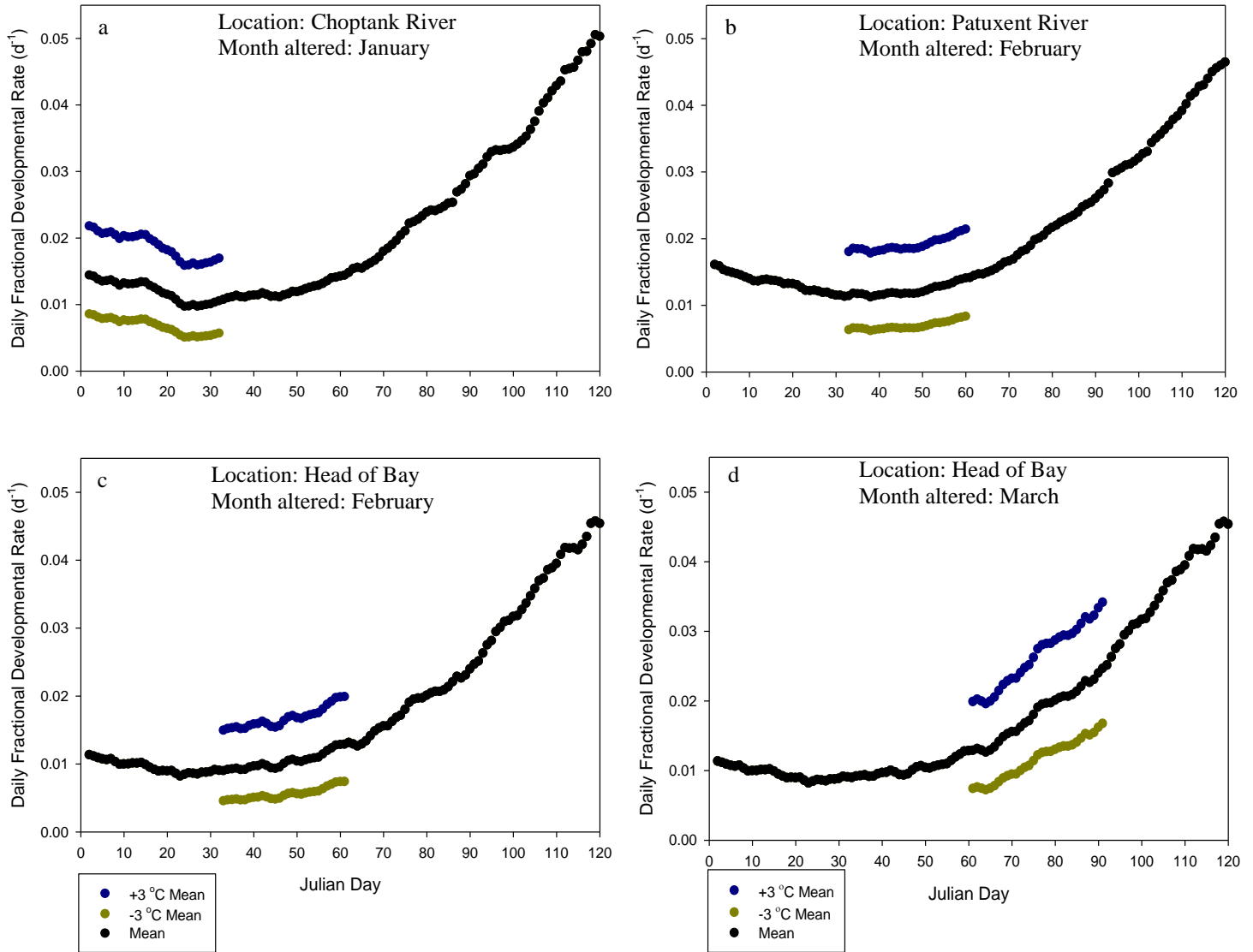
Results of Lilliefors normality test for untransformed and \log_{10} transformed YOY recruitment indices for Striped Bass and White Perch in the Choptank River, Head of Chesapeake Bay, and Patuxent River. Bold values indicate data were not normally distributed ($P < 0.05$).

Table 5.4

Location	Specific Factors	r ²
Striped Bass		
Choptank	Jan. Temperature, Jan. Temperature*Mar. Discharge	0.51
Head of Bay	Feb. Temperature	0.58
Patuxent	Feb. Temperature	0.33
White Perch		
Choptank	Jan. Temperature, Jan. Temperature*Jan. Discharge	0.70
Head of Bay	Mar. Temperature	0.55
Patuxent	Feb. Temperature	0.33

Results of multiple linear regression analysis, showing tests with the highest significant (P<0.05) r² value. Specific factors refer to monthly averages (Jan., Feb., Mar.) of temperature and discharge.

Figure 5.4



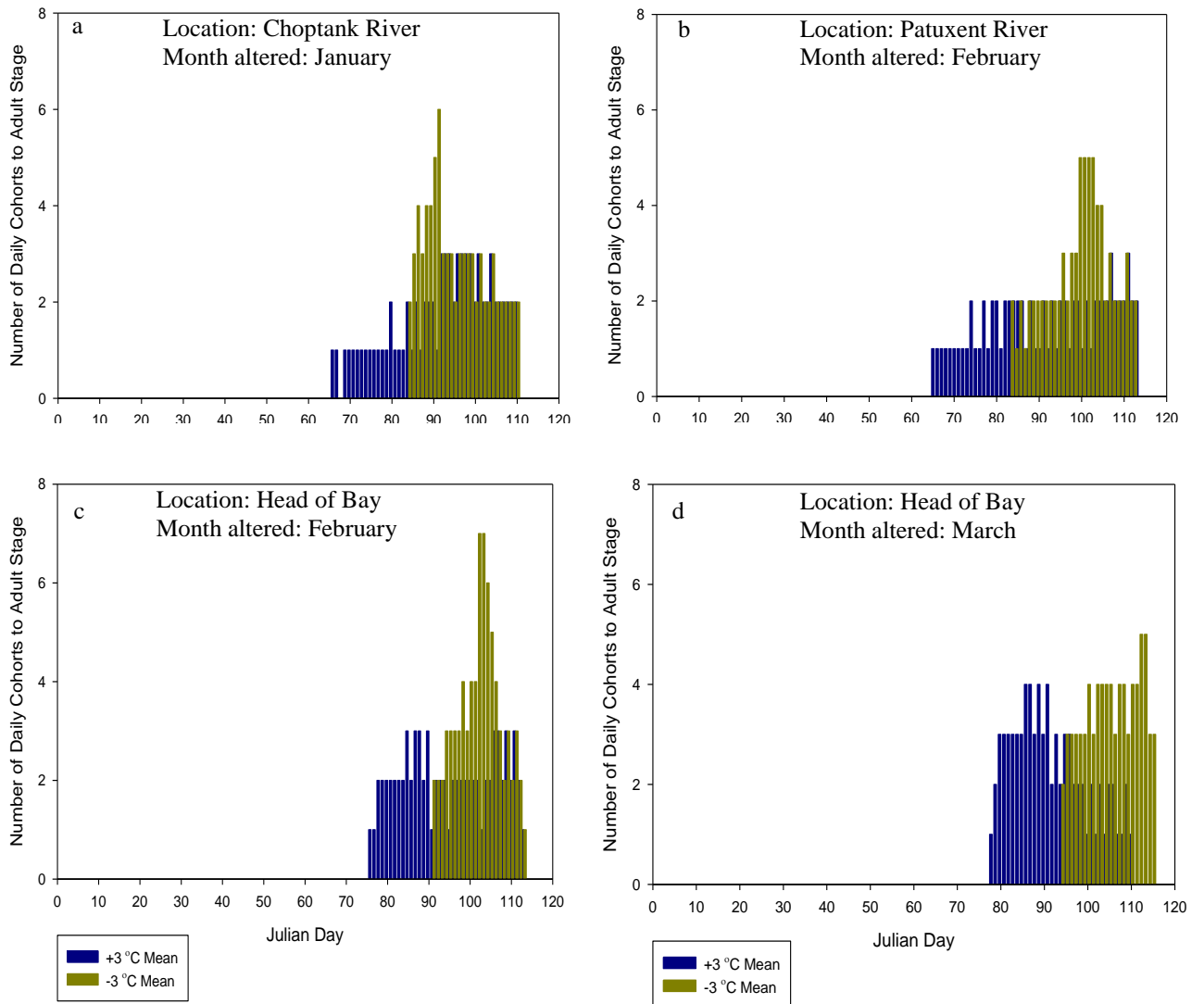
Fractional developmental rates at the climatologically averaged daily temperature (●) and when daily temperature was increased by 3 °C (●) and decreased by 3 °C (●) during (a) January for Choptank River temperature data, (b) February for Patuxent River temperature data, (c) February for Head of the Bay temperature data, and (d) March for Head of the Bay temperature data.

Table 5.5

Simulation	+3	-3	p-value
1. Choptank-Jan	52 ± 1.3	55 ± 1.7	<0.0001
2. Head of Bay-Feb	55 ± 1.4	61 ± 2.	<0.0001
3. Head of Bay -Mar	51 ± 1.6	65 ± 1.9	<0.0001
4. Patuxent-Feb	50 ± 1.3	58 ± 1.7	<0.0001

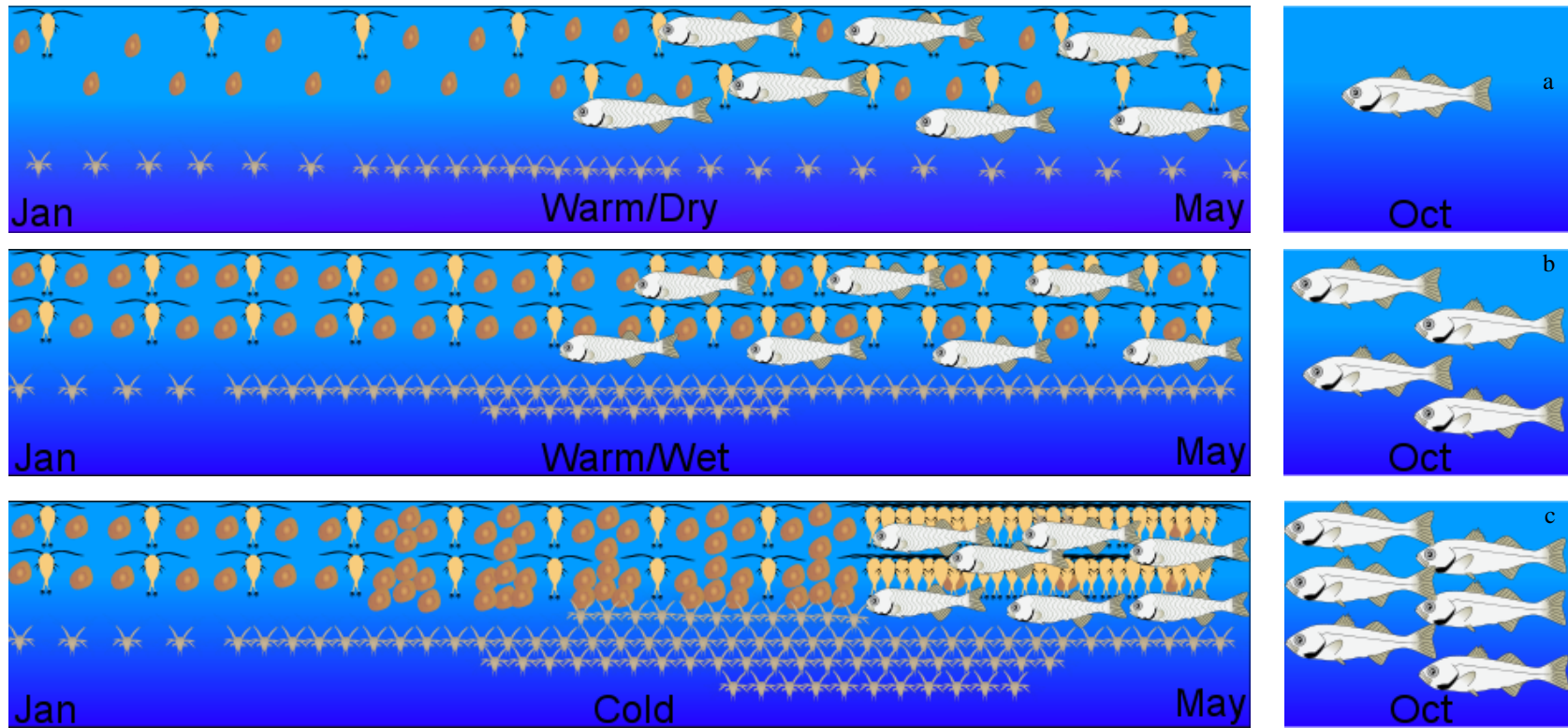
The average (\pm SE) generation time (d^{-1}) of *E. carolleae* that were hatched each day in winter for all the model simulations (Table 5.2). The p-value shows the result of a paired t-test comparing the *E. carolleae* generation time when temperature was increased by 3 °C to when it was decreased by 3 °C in each simulation.

Figure 5.5



The day each daily *E. carolleae* cohort hatched in winter reached the C6 stage according to my developmental model. For each model simulation I adjusted the average daily temperature ± 3 °C in (a) the Choptank River during January, (b) the Patuxent River during February, (c) the head of Chesapeake Bay during February, and (d) the head of Chesapeake Bay during March.

Figure 5.6



Conceptual diagram of how variability in the winter season impacts anadromous fish recruitment later in the year. (a) In winters with above average water temperature and below average discharge, *E. carolleae* copepodite and *H. rotundata* abundance is low. Few nauplii are produced and accumulate throughout winter. In early spring there is a small increase in *E. carolleae* adult abundances, but prey concentrations are low for first feeding larvae of anadromous fish. Young of the year (YOY) recruitment in the fall will be low. (b) In winters with above average water temperature and above average discharge, *E. carolleae* copepodite and *H. rotundata*

abundance is average. A higher concentration of *E. carolleae* nauplii are produced and survive throughout winter. At the same time in spring, *E. carolleae* nauplii hatched in winter reach the adult stage. This increases the concentration of prey available to fish feeding fish larvae. As a result, YOY recruitment is higher in the fall compared to warm, dry years. (c) Discharges do not appear to have any effect on anadromous fish recruitment in waters with below average water temperature. At the beginning of winter, *H. rotundata* and *E. carolleae* copepodite abundance is similar to warm, wet winters. Later in winter, a large *H. rotundata* bloom is likely to form. The combination of high *H. rotundata* abundance and decreased developmental rates caused by low temperatures, allows *E. carolleae* nauplii abundances to accumulate over winter. Later in spring, all *E. carolleae* nauplii hatched in winter reach the adult stage over a short period of time. This causes a large, distinct peak in *E. carolleae* abundances at the same time first fish larvae of anadromous fish start feeding. As a result, YOY recruitment in the fall is likely to be very high.

Conclusions

Over five years of research, my work has led to an improved understanding of winter plankton dynamics in a temperate estuary, of how some of the dominant plankton species interact with each other, and of how winter plankton dynamics can influence the spring ecosystem. Based on primary production rates collected over three winters at a specific location in the Choptank River, the photosynthetic community typically produces an average of $264 \pm 39 \text{ mg C m}^{-3} \text{ d}^{-1}$ in the top 1 m of the water column from the period December 21 to March 19. The highest production rate, $1012 \pm 15 \text{ mg C m}^{-3} \text{ d}^{-1}$, was measured in the middle of a *H. rotundata* bloom.

This project enhanced our understanding of how and why winter blooms of *H. rotundata* form. Winters with high rainfall create a more stratified water column that favors the growth of dinoflagellates over diatoms. My field observations showed that while wet winters can create preferred growth (μ , d^{-1}) conditions for dinoflagellates, zooplankton grazing (g , d^{-1}) can still control the phytoplankton net population growth ($\mu - g$). Therefore, for a phytoplankton bloom to form there must be a reduction in g . Water temperatures below $1 \text{ }^{\circ}\text{C}$ appear to reduce microzooplankton and copepod grazing enough to allow a dinoflagellate bloom to form. Under conditions of high rainfall and reduced grazing, *H. rotundata* is the dinoflagellate species that consistently forms winter blooms in the northern Chesapeake Bay region. At least one reason that *H. rotundata* can bloom under low irradiance winter conditions is because they can ingest bacteria which may partially compensate for low photosynthesis due to light limitation.

One of the major grazers on *H. rotundata* during the winter was the dominant winter copepod, *Eurytemora carolleeae*. Using laboratory cultures of *E. carolleeae* and

H. rotundata, I tested how variation in *H. rotundata* abundance could impact the copepod egg production rate, hatching success rate, and nauplii survival rate. Winter blooms of *H. rotundata* do not appear to impact winter copepodite abundances, but evidence suggests that *H. rotundata* can influence the potential spring copepodite abundances through its effects on survival of copepod nauplii hatched in winter. Laboratory experiments showed that as *H. rotundata* abundances increase, the percent mortality of copepod nauplii is reduced. Copepod nauplii that are hatched in winter reach the copepodite stages in spring, and large *H. rotundata* blooms should increase spring copepodite abundance by reducing mortality on nauplii in winter. I also examined the relationship between *H. rotundata* abundances and copepod egg production and hatching success rates in winter, but there was no clear link between these factors, even over a large range of *H. rotundata* abundances (30 – 25,000 cells mL⁻¹). This suggests that copepods were not food limited in winter. There was, however, a relationship between copepod egg production rate and temperature, with higher temperature leading to greater egg production.

In the final chapter I developed a model to explore how winter environmental conditions could affect anadromous fish recruitment through impacts on the copepod *E. carolleae*. The spring abundance of copepods, specifically *E. carolleae*, is important to the survival of first feeding stages of anadromous fish larvae. If high abundances of *E. carolleae* are available when anadromous fish larvae start to feed, then there is a match between predator and prey, which should lead to high recruitment for that year. The later in the spring that peak abundances of *E. carolleae* occur, the greater the probability of fish larvae being matched with their prey. In my model, I demonstrated how a winter with below average water temperature delays the development of copepod nauplii that

were hatched in winter, causing them to reach the adult stage later in spring and for cohorts to reach maturity around the same time, potentially resulting in a stronger population peak. In addition to delaying nauplii development, cold winters increase the probability of a *H. rotundata* bloom forming, which should increase the survival of *Eurytemora carolleeae* nauplii. The combination of increased survival and delayed development should result in a large abundance peak in *E. carolleeae* occurring later in spring, coinciding with spawning peaks for larval anadromous fish that feed on these copepods. This large, late peak in *E. carolleeae* abundances should increase the chance for successful anadromous fish recruitment.

All of my research was conducted in the Chesapeake Bay region and with dominant Chesapeake Bay winter plankton species. Therefore my findings cannot be directly applied to other coastal ecosystems with different species and environments, but it is likely that that in other temperate estuaries, winter plankton dynamics can impact spring planktonic food webs and anadromous fish recruitment. Estuaries around the world that experience a large range in annual temperature will likely see the same effect of winter temperature on copepod development.

Winter temperature is an annually reoccurring control on plankton processes and interactions in temperate estuaries. In the Chesapeake Bay region, *H. rotundata* appears to require water temperatures below 1 °C to bloom and below average temperatures also decrease *E. carolleeae* developmental rate, delaying the spring peak in *E. carolleeae* populations. This is important because average winter temperature is expected to increase as much as 5 °C by 2100 in the Chesapeake Bay region. Based on my results, this

projected increase in temperature would reduce winter primary production, occurrence of *H. rotundata* blooms, and decrease the likelihood of high anadromous fish recruitment.

It is worth noting that it has been suggested that other fish species in Chesapeake Bay may benefit from an increase in winter temperature. Alex Atkinson's master's thesis (<http://drum.lib.umd.edu/handle/1903/18169>, 2016) found that survival of juvenile Atlantic menhaden (*Brevoortia tyrannus*) was reduced during winters with below average temperature. Menhaden have a different life history than species such as striped bass and white perch. Whereas striped bass and white perch spawn in the late spring, menhaden spawn in the fall and over winter in Chesapeake Bay. Cold winters can indirectly benefit striped bass and white through their prey, while cold winters can directly harm menhaden by decreasing their survival. This means an increase in winter temperature caused by climate change may see an increase in menhaden populations but a decrease in striped bass and white perch populations.

My research has the potential to alter what are considered the primary factors controlling peak spring copepod abundances in temperate estuaries (e.g. spring phytoplankton blooms) and therefore, anadromous fish recruitment. The winter season is not static and dormant for plankton. Plankton productivity can be high, and production during the winter can impact other seasons, particularly spring.

Future Research

My research exposed numerous gaps in our current scientific knowledge in addition to highlighting the importance of winter plankton dynamics to the spring season.

I suggest several directions for future research that would lead to a better understanding of plankton community composition, ecology, development, and production in winter.

1. *Continue and expand upon weekly winter monitoring in the Choptank River and throughout the Chesapeake Bay.* Winter is the most under-sampled season and is often completely excluded from annual monitoring plans. Continuing the monitoring I started over the past five years will help us understand how frequently winter blooms form, how long they last, and the magnitude of a typical bloom. Expanding this monitoring to other tributaries, such as the Patuxent River, will help us understand how widespread winter blooms are in the Chesapeake Bay region. Monitoring in winter would be most effective if sampling was conducted at least semi-weekly (every other week), this would increase the likelihood of sampling during a phytoplankton bloom. I collected samples weekly and think I captured a majority of the variability in winter phytoplankton abundance. Sampling semi-weekly could still capture most variability in phytoplankton abundance while saving on sampling costs (See appendix).
2. *Improve our understanding of *H. rotundata* on a global level.* As I mentioned in Chapter 1, *H. rotundata* is a ubiquitous species in estuarine and coastal environments, but their importance and role in ecosystems is not well understood. Most of the studies in which this species is identified provide little or no abundance data. Therefore, it is unknown in which of these environments *H. rotundata* forms blooms, either during winter or other seasons. The next step would be to collect abundance data for *H. rotundata*

from different regions of the world. Collecting genetic data and measuring their growth rates under a variety of environmental conditions would help us understand intra-specific variability of this global species and the different niches it can and does occupy.

3. *Measure copepod rates (production, grazing, development, etc.) at lower temperatures.* Rate measurements below 4 °C are almost non-existent for copepod processes in temperate regions, despite water temperatures in winter often dropping to 4 °C or less. *E. carolleae* egg production, developmental, and ingestion rates between 0 and 4 °C need to be experimentally determined with cultures in the laboratory to isolate the effect of temperature from other effects on these rates.
4. *Confirm the impact of the winter season on anadromous fish larvae recruitment.* I show statistical evidence that spring recruitment is related to winter temperature and discharge. I then proposed a mechanism by which this is possible, but more field sampling including both process studies and monitoring in winter is needed to confirm whether this is true or not. Tracking winter copepodite and nauplii abundances into spring is necessary to show whether copepodite abundance peaks in spring are correlated to nauplii abundances in winter. It is also necessary to conduct this type of sampling over numerous winters to capture variation in warm vs. cold winters. Understanding what factors are controlling fish recruitment is important so management efforts are targeting things that are most likely to improve recruitment. Also, the impact of winter temperature on anadromous fish

recruitment means recruitment success is likely to be effected by climate change. As winter temperatures increase, as predicted, anadromous fish recruitment will be expected to decrease.

Appendix

Chapter 2

Calculations: To calculate the ingestion rate of an individual copepod on prey I used the calculations originally published in Frost (1972):

$$C_2 = C_1 e^{k(t_1 - t_2)} \quad (1)$$

C_1 is the starting concentration and C_2 is the ending concentrations of prey (cells mL^{-1} or $\mu\text{g Chl } a \text{ L}^{-1}$) for the control bottles over the one day experimental period. The growth constant, k (d^{-1}), for the dinoflagellates without predators present was calculated using equation (1).

$$C_2^* = C_1^* e^{(k-g)(t_2 - t_1)} \quad (2)$$

C_1^* and C_2^* are the concentrations of prey for the experimental bottles at the beginning and end of the one day period, t_1 and t_2 , respectively. 'k' is the value calculated with equation (1) The copepod grazing coefficient, g (d^{-1}), was solved with equation (2).

$$\langle C \rangle = \frac{C_1^* [e^{(k-g)(t_2 - t_1)} - 1]}{(t_2 - t_1)(k - g)} \quad (3)$$

The average prey concentration that copepods had access to, $\langle C \rangle$, for each experimental bottle during the 24 hour time period was calculated with equation (3).

$$F = \frac{Vg}{N} \quad (4)$$

The filtration rate, F ($\text{mL copepod}^{-1} \text{d}^{-1}$), was calculated with equation (4). V is the volume of the bottle, which in this case was 1L. N is the number of copepods in each bottle, and g is the grazing coefficient as calculated from equation (2). The number of copepods in each experiment was based on the number of copepods alive at the end of 24

hours. Any dead copepods found were assumed to have died during the setup of the experiments and to have no influence on the ingestion of prey in the experiment.

$$I = \langle C \rangle \times F \quad (5)$$

By multiplying the average cell concentration $\langle C \rangle$ and the filtration rate (F), the ingestion rate of an individual copepod (I, cells eaten copepod⁻¹ d⁻¹) was calculated with equation (5).

The experiments to estimate microzooplankton grazing and copepod grazing on prey result in different expressions of grazing rates, dilution experiments estimate a microzooplankton community grazing coefficient (g d⁻¹) and Frost (1972) experiments estimate the direct ingestion rate of an individual copepod (cells eaten copepod⁻¹ d⁻¹). In order to directly compare the grazing impact of microzooplankton and copepods, further calculations were needed to transfer the data into the same unit.

I used the method that Strom et al. (2001) used to transform the dilution experiment results into ingestion rates of the microzooplankton community. Strom et al. (2001) used modified versions of the Frost (1972) equations to estimate microzooplankton community ingestion rates. I used equation (3) to calculate the time averaged prey abundance $\langle C \rangle$ in the 100% whole water of the dilution experiments. The growth rate (μ , d⁻¹) and grazing rate (g, d⁻¹) estimated from the dilution experiments were used in place of k and g, respectively. The ingestion rate was calculated from a modified version of equation (5), instead of the filtration rate, g was multiplied by $\langle C \rangle$. This estimated the number of prey cells or chlorophyll *a* concentration ingested by the entire microzooplankton community. The individual copepod ingestion rates calculated by equation (5) were multiplied by the *in situ* copepod abundance to get the total ingestion

rate of prey by the copepod community in a day. The *in situ* copepod abundance was estimate from a vertical plankton tow collected at the same time water was collected for both types of grazing experiments.

Additional Data: Table A.1 and Table A.2 present the calculated μ and g from the dilution experiments for chlorophyll *a*, *H. rotundata*, and cryptophytes for winter 2013 and winter 2014. Table A.1 is μ and g calculated with the linear regression method and Table A.2 is μ and g calculated with the two – point method. As mentioned previously in chapter 2, there was no significant difference between the linear regression method and the two – point method so I used the conservative two – point method data for further analysis. There was no correlation between μ and g for chlorophyll *a* and μ and g for *H. rotundata* (correlation, $r = 0.014$, $p = 0.950$ (μ) and $r = 0.179$, $p = 0.414$ (g)) and cryptophytes (correlation, $r = 0.117$, $p = 0.595$ (μ) and $r = 0.035$, $p = 0.874$ (g)). The most likely reason for this is chlorophyll *a* includes the μ and g for all species with chlorophyll *a*, not just *H. rotundata* and cryptophytes. The focus of this project is on the phytoplankton the form winter blooms so I chose to focus on the direct measurements of specific species/groups and not the community as a whole.

I compared the growth rates for *H. rotundata* I estimated with the two-point method from the dilution experiment to growth rates estimated based on field abundances. I collected weekly abundance data for *H. rotundata*, with this data I estimate what the daily growth rate of *H. rotundata* would have to be to get from the abundance in week one to week two. The growth rate was calculated using the growth rate equation

$$\mu = \ln(t_f/t_o)/7$$

where t_f was *H. rotundata* abundance (mL^{-1}) week 2, t_o was *H. rotundata* abundance (mL^{-1}) week 1, and 7 was the number of days between the two time points.

The average growth rate estimated experimentally in 2013 was significantly higher compared to the growth rates estimated using weekly field abundance data (paired t-test, $p = 0.01$). This is likely because the growth rates estimated from dilution experiments were in the absence of predators, but growth rates estimated from abundance data included predation. The average growth rate estimated experimentally in 2014 was not significantly different compared to the growth rates estimated using weekly field abundance data (paired t-test, $p = 0.10$). Although between 1/27/2014 and 2/17/2014 (Table A.3), when a bloom formed, the growth rates estimated with abundance data was higher than growth rates estimated with dilution experiments. This suggests that some artifact of the dilution experiments was suppressing *H. rotundata* growth, although I have no data on what the artifact may be.

Winter 2013 provides the best data for growth rates of *H. rotundata* and cryptophytes compared to winter 2014. It is unclear why most measured growth rates for phytoplankton in winter 2014 were negative but weeks with high *H. rotundata* abundance could have reduced the effect of the dilution experiment by not decoupling *H. rotundata* from prey, even in the lowest dilution. As a result of the unreliable growth rates measured in winter 2014, I used GPP as a proxy for growth among the phytoplankton community, specifically for *H. rotundata*. There was a strong, positive correlation between *H. rotundata* abundance and GPP for 2013 and 2014 (correlation, $r = 0.915$, $p = <0.0001$). Since *H. rotundata* appears to be adapted to winter conditions, it would be expected that

H. rotundata would have the highest growth rates compared to all other phytoplankton and account for the largest portion of GPP.

In winter 2013 the average growth rate of *H. rotundata* was significantly higher than the average growth rate of cryptophytes (one tailed paired t-test, $p = 0.021$). This supports hypothesis that *H. rotundata* has higher growth rates in the winter compared to other phytoplankton. While the average growth rate for *H. rotundata* was 0.37 d^{-1} , their maximum estimated growth rate was 0.99 d^{-1} (Table A.2).

I fitted a functional response curve to the calculated ingestion and clearance rate of an individual copepod at different *H. rotundata* concentrations with data from winters 2012, 2013, and 2014 (Figure A.1). The I_{max} is $19.6 \mu\text{g copepod}^{-1} \text{ d}^{-1}$ and $K=$ is $376.7 \mu\text{g L}^{-1}$. There is a lot of variability in an individual copepods ingestion rate, especially at higher carbon concentrations ($>500 \mu\text{g L}^{-1}$). This high variability is most likely because the data was taken over three different winters. Under the right conditions an individual copepod could ingest close to $40 \mu\text{g d}^{-1}$. The graph appears to show two different potential response curves but further analysis would have to be done to see what is driving this difference (Figure A.1).

References

Frost, B.W. (1972) Effects of size and concentration of food particles on the feeding behavior of the marine planktonic copepod *Calanus pacificus*. *Limnol Oceanogr* 17:805-815.

Strom, S.L., M.A. Brainard, J.L. Holmes, and M.B. Olson (2001) Phytoplankton blooms are strongly impacted by microzooplankton grazing in coastal North Pacific waters. *Mar Biol* 138:355-368.

Table A.1

Date	Chlorophyll <i>a</i>		<i>H. rotundata</i>		Cryptophytes	
	Growth (μ d ⁻¹)	Grazing (g d ⁻¹)	Growth (μ d ⁻¹)	Grazing (g d ⁻¹)	Growth (μ d ⁻¹)	Grazing (g d ⁻¹)
12/23/2012	-1.50	-1.62	0.97	1.30	0.42	0.27
12/31/2012	0.67	0.54	0.20	0.80	-0.10	0.38
1/6/2013	0.41	0.34	1.10	0.59	0.21	0.23
1/12/2013	0.01	-0.31	0.42	-0.83	0.17	-0.15
1/20/2013	0.33	0.37	0.31	0.46	0.20	0.11
1/27/2013	0.04	-0.04	0.06	0.05	0.05	0.09
2/3/2013	0.05	-0.13	0.20	0.03	0.17	0.04
2/10/2013	0.06	-0.15	0.11	0.11	0.02	0.02
2/17/2013	-0.07	0.02	-0.01	0.45	-0.12	-0.49
2/24/2013	0.24	0.12	0.28	0.16	0.16	0.27
3/3/2013	0.02	-0.04	0.26	0.33	0.28	0.26
3/10/2013	0.08	-0.24	0.25	-0.24	0.42	0.06
Average	0.03 + 0.16	-0.10 + 0.16	0.35 + 0.10	0.27 + 0.16	0.16 + 0.05	0.09 + 0.07
12/30/2013	-2.68	-2.64	-0.03	0.14	-0.91	-0.52
1/6/2014	-0.54	-1.33	-0.18	0.01	-0.09	-0.11
1/13/2014	-0.33	-0.66	-1.10	2.99	-0.23	3.09
1/20/2014	-0.32	-0.20	-0.42	1.24	0.04	0.10
1/27/2014	0.17	0.12	-1.58	-1.58	-3.14	-2.75
2/3/2014	0.07	0.09	-0.02	-0.25	0.11	0.05
2/10/2014	0.04	0.15	0.06	0.09	0.12	0.41
2/17/2014	0.13	0.00	0.05	-0.05	-0.11	-0.22
2/24/2014	0.04	-0.01	-0.09	-0.14	0.07	-0.11
3/3/2014	-0.26	-0.26	-0.28	-0.24	-0.05	0.50
3/10/2014	-0.06	-0.03	-0.35	-0.24	0.25	0.51
Average	-0.34 ± 0.26	-0.43 ± 0.27	-0.36 ± 0.17	0.18 ± 0.36	-0.36 ± 0.31	0.09 ± 0.42

The growth (μ , d⁻¹) of and grazing (g, d⁻¹) on chlorophyll *a*, *H. rotundata*, and cryptophytes in winter 2013 and 2014 based off of linear regression analysis from dilution experiments. (\pm SE)

Table A.2

Date	Chlorophyll <i>a</i>		<i>H. rotundata</i>		Cryptophytes	
	Growth ($\mu \text{ d}^{-1}$)	Grazing (g d^{-1})	Growth ($\mu \text{ d}^{-1}$)	Grazing (g d^{-1})	Growth ($\mu \text{ d}^{-1}$)	Grazing (g d^{-1})
12/23/2012	-1.60	-1.67	0.99	1.27	0.41	0.26
12/31/2012	1.09	0.91	0.70	1.01	0.06	0.51
1/6/2013	0.26	0.22	0.92	0.63	0.35	0.63
1/12/2013	-0.07	-0.38	0.65	-0.62	0.27	-0.05
1/20/2013	0.30	0.34	0.52	0.63	0.20	0.10
1/27/2013	-0.01	-0.09	-0.06	-0.03	0.08	0.11
2/3/2013	0.00	-0.17	0.33	0.13	0.19	0.08
2/10/2013	0.05	-0.16	0.29	0.01	-0.07	-0.16
2/17/2013	-0.05	0.03	-0.27	0.22	0.18	0.03
2/24/2013	0.15	0.05	0.35	0.20	0.14	0.26
3/3/2013	0.04	-0.01	0.17	0.25	0.30	0.28
3/10/2013	0.10	-0.01	-0.12	-0.57	0.60	0.21
Average	0.02 + 0.18	-0.07 + 0.18	0.37 + 0.12	0.26 + 0.17	0.22 + 0.05	0.19 + 0.07
12/30/2013	-2.68	-2.20	0.39	0.49	-0.80	-0.38
1/6/2014	-0.54	-1.52	-0.34	-0.13	-0.05	-0.08
1/13/2014	-0.33	-0.64	-1.64	2.52	-0.52	2.81
1/20/2014	-0.32	-0.34	-0.57	1.08	-0.08	-0.04
1/27/2014	0.17	-0.01	-0.94	-1.04	-3.30	-2.95
2/3/2014	0.07	0.10	-0.06	-0.28	0.24	0.19
2/10/2014	0.04	0.26	-0.02	0.02	0.20	0.49
2/17/2014	0.13	0.00	0.13	0.01	0.14	-0.01
2/24/2014	0.04	-0.04	-0.18	-0.23	-0.02	-0.20
3/3/2014	-0.26	-0.20	-0.40	-0.35	0.20	0.73
3/10/2014	-0.06	0.00	-0.35	-0.25	0.11	0.37
Average	-0.34 ± 0.26	-0.42 ± 0.24	-0.36 ± 0.17	0.17 ± 0.30	-0.35 ± 0.33	0.09 ± 0.42

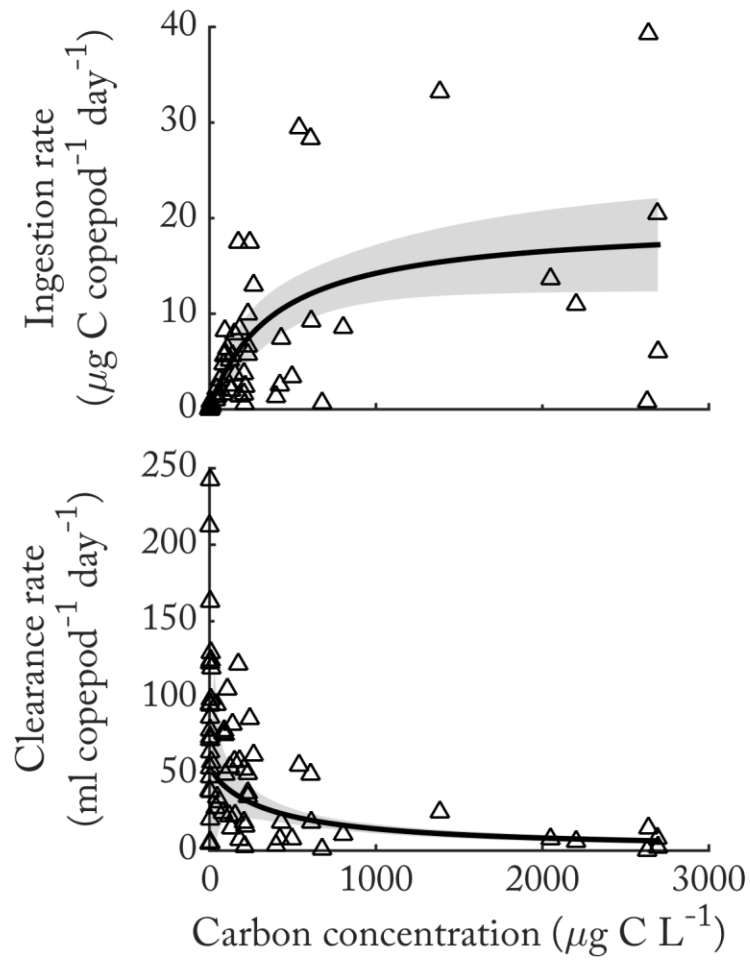
The growth (μ, d^{-1}) of and grazing (g, d^{-1}) on chlorophyll *a*, *H. rotundata*, and cryptophytes in winter 2013 and 2014 based off of 2-point method analysis from dilution experiments. (\pm SE)

Table A.3

Date	<i>H. rotundata</i>	
	Exp Growth (μ d ⁻¹)	Field Growth (μ d ⁻¹)
12/23/2012	0.99	-0.16
12/31/2012	0.70	0.39
1/6/2013	0.92	-0.28
1/12/2013	0.65	0.12
1/20/2013	0.52	-0.12
1/27/2013	-0.06	0.14
2/3/2013	0.33	-0.04
2/10/2013	0.29	0.04
2/17/2013	-0.27	-0.01
2/24/2013	0.35	0.04
3/3/2013	0.17	-0.13
3/10/2013	-0.12	-
Average	0.37 ± 0.12	-0.001 ± 0.06
12/30/2013	0.39	-0.15
1/6/2014	-0.34	-0.56
1/13/2014	-1.64	-0.09
1/20/2014	-0.57	0.30
1/27/2014	-0.94	0.18
2/3/2014	-0.06	0.13
2/10/2014	-0.02	0.12
2/17/2014	0.13	0.15
2/24/2014	-0.18	-0.004
3/3/2014	-0.40	-0.04
3/10/2014	-0.35	-
Average	-0.36 ± 0.17	0.01 ± 0.08

The growth (μ , d⁻¹) of *H. rotundata* based off of 2-point method analysis from dilution experiments (Exp Growth) and weekly field abundance data collected from the Choptank River (Field Growth). (\pm SE)

Figure A.1



The ingestion rates (a, $\mu\text{g C copepod}^{-1} \text{ day}^{-1}$) and clearance rates (b, $\text{ml copepod}^{-1} \text{ day}^{-1}$) of *E. carolleae* copepods measured at various *in situ* carbon concentrations ($\mu\text{g C L}^{-1}$) of *H. rotundata* with a type II functional response curve. Grey area denotes 95% confidence intervals.

Chapter 3

2015 field experiments: Between December 29th, 2014 and March 9th, 2015 I set up weekly dilution experiments to measure $\leq 10 \mu\text{m}$ nanoplankton and $\leq 200 \mu\text{m}$ microplankton community grazing coefficients on bacteria. Water for the experiments was collected from the same location, Bill Burton fishing pier, described in previous chapters. All water was gently filtered through $200 \mu\text{m}$ mesh to remove any large zooplankton, than half of the water was filtered through $10 \mu\text{m}$ mesh to remove all phytoplankton and zooplankton between $11 \mu\text{m}$ to $200 \mu\text{m}$ long.

The set up for the $\geq 10 \mu\text{m}$ dilution experiment was a slightly modified version of Landry & Hasset (1982) based on experiments done in Tsai et al. (2013) to measure community grazing coefficients (day^{-1}) for $\leq 10 \mu\text{m}$ nanoplankton on bacteria and apparent bacterial growth rate (day^{-1}). I autoclaved the $0.2 \mu\text{m}$ filtered water used to dilute the whole water. Viruses can slip through $0.2 \mu\text{m}$ filters and inflate the grazing rates on bacteria through viral lysis (Tsai et al. 2013). Autoclaved water can remove viruses and reduce a potentially large source of error; this method ensured more accurate estimates of $\leq 10 \mu\text{m}$ nanoplankton grazing rates on bacteria. Filtered water was collected twice throughout the season and autoclaved in large batches and maintained at 4°C in the dark until used for experiments. $\leq 200 \mu\text{m}$ microplankton grazing experiments were set up as described in Landry & Hasset (1982) and in Chapter 1.

The dilution treatments used in my experiments were 100%, 20%, 10%, and 5% whole water. Triplicate 250 mL bottles were used for each treatment with $10 \mu\text{m}$ filtered water and triplicate 1000 mL bottles were used for each treatment with $200 \mu\text{m}$ filtered water. The bottles were placed in one layer mesh bags and ran for 24 hours in a protected

cove. A 4.0 mL water sample take at 0 and 24 hours from each bottle was preserved in 2% sterilized buffered paraformaldehyde in a Thermo Scientific 5.0 mL Cyrovial. Samples were stored frozen at -80.0°C for less than a week from the time of sample collection. When the samples were ready to be run they were thawed and stained with SYBR green in a dark room. Bacteria from these samples were counted using a BD Acurri C6 flow cytometer. PolyScience SureCount beads were used to calibrate the flow cytometer.

Initial analysis of dilution experiments to calculate community grazing coefficient (g, d^{-1}) and apparent bacteria growth rate (μ, d^{-1}) was the same as described in Chapter 2, using the 2-point dilution method. The microzooplankton grazing coefficient on bacteria in the $\leq 200 \mu m$ dilution experiments represents the combined grazing coefficient of $\leq 10 \mu m$ nanoplankton and microzooplankton on bacteria. In order to estimate just the grazing coefficient of microzooplankton on bacteria I took the difference of estimated bacterial growth rate at the 100% whole water dilution for both dilution experiments (Tsai et al. 2013). If microzooplankton are grazing on bacteria, then the apparent growth rate for bacteria in $\leq 200 \mu m$ dilution experiments is lower than their growth rate in $\leq 10 \mu m$ dilution experiments. If the apparent bacterial growth rate is higher in the $\leq 200 \mu m$ dilution experiment, then microzooplankton are not grazing on bacteria and could be releasing them from grazing pressure from $\leq 10 \mu m$ through a trophic cascade.

$\leq 10 \mu m$ Nanoplankton were grazing on bacteria for all but one week, and $\leq 200 \mu m$ microplankton were not grazing on bacteria for all but one week (Table B.1). The one week $\leq 200 \mu m$ microplankton were grazing on bacteria the rate was very low (Table B.1). When the $\leq 200 \mu m$ microplankton were included, the growth rates of bacteria

significantly increase in the 100% experimental bottles compared to 100% experimental bottles where 11-200 μm microplankton were excluded for 6 out of the 11 weeks (Figure B.1, Table B.1). The results suggest there is a trophic cascade between ≤ 200 μm microplankton, ≤ 10 μm nanoplankton, and bacteria for about 50% of winter. The presence of microplankton can increase the apparent growth rate of bacteria, suggesting it releases grazing pressure on bacteria from ≤ 10 μm nanoplankton.

Microplankton is known to graze on nanoplankton, particularly *Heterocapsa rotundata*, in the winter (Millette et al. 2015) and *H. rotundata* grazes on bacteria (chapter 3). Therefore, microplankton could increase bacterial growth and abundance by consuming their primary predator. If this is true, then we have to understand more than just the grazing rates of predators on bacteria if we want to know what controls bacterial populations.

It is possible that the difference in bacterial growth rates between the two treatments is an artifact of the experiments. The filtered seawater used to set up the dilution experiment was different for the ≤ 10 μm experiments than the ≤ 200 μm experiments. Filtered seawater used to dilute the ≤ 200 μm experiments was filtered through a 0.2 μm filter and used right away while seawater used to dilute the ≤ 10 μm experiments was filtered through a 0.2 μm filter, autoclaved for two hours, and stored in the dark at 4 °C. It is possible 0.2 μm filtered water had higher amounts of DOM than the 0.2 μm filtered and autoclaved water that stimulated growth of bacteria in the ≤ 200 μm experiments.

There is evidence to suggest a trophic cascade exists in the winter between microplankton, nanoplankton, and bacteria. More research is necessary to confirm if this

cascade is real or an artifact of the experimental design. If a cascade does exist, then the impact of *H. rotundata* grazing on bacterial populations is controlled by more than just light and *H. rotundata* abundance as discussed in chapter 3.

Microsphere uptake rate: To determine how long to run my field experiments with 0.5 μm microspheres I had to measure how long *H. rotundata* ingested the microspheres before they started to egest them. At the start of experiments *H. rotundata* is only ingesting microspheres but eventually they will start egesting the microspheres as well. Once *H. rotundata* starts ingesting and egesting microspheres *H. rotundata*'s ingestion rate can no longer be accurately measured.

I set up five sets of 3 250 mL bottles with 100 mL of 20 μm filtered water collected from the HPL dock. A concentration of 2.5×10^5 microspheres mL^{-1} was added to each bottle. The experiment ran for 120 minutes in the same environmental chamber as the laboratory experiments in chapter 3. Samples to measure microsphere uptake were taken from one of the experimental sets at 15, 30, 60, 90, and 120 minutes. Each sample was preserved on to a glass slide as described in the field experiments in chapter 3.

H. rotundata linearly took up microspheres for 60 minutes (Figure B.2). At 90 and 120 minutes there was no change in the rate at which microspheres were ingested, suggesting that *H. rotundata* had started to egest the microspheres. I decided to run my field experiments in chapter 3 for 30 minutes because at 60 minutes the standard error was higher compared to 30 minutes (Figure B.2).

Laboratory experiment #1: additional data: One of the goals of the first laboratory experiment I did looking at the effect of ammonium concentration and irradiance levels on *H. rotundata* bacterial grazing was to establish methods for future experiments. I

chose to run the experiment for 72 hours to test how long I needed to run future experiments for, so I measured the grazing rates every 24 hours. During the first 24 hours (0-24), based on statistical analysis there was a significant interactive effect of ammonium and irradiance levels (p-value = <0.0001 , two-way ANOVA), but I did not identify any pattern between grazing rates and ammonium concentrations and irradiance levels (Figure B.3a).

During the last 24 hours (48-72) the experiment failed. I did not detect growth of bacteria in any of the controls, which was high during the earlier 48 hours, and resulted in the grazing rates being below or near zero (Figure B.3b). Estimates of *H. rotundata* abundances did not make sense and I could not retest them because the sample size was too small. I decided to include the results from the 24-48 hr time point because the results from them were supported by later experiments and were the reason I focused on irradiance over ammonium. In laboratory experiments #2 I made numerous adjustments to the methods based on the first set of experiments, including increasing the volume of bottles, increasing the amount of water, and reducing the run time of the experiment.

Field Experiments: additional data: I fitted two different equations to the data in Figure 3.4 in addition to the log function (Figure B.4). The other two equations fitted to the data were a simple linear regression and power function. Both of the Akaike information criterion (AIC) values for the simple linear regression and power function were higher compared to the log function (Figure B.4). Therefore, I selected the log function as the equation to fit to my data.

References

Landry, M.R. and R.P. Hassett (1982) Estimating the grazing impact of marine microzooplankton. *Mar Biol* 67:283-288.

Millette, N.C., D.K. Stoecker, and J.J. Pierson (2015) Top-down control of micro- and mesozooplankton on winter dinoflagellate blooms of *Heterocapsa rotundata*. *Aquat Microb Ecol* 76:15-25.

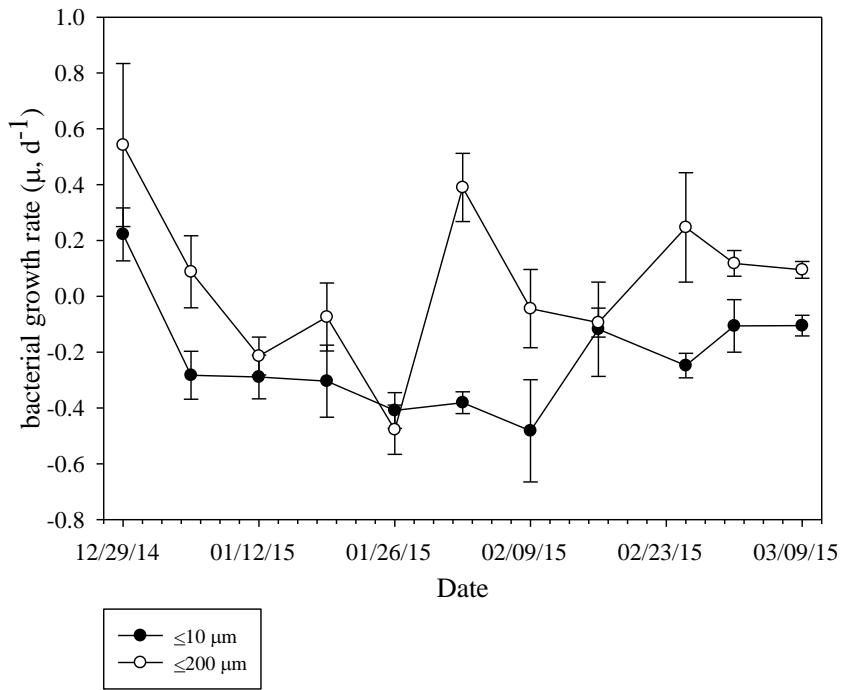
Tsai, A.Y., G.C. Gong, and Y.W. Huang (2013) Variations of microbial loop carbon flux in western subtropical Pacific coastal water between warm and cold season. *Journal of Experimental Marine Biology and Ecology*. 449:111-117.

Table B.1

Date	$\leq 10 \mu\text{m}$ nanoplankton grazing (d^{-1})	$\leq 200 \mu\text{m}$ microplankton grazing (d^{-1})
12/29/2014	0.099 ± 0.203	-0.320 ± 0.248
1/5/2015	0.495 ± 0.037	-0.370 ± 0.195
1/12/2015	-0.038 ± 0.170	-0.075 ± 0.137
1/19/2015	0.338 ± 0.212	-0.231 ± 0.238
1/26/2015	0.470 ± 0.119	0.069 ± 0.056
2/2/2015	0.052 ± 0.169	-0.770 ± 0.160
2/9/2015	0.693 ± 0.396	-0.438 ± 0.182
2/16/2015	0.609 ± 0.358	-0.025 ± 0.229
2/25/2015	0.188 ± 0.096	-0.494 ± 0.200
3/2/2015	0.505 ± 0.030	-0.223 ± 0.119
3/9/2015	0.401 ± 0.071	-0.280 ± 0.065

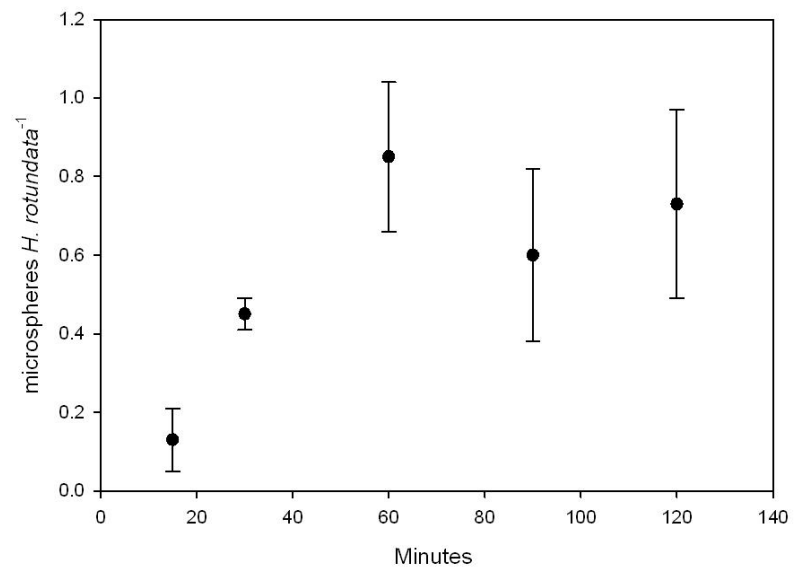
Weekly grazing rates on bacteria by $\leq 10 \mu\text{m}$ nanoplankton and $\leq 200 \mu\text{m}$ microplankton in the 2015 winter. $\leq 200 \mu\text{m}$ microplankton grazing rates were the difference between bacterial growth rate in the 100% whole water treatments of $10 \mu\text{m}$ and $200 \mu\text{m}$ dilution experiments. Bold numbers are significant grazing rates, for $\leq 200 \mu\text{m}$ microplankton they also note when $\leq 200 \mu\text{m}$ microplankton grazing significantly reduced $< 10 \mu\text{m}$ nanoplankton grazing.

Figure B.1



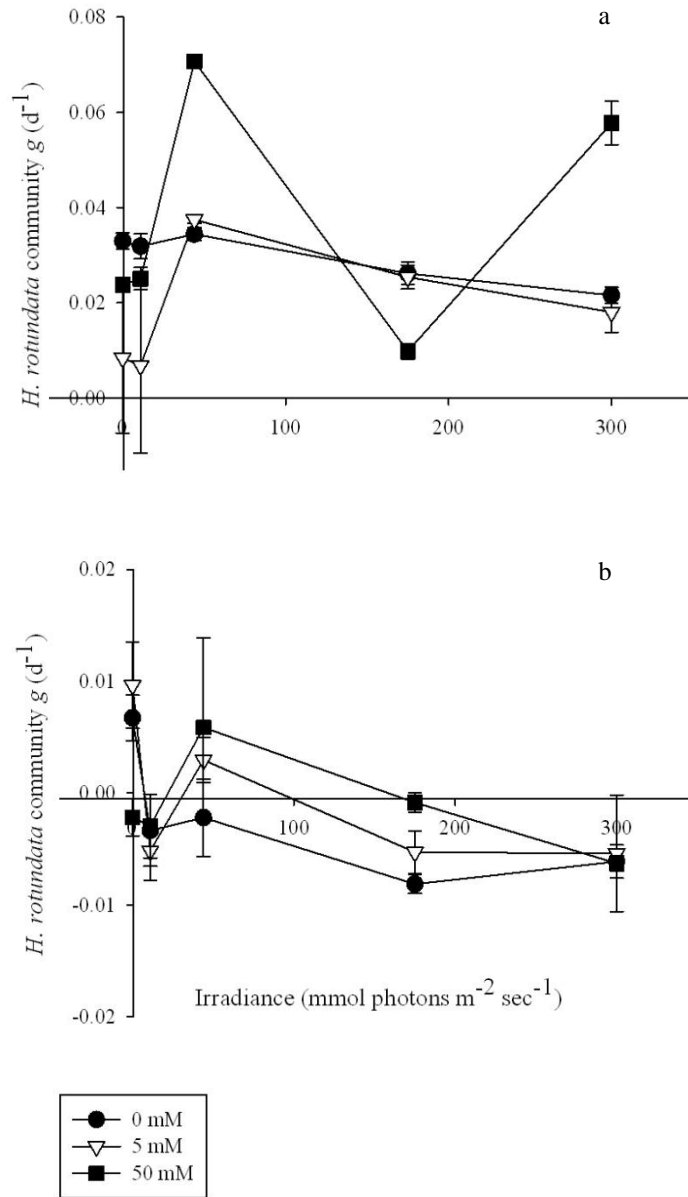
Weekly growth rates of bacteria (d^{-1}) in experimental bottles with 100% 10 μm and 200 μm filtered water during the 2015 winter. Error bars = standard error.

Figure B.2



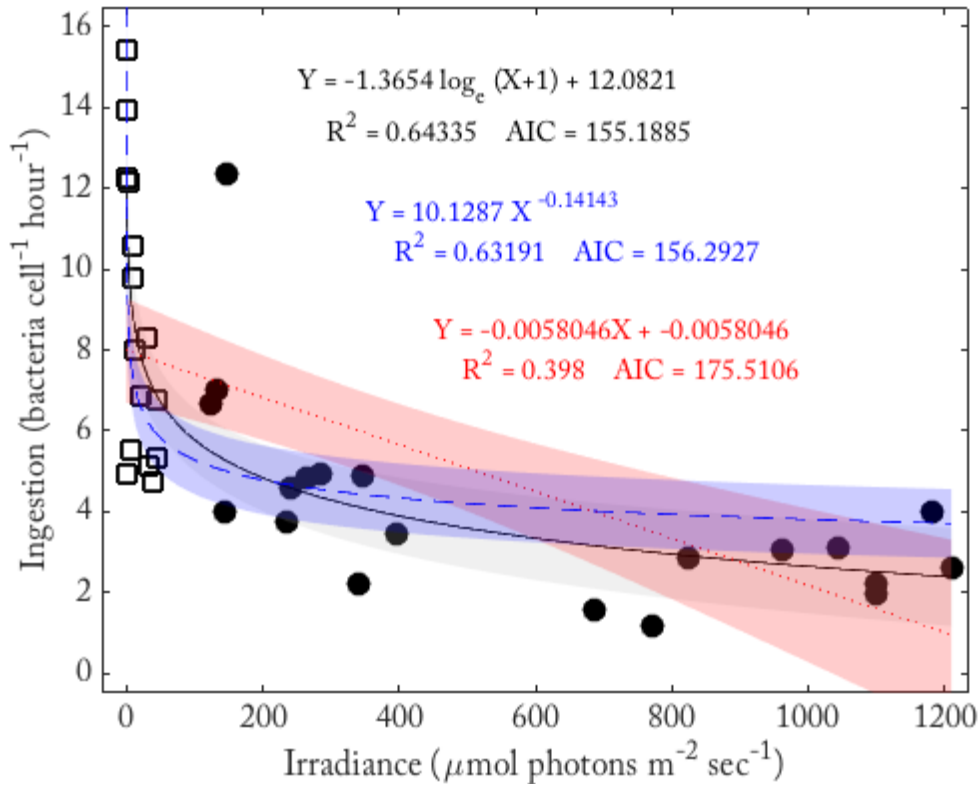
The uptake rate of microspheres per *H. rotundata* over 120 minutes.

Figure B.3



Heterocapsa rotundata community grazing coefficient g (d^{-1}) at different irradiance levels ($\mu mol\ photons\ m^{-2}\ s^{-1}$) for three different ammonium concentrations (μM) during (a) 0-24 hr and (b) 48-72 hr. Bars indicate SE.

Figure A.4



A comparison of a log function (black), power function (blue), and linear regression (red) fitted to ingestion rates of *H. rotundata* (bacteria hr⁻¹) at different irradiance levels. Color shaded areas denotes 95% confidence intervals.

Chapter 5

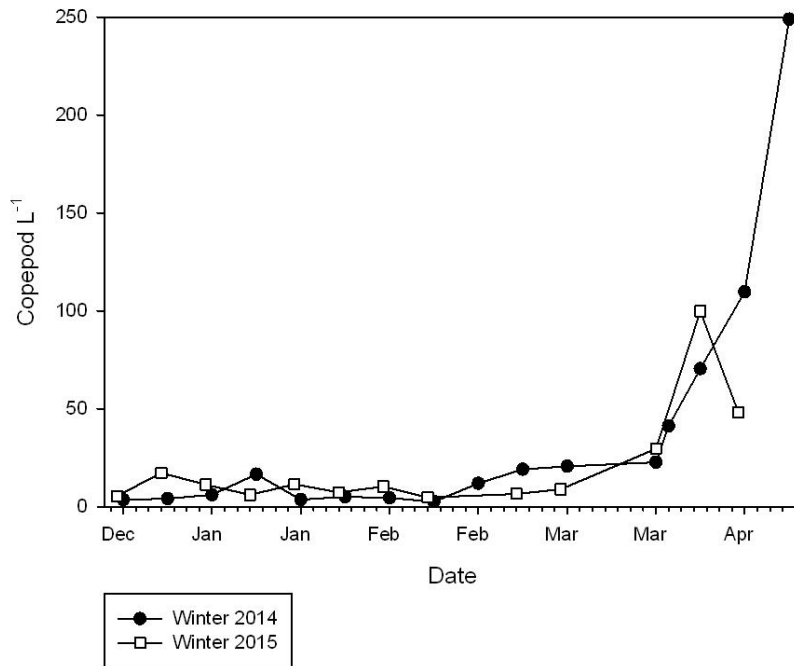
In winter 2014 and 2015 I continued collecting copepod samples to estimate copepodite abundances into the spring. In both of these years there was a bloom of *H. rotundata* that persisted past winter and into the spring, so I kept sampling until the bloom disappeared. In 2014 I collected five additional samples between 3/24/2014-4/14/2014 and in 2015 I collected three additional samples between 3/24/2015-4/6/2015.

In spring 2014 the copepodite abundances started to exponentially increase from 22 copepodites L⁻¹ to 249 copepodites L⁻¹ over twenty-one days (Figure C.1). In spring 2015 the copepodite abundances started to exponentially increase from 29 copepodites L⁻¹ to 100 copepodites L⁻¹ over seven days (Figure C.1). During this time the copepodite community was composed of 95-99% *E. carolleae*. These rapid increases in copepodite abundances are what would be predicted by the temperature based developmental model, but I cannot confirm the rapid increase is related to winter water temperature.

More sampling in spring is required to confirm temperatures in winter contribute to the timing of peak spring copepod abundance. When I finished sampling in spring 2014 copepod abundance was still increasing, it is unknown how high copepod abundances got that year or how long the copepod abundance peak lasted. In 2015, after copepod abundance reached 100 copepodites L⁻¹, abundances dropped to 49 copepodites L⁻¹ the following week (Figure C.1). It is unknown if copepodite abundances increased the following week and reached peak abundances later in the spring. In fact, based on average temperature, copepod abundances should have peaked later in 2015 (1.6 °C) compared to 2014 (3.0 °C).

The copepod abundances I collected between winter and spring in 2014 and 2015 suggest that copepod abundances are relatively stable in winter, than rapidly increase over a short period of time in spring. In order to confirm this is related to winter temperature, more intense sampling through winter and spring over multiple years is necessary.

Figure C.1



Copepodite abundances of *E. carolleae* and *A. tonsa* in the Choptank River for winter and spring 2014 (12/30/2013-4/14/2014) and 2015 (12/29/2014-4/6/2015).

Future Research

For all five years I sampled, I collected phytoplankton abundance data at least once a week (Chapter 1). This provided some of the highest resolution on phytoplankton abundance over multiple winters in Chesapeake Bay. The Chesapeake Bay Program (CBP) is the major monitoring group that consistently collects phytoplankton abundance data in the Bay. Currently, they collect one sample for winter phytoplankton abundance sometime in March every year. This is not enough sampling to capture the variability of phytoplankton abundance throughout winter (Chapter 1). Although, it is also not feasible for the CBP to conduct weekly sampling throughout at the year at all their monitoring stations.

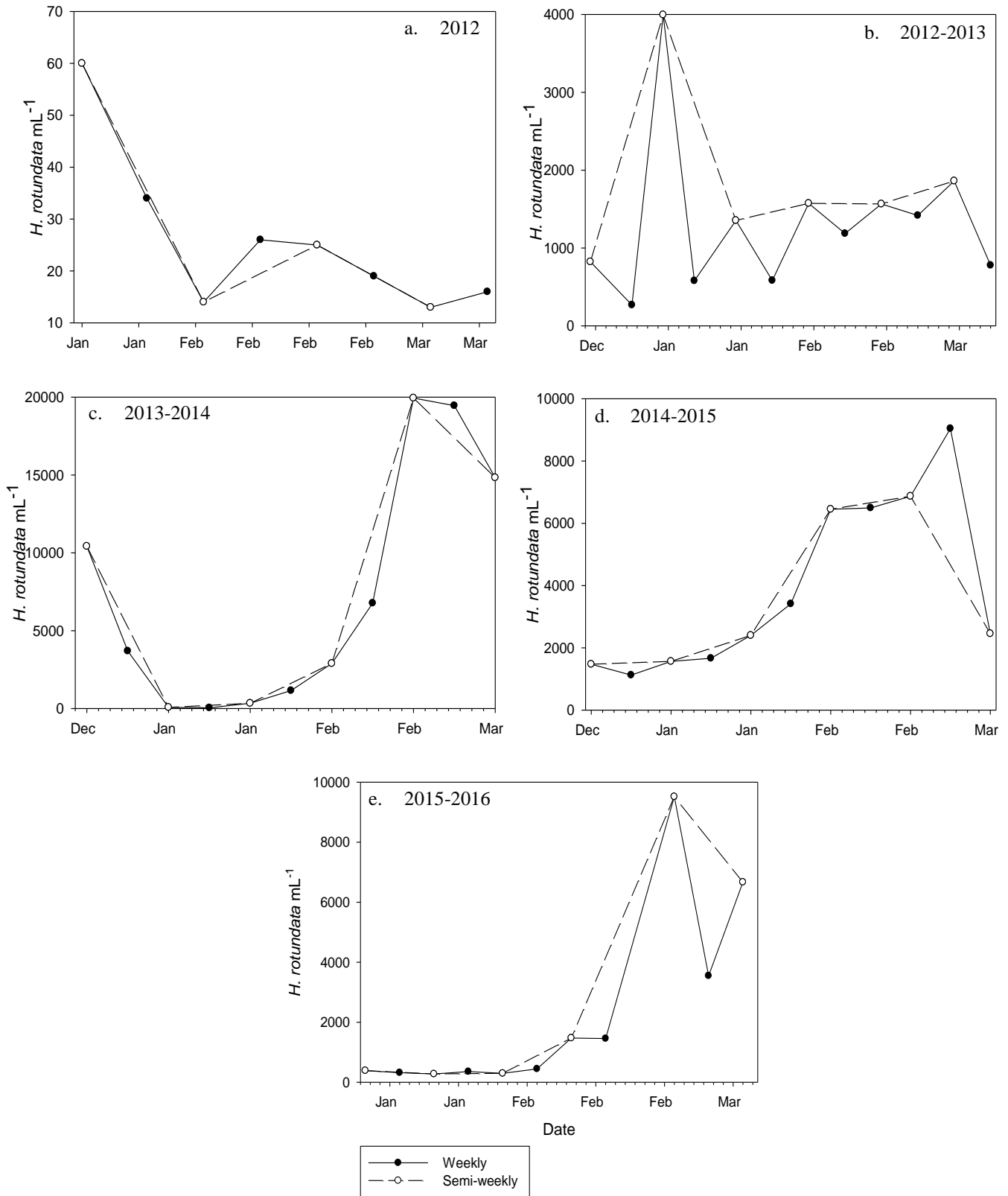
In the spring, summer, and fall the CBP typically samples twice a month. Extending this sampling into winter months is the easiest way start collecting more data on winter phytoplankton abundance. Ideally though, CBP phytoplankton samples should be collected semi-weekly. Two-sampled unpaired t-tests showed that the average winter *Heterocapsa rotundata* abundance from weekly sampling was not statistically different from the average *H. rotundata* abundance when sampling was reduced to semi-weekly (Table D.1). Additionally, semi-weekly sampling would still capture most of the variability of weekly sampling (Figure D.1), but would save on costs by reducing the number samples collected by half.

Table D.1

Year	Weekly	Semi-weekly	P-value
2012	26 ± 6	26 ± 13	0.87
2012-2013	1332 ± 292	3195 ± 1308	0.18
2013-2014	7236 ± 2445	8081 ± 3702	0.84
2014-2015	3904 ± 878	3535 ± 1099	0.78
2015-2016	2249 ± 985	3103 ± 1786	0.66

The average abundance of *H. rotundata* ($\text{mL}^{-1} \pm \text{SE}$) over winter when weekly abundance data was collected compared to semi-weekly data. A two-sampled unpaired t-test was used to test whether the average winter abundance from weekly and semi-weekly sampling was statistically different ($P < 0.05$).

Figure D.1



A comparison of variability in winter *Heterocapsa rotundata* abundance (mL^{-1}) from weekly sampling compared to semi-weekly sampling in the Choptank River for (a) 2012, (b) 2012-2013, (c) 2013-2014, (d) 2014-2015, and (e) 2015-2016.